TALLINN UNIVERSITY OF TECHNOLOGY
DOCTORAL THESIS
68/2023

Research and Development of Explicit Demand Flexibility Management Methods for Ventilation Systems

VAHUR MAASK

TAL TECH PRESS

Content

List of Publications

The list of author's publications, on the basis of which the thesis has been prepared:

I **Maask, V.**, Rosin, A., Korõtko, T., Thalfeldt, M., Syri, S., Ahmadiahangar, R. (2023), "Aggregation ready flexibility management methods for mechanical ventilation systems in buildings," Energy and Buildings, vol. 296, Oct. 2023 doi: https://doi.org/10.1016/j.enbuild.2023.113369.

II **Maask, V.**, Rosin, A., Korõtko, T. (2023), "Virtual Energy Storage Model of Ventilation System for Flexibility Service," 17th IEEE International Conference on Compatibility, Power Electronics and Power Engineering, CPE-POWERENG 2023 (1–6). IEEE.

III **Maask, V.**, Mikola, A., Korõtko, T., Rosin, A., Thalfeldt, M. (2021), "Contributions to ventilation system demand response: a case study of an educational building," Cold Climate HVAC & Energy 2021 (1–6). E3S Web of Conferences.

IV Ferrantelli, a., Aljas, H. K., **Maask, V.**, Thalfeldt, M. (2021), "Tenant-based measured electricity use in 4 large office buildings in Tallinn, Estonia," Cold Climate HVAC & Energy 2021 (1–10). E3S Web of Conferences.

V **Maask, V.**, Häring, T., Ahmadiahangar, R., Rosin, A., Korõtko, T. (2020), "Analysis of Ventilation Load Flexibility Depending on Indoor Climate Conditions," 21st International Conference on Industrial Technology, ICIT2020 (1–6). IEEE.

VI **Maask, V.**, Rosin, A., Roasto, I. (2018), "Development of Experimental Load Management System for Nearly Zero-Energy Building," 59th International Scientific Conference on Power and Electrical Engineering of Riga Technical University, RTUCON 2018 (1–5). IEEE.

Author's Contribution to the Publications

Contribution to the papers in this thesis are:

I Vahur Maask, as the paper's main author, developed the concept for the publication. Researched and developed novel methods to quantify energy flexibility in ventilation systems, conducted simulations, and analyzed the results.

II Vahur Maask, as the paper's main author, developed the concept for the publication. Researched and developed novel methods to describe ventilation systems as virtual energy storage, conducted simulations, and analyzed the results.

III Vahur Maask, as the paper's primary author, was responsible for the method development, conducting the experiment, and analysis of the results.

IV Vahur Maask, as the third author of the paper, was responsible for the data collection and pre-processing.

V Vahur Maask, as the main author of the paper, developed the concept for the publication, selected research methods, constructed models, and carried out the analysis.

VI Vahur Maask, as the paper's main author, was responsible for developing the concept for the publication, creating models, and analyzing the results.

Abbreviations

AHU	Air handling unit
AIC	Akaike information criterion
ARMA	Autoregressive moving average
BES	Battery energy storage
BMS	Building management system
CAV	Constant air volume
CO_2	Carbon dioxide
DR	Demand response
EMS	Energy management system
EU	European Union
FMS	Flexibility management system
FVR	Forced ventilation rate
HVAC	Heating, cooling, and air conditioning
IAQ	Indoor air quality
IPS	Integrated power system
MAPE	Mean absolute percentage error
nZEB	Nearly zero-energy building
OECD	Organization for Economic Co-operation and Development
PV	Photovoltaic
QoS	Quality of service
RMSE	Root means square error
SoC	State of charge
SPG	Specific pollutant generation
TSO	Transmission system operator
UPS	Unified power system of Russia
V2G	Vehicle to grid
V2L	Vehicle to load
VAV	Variable air volume
VES	Virtual energy storage
VPP	Virtual power plant

Symbols

A_D	The DuBois surface area (m^2)
A_R	Zone floor area (m^2)
C	CO_2 concentration in a zone (ppm)
C_{amb}	Ambient CO_2 concentration (ppm)
c_{amort}	The regulation cost on amortization (€)
c_{comf}	The regulation cost on comfort (€/kWh)
C_{design}	The design CO_2 concentration for a zone (ppm)
$C_{h,i}$	The guideline value of the substance (µg/m^3)
c_{mgn}	Margin for regulations (€/kWh)
C_{limit}	CO_2 concentration limit value (ppm)
$C_{h,o}$	The concentration of the substance in the supply air (µg/m^3)
C_t	CO_2 concentration at timestep *t* (ppm)
C_{t-1}	CO_2 concentration at previous timestep *t* - 1 (ppm)
$c_{t,el}$	Electricity price including electricity market price and electricity supplier profit margin at timestep *t* (€/kWh)
$c_{t,fees}$	The sum of all the fees includes transmission costs and taxes added to the consumed energy price at timestep *t* (€/kWh).
$C_{t,min}$	Minimum CO_2 concentration for maximum airflow rate at timestep *t* (ppm)
C_t^{st}	Stable condition CO_2 concentration at timestep *t* (ppm)
$E_{t,\,dec}$	The energy capacity for up-regulation at timestep *t* (kWh)
$E_{t,\,inc}$	The energy capacity for down-regulation at timestep *t* (kWh)
G	CO_2 generation rate (m^3/s)
g	Local acceleration of gravity (m/s^2)
G_h	The generation rate of the substance (µg/s)
G_{pers}^{co2}	CO_2 generated by a person (m^3/s)
G_{pers}^{w}	Humidity generated by a person (m^3/s)
G_{max}^{co2}	Maximum estimated CO_2 generation rate (m^3/s)
G_t^{co2}	CO_2 generation rate during the timestep *t* (m^3/s)
G_t^{heat}	Heat generation rate during the timestep *t* (W)
G_t^{w}	Humidity generation rate during the timestep *t* (g/s)
K_{design}	Design value for the number of persons in a zone (pers)
K_t	Number of people inside a zone at timestep *t* (pers)
K_{t-1}	Number of people inside a zone at timestep *t* - 1 (pers)
k_t^{self}	The self-discharge or self-charge rate at timestep t (Ws/s)
MET	The level of physical activity
m_{final}	The final mass of a zone (kg)
m_{in}	The mass of the entering medium (kg)
$m_{initial}$	The initial mass of a zone (kg)

m_{out}	The mass of leaving medium (kg)
n	Total number of rooms
N_1	Fan rotational speed for the state 1 (rpm)
N_2	Fan rotational speed for the state 2 (rpm)
p	The order of the autoregressive polynomial or pressure (Pa)
P_1	Power consumption for the state 1 (kW)
P_2	Power consumption for the state 2 (kW)
P_{bias}	Power consumption bias (kW)
$p_{s,1}$	Pressure for the state 1 (Pa)
$p_{s,2}$	Pressure for the state 2 (Pa)
P_{max}	Maximum power consumption (kW)
P_{min}	Minimum power consumption (kW)
$price_t$	The calculated regulation price at time *t* (€/kWh)
$p_{s,1}$	Pressure for the state 1 (Pa)
$p_{s,2}$	Pressure for the state 2 (Pa)
P_t	Power consumption for timestep *t* (kW)
$P_{t,dec}$	Flexible power for up-regulation at timestep *t* (kW)
$P_{t,inc}$	Flexible power for down-regulation at timestep *t* (kW)
Q	Ventilation rate for the zone (m^3/s)
q	The order of the moving average polynomial or heat generated inside a zone (J)
Q_1	Airflow rate for the state 1 (m^3/s)
Q_2	Airflow rate for the state 2 (m^3/s)
Q_B	Ventilation rate for emissions from the zone ($l/[s \cdot m^2]$)
Q_{fvr}	Forced ventilation rate (m^3/s)
Q_h	The ventilation rate required for dilution (m^3/s)
Q_i	Airflow rate from a room *i* (m^3/s)
Q_{max}	Maximum ventilation rate (m^3/s)
Q_{min}	Minimum ventilation rate (m^3/s)
Q_p	Ventilation rate for the number of persons in the zone (l/s)
Q_{resp}	Person respiration rate (m^3/s)
Q_{return}	Airflow rate in the return air duct (m^3/s)
Q_t	Ventilation rate at timestep *t* (m^3/s)
q_t	The heat generated inside a zone during timestep *t* (J)
Q_{t-1}	Ventilation rate at previous timestep *t* - 1 (m^3/s)
Q_t^{return}	Airflow rate in the return air duct at the timestep *t* (m^3/s)
Q_t^{room}	Airflow rate from the room (m^3/s)
Q_{tot}	Total ventilation rate for the zone (l/s)
$Q_{tot,min}$	Total minimum ventilation rate for the zone with zero occupancy (l/s)
RH	Relative humidity (%)

RQ	A respiratory quotient
SPG_t^{room}	Specific pollutant generation for the room at the timestep *t* [(m³/s)/m², W/m² or (g/s)/m²]
SPG_t^{zone}	Specific pollutant generation for the zone at the timestep *t* [(m³/s)/m², W/m² or (g/s)/m²]
T	The temperature of the air (K)
T_i	Indoor air temperature (°C)
T_{supply}	Supply air temperature (°C)
T_t	Temperature at timestep *t* (°C)
T_{t-1}	Temperature at the previous timestep *t* – 1 (°C)
u	Internal energy per unit mass (J/kg)
V	Air volume in a zone or specific volume (m³)
v	The velocity of molecules (m/s)
W	Absolute humidity (g/m³)
W_i	Water vapor concentration in indoor air (g/m³)
W_{limit}	Humidity concentration limit value (g/m³)
W_{supply}	Supply air humidity concentration (g/m³)
W_t	Humidity concentration at timestep *t* (g/m³)
W_{t-1}	Humidity concentration at previous timestep *t* – 1 (g/m³)
w	Energy converted into work (J)
X_i	IAQ parameter value in room *i* (ppm, °C or g/m³)
X_{limit}	IAQ parameter limit according to the standard or set value (ppm, °C, or g/m³)
X_t^{limit}	IAQ parameter calculated limit for the timestep *t* (ppm, °C, or g/m³)
X_{return}	IAQ parameter value in return air (ppm, °C or g/m³)
Y_t^{fcst}	ARMA(p, q) model forecast for timestep *t*
Y_{t-i}	The autoregressive model lag
z	Elevation above the horizontal reference plane (m)
α	ARMA model constant
β_i	The autoregressive model's coefficient for the lag *i*
ΔP_t	Available flexible power at timestep *t* (kW)
Δt	Timestep length (s)
ε_t	Error terms
ε_{t-i}	The moving average model's error lag
ε_v	Effectiveness of ventilation
τ_t	FVR duration estimate at timestep *t* (s) or duration of regulation at timestep *t* (h)
τ_{t-i}	FVR duration estimate lag (s)
τ_t^{FVR}	Forced ventilation rate duration at time *t* (s)
$\tau_{t,i}^{FVR}$	An estimate of FVR duration at timestep *t* during correction iteration *i* (s)

$\tau_{t,i-1}^{FVR}$	An estimate of FVR duration at timestep *t* during previous correction iteration *i* – 1 (s)
$\tau_t^{FVR,co2}$	CO_2 concentration based FVR duration at timestep *t* (s)
$\tau_t^{FVR,T}$	Temperature based FVR duration at timestep *t* (s)
$\tau_t^{FVR,W}$	Humidity-based FVR duration at timestep *t* (s)
$\tau_t^{rb,CO2}$	CO_2 concentration based rebound duration at timestep *t* (s)
ϕ_i	The moving average model's coefficient for the lag *i*

1 Introduction

1.1 Background

Increasing environmental awareness and climate change have pushed the EU towards climate neutrality. Renewable Energy Directive [1] will force member states to fulfill at least 32% of overall energy needs with renewable energy by 2030. Furthermore, the provisional agreement is to increase the share of renewable energy goal from 32 to 42.5%. The European Green Deal [2] states that the long-term strategy will become the first climate-neutral continent by 2050. According to the Eurostat [2], the share of renewable energy consumption in gross final energy consumption during the period from 2010 to 2021 has increased from 12.5 to 21.8% in the EU, while in Estonia, renewable energy share during the same period has increased from 24.6 to 38%. Increasing the share of distributed volatile renewable energy generation makes maintaining the equilibrium between supply and demand increasingly challenging. It raises the importance of demand response and energy flexibility managed by aggregators, as described in [3]. Furthermore, the Baltic desynchronization of the IPS/UPS synchronous area will be conducted by 2026 [4]. It will further increase the importance of grid services, which Baltic electricity consumers could provide to system operators by taking advantage of their flexible loads.

According to the European Commission [5], buildings consume around 40% of the total energy produced in the EU, being the largest energy consumers in Europe. It is applying pressure on building more energy-efficient buildings and raising interest in flexible loads inside a building. In Estonia, all new buildings must be nZEB from 2020 onwards, which means that the building must not exceed the set energy performance indicator value, which for multi-apartment and office buildings is 100 kWh/(m^2·y) [6]. Another aspect is the demand-side flexibility inside a building. According to Eurelectric [7], flexibility is the modification of energy generation or consumption in reaction to an external signal to provide a service to the grid. Flexibility can be characterized by the following parameters: the amount of power modulation, the duration, the rate of change, the response time, the location, etc.

Typical flexible loads in buildings are heating, ventilation, air conditioning, lighting, appliances (e.g., laundry, dishwasher, tumble dryer), and electric vehicle chargers [8]–[10]. The study in [11] showed that HVAC systems account for up to 62% of overall electrical energy consumption in a building. In contrast, ventilation system fans can have up to 20% of the share. Therefore, ventilation systems are the biggest electricity consumers in a building after heating, cooling, and lighting. While heating, cooling, and lighting electricity consumption relies on ambient conditions and has high seasonal dependence, a ventilation system operation correlates with building usage, thus making it a valuable flexibility source throughout the year.

Ventilation systems can be characterized by their system type or control topology (Figure 1.1). There are two types of ventilation systems: natural and mechanical. Natural ventilation systems rely on airflows driven by gravity forces without electricity consumption [12]. Therefore, natural ventilation systems have no value from an energy flexibility standpoint. Mechanical ventilation systems depend on airflows generated by fans and can be divided into four: exhaust, supply, balanced, and energy recovery [13]. Exhaust and supply ventilation systems commonly use only one extract or supply air fan. Balanced ventilation systems use at least two fans, one installed in the exhaust and the

other in the supply air duct. It gives better indoor climate control and is universally applicable to all climates. The energy recovery ventilation type also has at least two fans but includes additional equipment to provide energy recovery that is essential for constructing nZEB. Energy recovery can be in the form of heat recovery or enthalpy recovery. Both have a heat exchanger, but the enthalpy recovery system retracts some water vapor from the exhaust air and transfers it back to the supply air.

From the control perspective, a ventilation system can be divided into a constant air volume (CAV) and variable air volume (VAV) type of a system. CAV system has the simplest control topology and commonly operates in an open loop configuration without feedback. This system type does not change its ventilation rate and has power consumption with low fluctuation. CAV is controlled by switching the system on, off, or between operation modes. Only adjustments are made in temperature control where the temperature can be regulated in a single point (single-zone) or multiple points (multi-zone). VAV system has a more complex system control topology and can handle the ventilation rate according to indoor air quality (IAQ). A single-zone VAV ventilation system adjusts its ventilation rate mainly by changing the fans' rotational speed directly through IAQ parameters (e.g., pollutant concentration, temperature, humidity). A multi-zone VAV type system has multiple dampers that adjust their position according to the zone's IAQ parameter, and the fans' rotational speed is changed through pressure shifts in air ducts.

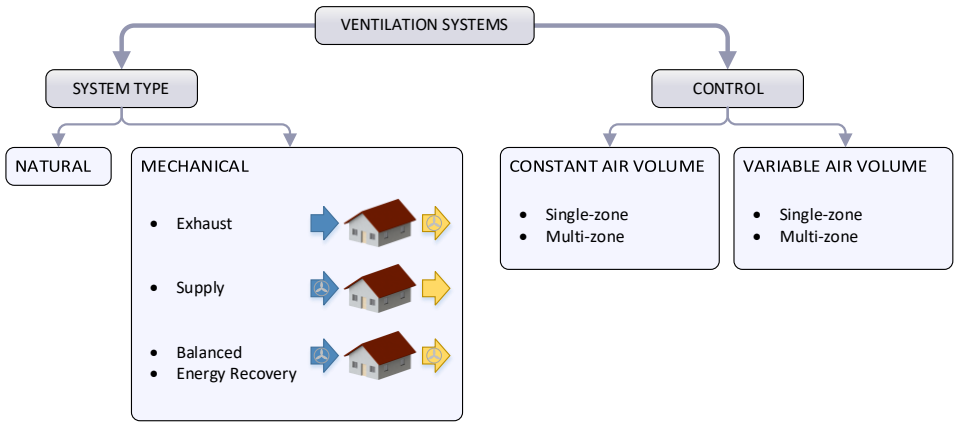

Figure 1.1. Characterization of ventilation systems by system type and control.

The installation and electrical loads of a building can be considered one nanogrid [14]. As proposed in studies [15]–[17], a central controller is used to manage nanogrid's energy flows and flexibility, which in this thesis is denoted as a flexibility management system (FMS). Changes in the ventilation system structure must be introduced to provide flexibility service to the grid. The concept of flexible control is explained in Figure 1.2, where the structure is divided into four hierarchical layers: ventilation system, measurement, management, and aggregation. On the ventilation system level, no changes are needed.

Based on the system type, an appropriate flexibility management algorithm is chosen. On the measurement level, power metering must be achieved. It is required to install an electricity meter to measure the power consumption of a ventilation system, or an existing meter will be used if available. Air duct sensors are needed to boost the performance of

the flexibility estimation algorithm, and room IAQ sensors are recommended for improvements. The flexibility can also be estimated in a sensorless mode, increasing the uncertainty in flexibility estimations. On a management level, an FMS must be installed. It can also be a remote server communicating with the building management system (BMS). If the building has no BMS, the FMS must directly control the ventilation system and acquire sensor data. ADepending on the system configuration, a ventilation system can be controlled through switches or frequency converters. The aggregation level consists of the aggregator communicating with different FMSs and providing services to the transmission system operator (TSO).

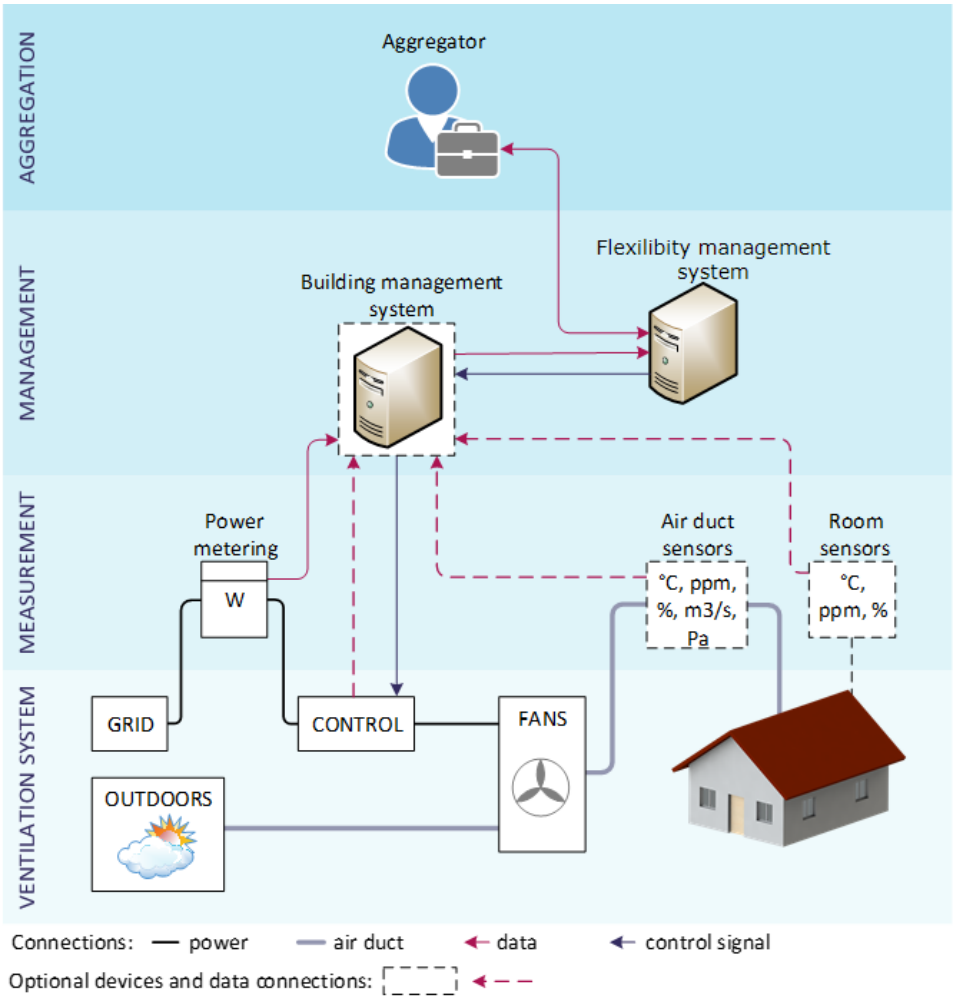

Figure 1.2. The concept of flexible control of a ventilation system.

1.2 Motivation

The author of this thesis carried out a comprehensive study on ventilation systems and addressed restrictions that can jeopardize the use of these systems in the flexibility service. The motivation to conduct this research came from the lack of appropriate methods that could be used to assess and include ventilation systems in the flexibility service. This research will bridge the gap in research by proposing appropriate methods for ventilation system flexibility management. The developed methods are modeled and tested in simulations, and experiments have been conducted on an actual building to verify the applicability of the developed method. Based on the results presented here, it is possible to assess the flexibility potential of the selected system and select an appropriate control algorithm to include the ventilation system in the flexibility service. The thesis can also be a source for future developments and research topics in the field of energy flexibility and load aggregation. This research was supported by the Estonian Research Council grant (PUT1680), Estonian Centre of Excellence in Zero Energy and Resource Efficient Smart Buildings and Districts ZEBE (grant 2014-2020.4.01.15-0016) funded by the European Regional Development Fund. Additional support was received from the European Commission through the H2020 project Finest Twins (grant no 856602). This doctoral thesis was supported by the project "Increasing the knowledge intensity of Ida-Viru entrepreneurship" co-funded by the European Union (2021-2027.6.01.23-0034).

1.3 Aims, hypotheses, and research tasks

The main aim of this Ph.D. research is to study and develop methods for harvesting mechanical ventilation system flexibility on the building level to ensure electricity cost reduction, create conditions for wider use of renewable energy in buildings, and provide services to a balancing authority.

Hypotheses:

1. Combining mass and energy balance analysis with sensor data will enable estimating forced ventilation rate duration.
2. The forced ventilation rate duration methods will forecast the maximum delivery period, wherein, in at least 95% of cases, the requirements for indoor air quality are guaranteed.
3. With the implementation of ventilation system flexibility management methods, it is possible to provide up-regulations for at least 30 min without exceeding set requirements for indoor air quality in at least 50% of the cases where the reserve is activated.
4. Using flexibility management methods to provide the flexibility service with a ventilation system will reduce the total energy cost of ventilation by at least 5%.

Research tasks:

- Analysis and classification of approaches for managing ventilation system flexibility to develop novel mathematical methods to quantify the flexibility.
- Development of novel ventilation system flexibility management methods to consider different system configurations and available sensor data.
- Improvement and validation of developed flexibility management methods on a simulated building model to analyze the performance characteristics and behavior of these methods.

- Improvement and validation of the developed flexibility management methods on a test building to test these methods under the conditions that would occur in actual use.

1.4 Contribution and dissemination

This thesis addresses comprehensive research on demand flexibility in ventilation systems, focusing on quantifying this flexibility and integrating the selected system into the flexibility service. The author proposes flexibility management methods that consider system type, available sensor data, and layout, covering most of the ventilation systems used in buildings. Knowledge and results included in this research have increased the awareness of ventilation system usability in flexibility service programs and facilitated the integration of these systems.

The findings of this research have been introduced in six research publications. Five of the papers have been published at Scopus-indexed conferences. One of the articles was published in a peer-reviewed journal. Intermediate results of the research have been presented in four sequential doctoral schools.

Scientific novelties:

- A novel method for calculating forced ventilation rate duration that considers sensor data, building size, and ventilation system parameters without the need for complex system models, large training datasets, and tuning of the hyperparameters. The method is applied to different pollutants to calculate changes in their concentration.
- A novel approach to cope with limited or nonexistent sensor data in applications where it is impossible or infeasible to install additional measurement devices.
- Definitions of ventilation system flexibility characteristics, instructions to aid the recognition process of these characteristics, and specification of ventilation system parameters that affect the flexibility.

Practical novelties:

- A set of methods developed from an aggregator's viewpoint enables integrating most ventilation systems into flexibility service.
- Comprehensive guidelines on integrating a ventilation system in a flexibility service include the needed parameters, sensor data, sources of the input, and algorithm selection procedure.
- Calculations made on the 2022 energy prices and reserve activations provide a clear picture of how the ventilation system exploitation in the flexibility service can reduce energy consumption and most importantly, the total energy costs.

1.5 Application

Within the last decade in Estonia, 212 new office buildings, 583 new commercial buildings, and 46,723 new dwellings were built, which corresponds to a floor area of 794,800 m^2 for office buildings, 1,038,300 m^2 for commercial buildings, and 4,571,600 m^2 for dwellings [18]. According to the Estonian regulation [19] the airflow rate for office and commercial buildings is 2 $l/(s \cdot m^2)$. The same regulation states the airflow rate for dwellings, which is 0.5 $l/(s \cdot m^2)$. The total calculated airflow rate is 5,952 m^3/s for all the office, commercial buildings, and dwellings built within the last decade. The average specific fan power is

between 2.0 and 2.7 kW/(m^3/s) [20]. Therefore, the total installed power for selected buildings built during the last ten years is 11.9 MW and 16.1 MW. The share of total power consumption of the ventilation system of each building type is roughly equal (Figure 1.3). Considering building size, office and commercial buildings have larger ventilation systems, which makes them preferable in the flexibility service. It does not mean that dwelling ventilation systems should be set aside. If many dwelling ventilation systems are concentrated under an aggregator, considerable power for the flexibility service can be harvested. According to the study [22], up to 15% of the rated fan power can be used for flexibility services without substantially affecting the IAQ of the building. The total available power for the flexibility service in the selected buildings is around 2.1 MW.

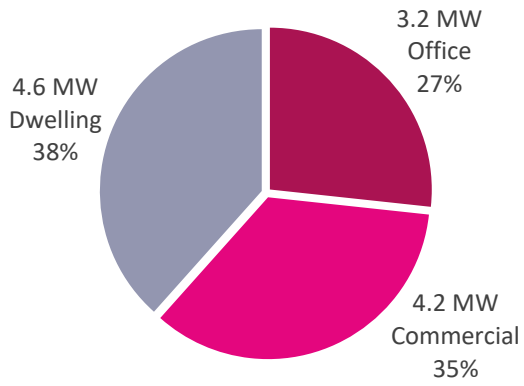

Figure 1.3. Share of the installed power of the ventilation system for each building type during the last decade.

According to Estonia's 2022-year manual frequency restoration reserve (mFRR) activations, the average energy utilized during up-regulation was around 8.7 MWh [22]. During the same time frame, regulations consumed a maximum of 98.9 MWh of energy. According to Elering AS [23], an Estonian transmission system operator (TSO), the average hourly energy usage in 2022 was 934 MWh. Since ventilation systems are known to use at least 2% of the energy generated in the EU, their greatest potential is to provide about 19 MWh of energy for the flexibility service. Therefore, ventilation systems use more energy than is needed during most regulations. As a result, the potential for the flexibility offered by ventilation systems is rather significant.

1.6 Thesis outline

The thesis is divided into four main topics and sections. Chapter 2 covers the previous research on demand-side flexibility and gives an overview of ventilation types and relevant parameters. Chapter 3 discusses the development of ventilation system flexibility management methods where different system types and available data are used to propose an appropriate flexibility management algorithm. Chapter 4 presents modeling and assessment of the flexibility management methods developed in Chapter 3 based on the results acquired from simulations. Chapter 5 addresses case studies with flexibility management methods on a test building to evaluate the performance of the method under real conditions. Finally, Chapter 6 concludes all the results gathered during this research and recommends future research topics.

2 State of the art

This chapter presents a background study of flexibility, characterization of demand-side flexibility, flexibility management algorithms, and ventilation system control from a flexibility standpoint. The state of the art study is based on various research papers to give insight and an overview of current trends and relevant research results. Firstly, energy flexibility definitions and relevant research are addressed, with the focus mainly on buildings and demand-side flexibility. Secondly, the characterization of the flexibility algorithm is given, and the main approaches are discussed. Lastly, ventilation systems and their control discussed in research papers are studied.

2.1 Energy flexibility

Energy flexibility in the context of electric system flexibility is the system's ability to adjust generation or consumption to maintain a secure system operation considering grid stability constraints and volatile renewable energy sources [24]. By Eurelectric [7] definitions, the modification of generation or consumption is done through an external signal, which can be price or activation. Electric system flexibility can be divided into demand-side and generation flexibility (Figure 2.1). Demand-side flexibility can be differentiated into explicit and implicit demand flexibility. Implicit demand flexibility uses different electricity tariffs to stimulate prosumers to consume or generate at certain hours [24]. With advancements in smart grid technology and distributed energy generation, a passive energy consumer can become an active energy prosumer [25]. Explicit demand flexibility considers committed prosumers who increase or decrease consumption or generation in response to the system's needs [24].

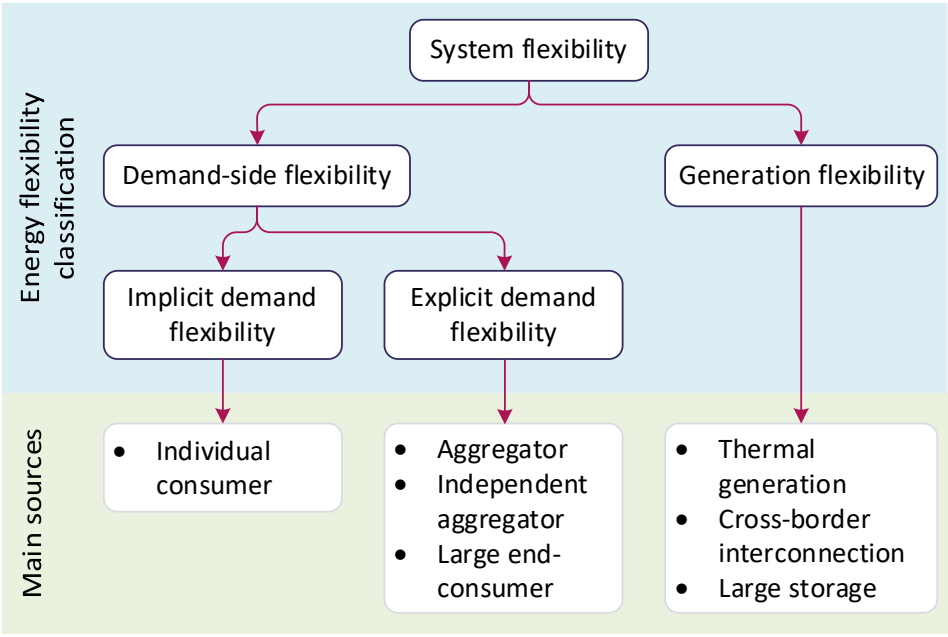

Figure 2.1. Classification of energy flexibility and main sources of flexibility [24].

Generation flexibility has been the main source of system flexibility long before the cost-effectiveness of changing demand patterns was evaluated [26]. The primary sources of generation-side flexibility have been:

- **Thermal generation** uses fossil fuel-based power plants to provide flexibility to the system. If there is a need for more energy, then more fuel is burned and vice versa [24].
- **Cross-border interconnection** enables large-scale sharing of energy, ancillary services, and backup resources [27].
- **Large energy storage** can adapt its energy production and consumption according to the system's needs. Hydroelectric plants have been the main energy storage for a long time but are limited by the location where they can be installed [28]–[30]. With the advancements in battery technology and increased efficiency in production, energy storage can have a significant role in providing stability to the energy system if safety and environmental aspects are addressed [31], [32].

2.1.1 Demand-side flexibility

In 2019, the total electricity consumption in the world reached 22.8 PWh, with a 1.7% increase compared to the previous year. In the same year, the total electricity consumed in OECD countries was 9.7 PWh, around 42% of the total electrical energy consumption in the world. Compared to the previous year, electricity consumption in OCED countries decreased by 1.1%. The main sectors where electricity is consumed are residential, industrial, commercial, and public services (Figure 2.2). Under others, electricity consumption in agriculture, forestry, fishing, and other non-specified sectors is presented [33].

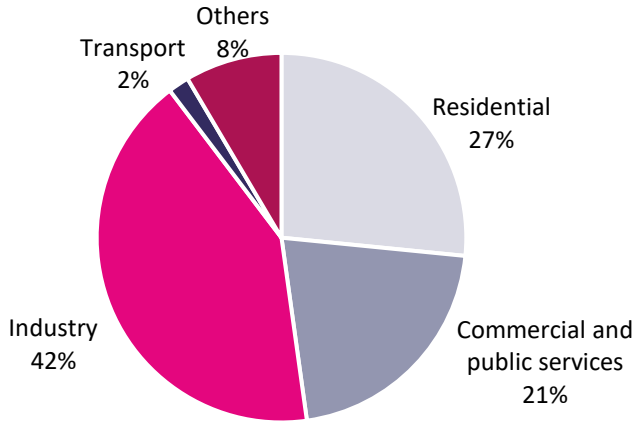

Figure 2.2. World electricity consumption by sector in 2019 [33].

According to the Global Alliance for Buildings and Construction, nearly 55% of global energy consumption is represented by buildings. A share of energy consumed by residential buildings is around 73%, and non-residential buildings are around 27%. In Estonia, 76% of the floor area in the building stock comprises residential buildings. Annual energy consumption per floor area in Estonian residential buildings is around

270 kWh/m^2, while the same parameter for non-residential buildings is around 400 kWh/m^2. Non-residential buildings in Estonia by floor area are about 20% wholesale and retail trade, 18% hotels and restaurants, 18% health care, 19% education, and the rest of 25% are used by other non-residential sectors. Residential buildings can be classified into multi- and single-family dwellings, where the share of the residential building stock is 75% and 25%, respectively. In summary, buildings can be considered valuable assets in demand-side flexibility programs [34], [35].

Flexible loads in buildings play a crucial role in the demand-side flexibility. Flexible loads are differentiated from all the other devices and systems by the ability to vary power consumption over their baseline demand without jeopardizing their Quality of Service (QoS). The amount of deviation from the baseline demand requested by an aggregator or balancing authority (usually TSO) is the reference signal [36]. Buildings, devices and systems that correspond to flexible loads have electrical storage, discrete (on/off) and dimming control of the lighting system, discrete and variable frequency control of the components in an HVAC system, and shiftable appliances [37]. According to the study [11] where electricity consumption in two office buildings was measured, it can be stated that most of the energy in office buildings is consumed by HVAC systems (Figure 2.3). The mentioned study was conducted in Estonian office buildings where the need for building cooling is around 3% of total electricity consumption, which is insignificant compared to the heating load. Ventilation systems with air heaters account for about 31% of total energy consumption in the monitored buildings. In the residential sector, space heating has the highest share of total electricity consumption in Estonian dwellings, while cooling load is non-existent in residential buildings (Figure 2.4) [35].

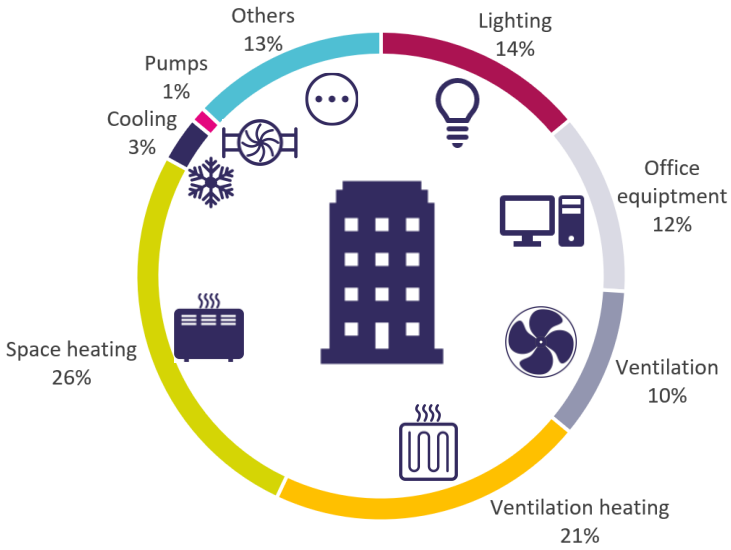

Figure 2.3. Weighted distribution of electricity consumption in two office buildings [11].

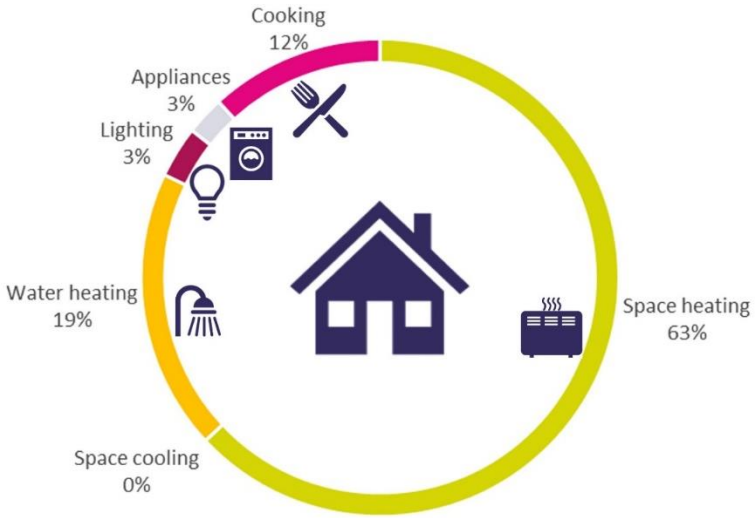

Figure 2.4. Distribution of electricity consumption in Estonian residential buildings [35].

Flexible loads and their usage in the flexibility service are as follows:

- **Electrical storage** has increased its necessity in energy flexibility in buildings aided by the wider use of stationary battery systems in buildings and electric vehicles with bidirectional charging possibilities, e.g., vehicle to load (V2L), vehicle to grid (V2G) [38]. One of the research topics is to use electrical storage to increase the share of locally produced electrical energy from on-site renewable energy generation, also called self-consumption. Luthander et al. [39] have reported that a battery storage system of 0.5 to 1 kWh per kWp of PV panels can increase the relative self-consumption rate by 13 to 24%. Kempener and Borden [40] showed that 4 kWh electric storage with 5 kWp PV panels could improve self-consumption from 30 to 60%. Another field of research is to optimize electrical storage's discharging/charging process to smoothen load fluctuations and shape load profiles for economic benefits [41], [42]. Phan et al. [43] proposed a method to optimize battery usage over a 24-hour period, which can achieve cost reduction on consumed energy by 28 to 31%. Battery energy storage is also used to provide services to the electrical system. The study [44] showed that when using batteries in both the energy and regulation market, 12% of total revenue is gathered from regulations.
- **A lighting system** in buildings has changed in the last two decades from being manually controlled by the occupants to automatically adjusting to visual comfort, efficiency, and economics [45]. Compared to other flexible loads in buildings, a lighting system's power consumption can be altered within seconds [46]. In the study [46], it is reported that for large California buildings (i.e., more than 4645 m^2), a 25% reduction in lighting system power consumption could provide a 2.5 GW regulation reserve. The same report found that when the lighting system operates around 80% light level, then ±8% power consumption can be altered without notice.
- **HVAC systems** are the largest energy consumers in a building, and through demand-side management, substantial environmental and economic benefits can be gained [47], [48]. Nyholm et al. [49] showed that pre-heating and operation

duration of 5.5 GW of peak-load shifting can be achieved by optimizing an electric heating system in Sweden based on the Swedish electricity prices during the study. The study [51] analyzed load shifting for a heat pump and a thermal storage tank by considering different temperature setpoints and tank sizes. The results showed that the proposed method can save 10% of annual costs. During up-regulations, when air-conditioners are switched off, the delay after giving the activation signal (to switch off) is around 12 to 60 s until the final load curtailment [50]. Bode et al. [51] made a similar study about shutting down and cycling air-conditioning compressors, which responded within 60 s after the activation signal was given and reached total capacity within 6 min. Cai and Braun [52] proposed a control method for a rooftop unit with a variable speed supply fan, compressor, and condenser fan to provide frequency regulation service, reducing the energy cost for buildings by 12 to 26%. Authors of the study [53] reported that 15% of the ventilation system-rated power could be used for the flexibility service without jeopardizing occupants' thermal comfort.

- **Shiftable appliances** have a significant potential to provide flexibility in the residential sector where washing machines, dishwashers, tumble dryers, and other similar home equipment time of use can be altered [37]. According to the study [54], an average maximum down-regulation of 430 W at midnight on the weekend and an average maximum up-regulation of 65 W during the weekend can be achieved per household. The study in [55] used a mixed-integer nonlinear optimization model to control shiftable appliances and reduce the cost of electricity by 25%.

Nearly half of the global energy consumption is represented by buildings, making them valuable sources for the demand-side flexibility. In Estonia, around 60% of energy consumption is represented by the HVAC systems, and when comparing different flexible loads, they can provide cost-effective capacity to the flexibility service.

2.1.2 Aggregation and explicit demand flexibility

The explicit demand flexibility approach involves re-scheduling consumption or onsite generation with a specific objective. For example, to stabilize the electric system, lessen the effect of peak electricity prices, or deal with congestion problems [24], [56]. Therefore, offering competition to power plants in the form of Virtual Power Plants (VPP), which aggregates distributed energy generation and flexible loads to participate in the wholesale market, balancing markets, reserves markets, and providing grid services [24], [57], [58]. For large prosumers, individual participation in the mentioned markets can be considered. In all other cases, aggregation is needed to concentrate multiple prosumers' ability to change their consumption or generation to fulfill all the requirements stated by the market operator [59], [60]. Aggregators concentrate and manage the flexibility offered by buildings or other sources and make a combined offer to the balancing authority or transmission system operator (Figure 2.5) [61].

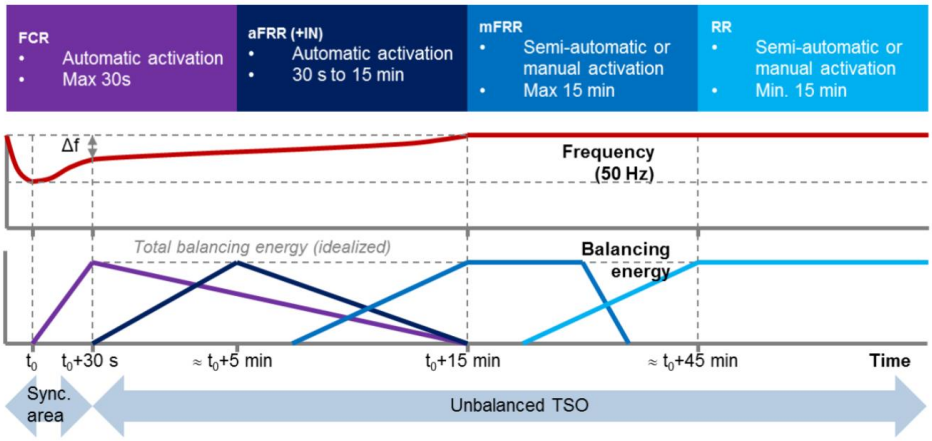

Figure 2.7. Activation process of balancing market reserves [81].

In Europe, harmonizing different balancing services is essential, meaning that regulatory measures are unified and markets are extended internationally between countries. For this balancing, service platforms are introduced:

- **PICASSO** is the Platform for the International Coordination of Automated Frequency Restoration and Stable System Operation. It is a platform to exchange balancing energy from aFRR with an activation time of 30 s to 15 min. Estonia is an observer state of this platform [82].
- **MARI** is the Manually Activated Reserves Initiative for the mFRR service. Activation time in this platform is less than 15 min. Estonia is a member state of this platform [83].
- **TERRE** is the Trans European Replacement Reserves Exchange for the RR service. Activation time in this platform for the RR service is up to 30 min. Currently, Estonia has no interaction with this platform [84].

Currently, the main balancing service available in the Baltic electric system is the Manual Frequency Restoration Reserve (mFRR). It states the limitation for the flexible load, meaning that the reaction time with the transition from one power level to another cannot be longer than 12.5 min (Table 2.1). Other parameters constrain the prospective systems to be used in the flexibility service. The minimum quantity is most important, meaning that 1 MW of ventilation systems must be combined to achieve the set minimum power level [85].

statistics. Randomization is the ability of the method to draw a pattern from a random dataset. Adaptability assumes that the same technique can be combined with other optimization techniques or used in a different environment. Artificial Neural Network has the highest score based on the MCA.

Table 2.2. List of algorithms used in energy management systems [103].

Algorithm	**MCA score**
ANFIS (Adaptive Neural Fuzzy Interference System)	187
ANN (Artificial Neural Network)	189
MLR (Multiple Linear Regression)	170
XGBoost (eXtreme Gradient Boosting)	185
WNN (Wavelet Neural Network)	181
SVM (Support Vector Machine)	169
ARIMA (Auto Regressive Integrated Moving Average)	140
Gaussian Process Regression	144

2.3 Ventilation systems

A ventilation system is used to provide fresh air to the building and to extract polluted air. Ventilation system operation depends on the usage of a building while providing required indoor air quality [104].

2.3.1 Ventilation system control

The traditional ventilation system is set up to provide a fixed minimum ventilation rate per person based on the maximum occupancy of a building or a space [105]. According to the standard EN-16798 [106] ventilation rate for normal conditions is 7 l/s per person and 0.7 l/s per m^2. The standard ventilation rates differ based on the building type and pollutant generation. Since the building is not occupied by the maximum number of people daily, this ventilation rate is higher than needed. Demand Controlled Ventilation (DCV) uses one or multiple Indoor Air Quality (IAQ) parameters to control the ventilation system according to the setpoint or limit values where actual demand for fresh air is estimated. It has been found that with DCV, about 62% of ventilation reduction can be achieved compared to a system without DCV [105].

DCV can be based on temperature [107], [108] or based on CO_2 concentration, which is discussed in [109], [110]. DCV with closed-loop control needs sensors to monitor IAQ. These sensors can be placed in rooms or air ducts. As suggested in [111], placing sensors in both the supply and return air ducts allows one to actively see contamination or temperature differences. The drawback of this setup is that during ventilation shutdown, the state of IAQ is unknown, and contamination or temperature can exceed the limits. Placing sensors in each room or space of the building requires higher investment costs and a complex sensor network.

Closed loop control needs a regulator to control the airflow accurately. A conventional system uses PID control to hold the IAQ within its setpoint value. The drawback of PID control is high overshoot and oscillation. In [100], direct feedback linearization is applied to overcome this issue to obtain a linear input-output model characterized by no overshoot and minimal oscillation.

Multiple studies consider temperature-based ventilation control with the thermal comfort of occupants. Ventilation demand response is considered in [110] where a study was made for commercial buildings to minimize the sum of HVAC energy and thermal discomfort costs related to occupants.

2.3.2 Methods used for ventilation systems

Studies in [10], [11] focus on temperature-based ventilation control while also considering the thermal comfort of occupants. Ventilation DR is considered in [10], where the study was made for a commercial building to minimize the sum of HVAC energy- and thermal discomfort costs related to occupants. In [11], testing was not based on any detailed model but on the actual measurement from the on-site experiments. Those studies did not consider all IAQ parameters but focused merely on the temperature. Controlling a ventilation system only by measured indoor temperature does not guarantee that other IAQ parameters are within the required limits.

An HVAC system for frequency regulation service is studied in [12]. Up to 15% of the rated fan power can be implemented in the frequency regulation without substantially affecting indoor temperature. The DR potential of ventilation systems in residential buildings is discussed in [13], where it is stated that a single 13 kW ventilation system in a 12-story apartment building can provide 4.5 kW of power increase and 1.0 kW of power reduction when needed without compromising IAQ. The outcome of the study was that an automated DR for ventilation systems could provide prolonged load sheds and ancillary services without jeopardizing IAQ. Research in [4] shows that buildings can provide short-term energy flexibility without requiring substantial changes and extra investments in the HVAC system. The mentioned studies do not consider ventilation shutdown as an option to provide load flexibility. Furthermore, existing research mainly focuses on one IAQ parameter while discarding the influence of other parameters on system flexibility.

The study in [14] monitored indoor air pollutant concentration and climate factors based on occupants' number and activities. The measured parameters included particulate matter and the CO_2 concentration. It was found that the pollutant concentration increases along with the rise in the number of occupants and the level of their physical activities. The occupants' behavior was studied in [15], where it was concluded that the CO_2 concentration and the absolute humidity level correlate since both the CO_2 and the water vapor are generated during respiration. The findings imply that the absolute humidity level can be estimated based on CO_2 concentration measurements. In [16], classroom measurements were carried out to investigate the dependence of CO_2 concentration on the ventilation rate and the number of students. The study showed that in a poorly ventilated space with a volume of 210 m^3 and an occupancy of 20 persons, the CO_2 concentration rose from 472 ppm to 1732 ppm within 4 hours.

2.3.3 Ventilation in nearly zero-energy buildings

Estonian Government has issued a regulation [6] that states: *"A nearly zero-energy building is a building that is characterized by sound engineering solutions, that is built according to the best possible construction practice, that employs solutions based on energy efficiency and renewable energy technologies and whose energy performance indicator is greater than 0 kWh/($m^2 \cdot y$) but does not exceed the limit values (Table 2.3)."*

3.1.2 Variable air volume type system

A VAV type ventilation system can also operate according to a schedule, but the airflow rate during the operational hours of a ventilation system is dependent on the building usage. It causes a situation where the power consumption of a ventilation system is not constant but is fluctuating. The schedule may differ for office buildings within a day, but it can be assumed that the ventilation system is operational during working hours and shut down for the rest of the time. Figure 3.3 shows an example of power consumption in a single-zone VAV type system during a week in an educational building. In a single-zone ventilation system, fluctuations are caused by a single sensor in the return air duct or the room. According to this sensor, the ventilation system changes the rotational speed of fans through a variable frequency drive and therefore, causes changes in the airflow rate.

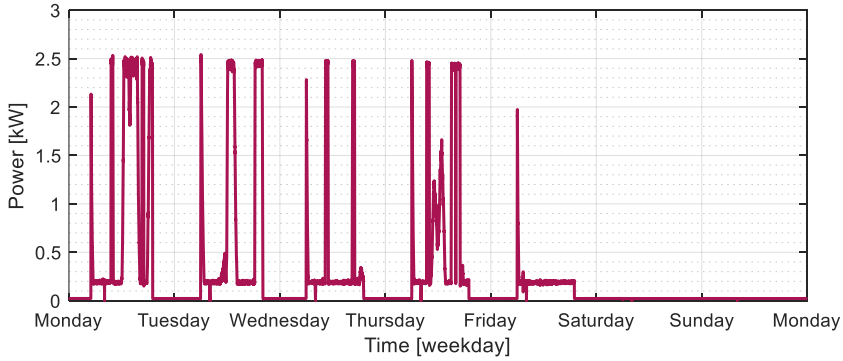

Figure 3.3. Example of weekly power consumption of a single-zone VAV type system.

Similar to a single-zone VAV type ventilation system, a multi-zone ventilation system can also operate according to a schedule. The difference is that the power consumption of the ventilation system is influenced by multiple valves that open and close according to the zone usage. The schedule may differ for office buildings within a day, but it can be assumed that the ventilation system is operational during working hours and shut down for the rest of the time. Figure 3.4 shows an example of a multi-zone VAV type system in an educational building where static pressure in the air duct is maintained. Power consumption fluctuations in this type of configuration are lower than for the single-zone VAV type system, which affects the forecasting accuracy positively.

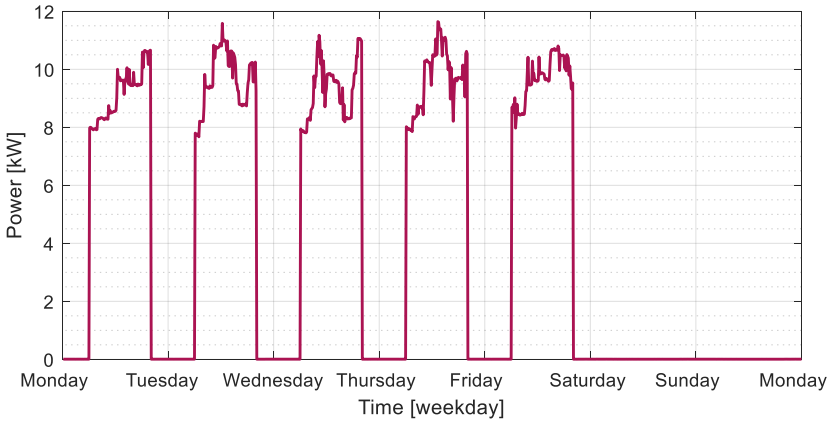

Figure 3.4. Example of weekly power consumption of a multi-zone VAV type system.

$$V\frac{dC}{dt} = G + QC_{amb} - QC \tag{3.7}$$

where V – air volume in a zone (m^3),
C – CO_2 concentration in a zone (ppm),
G – CO_2 generation rate (m^3/s),
Q – airflow rate for the zone (m^3/s),
C_{amb} – ambient CO_2 concentration (ppm).

To estimate CO_2 generation in a zone serviced by a selected ventilation system, the maximum number of people in this zone must be acquired. It is done according to the number of workplaces and seats in the zone, or the other alternative is to use values given in the standard EN 16798-1:2019 (Table 3.1). Maximum occupancy can be calculated accordingly if the zone floor area is known. CO_2 generated by a person during respiration is, according to the EN 16798-1:2019, around 20 l/h, or a more precise estimation can be done by calculating one person's CO_2 generation through DuBois surface area, MET, and RQ (i.e., the rate of CO_2 produced to oxygen consumed) value, as shown in (3.8). An average size adult has a DuBois surface area of around 1.8 m^2 and an *RQ* of 0.83 [13]. The standard EN 16798-1:2019 states that humans in residential, educational, and office buildings are mainly occupied with sedentary activities; therefore, the MET value is 1.2.

$$G_{pers}^{co2} = \frac{0.00276 \cdot A_D \cdot \mathrm{MET}}{(0.23RQ + 0.77) \cdot 10^3} \tag{3.8}$$

where A_D – the DuBois surface area (m^2),
MET – the level of physical activity,
RQ – a respiratory quotient [125].

$$\tau_{t,i}^{FVR} = \begin{cases} \tau_{t+1,i-1}^{FVR} + \Delta t, & \tau_{t+1,i-1}^{FVR} < \tau_{t,i-1}^{FVR} - \Delta t \\ \tau_{t,i-1}^{FVR}, & \tau_{t+1,i-1}^{FVR} \geq \tau_{t,i-1}^{FVR} - \Delta t \end{cases} \quad (3.22)$$

where $\tau_{t,i}^{FVR}$ – an estimate of FVR duration at time *t* during correction iteration *i*,
$\tau_{t,i-1}^{FVR}$ – an estimate of FVR duration at time *t* during previous correction iteration *i* - 1,
Δt – timestep length (s).

$$\sum_{t=1}^{n} \tau_{t,i}^{FVR} = \sum_{t=1}^{n} \tau_{t,i-1}^{FVR} \quad (3.23)$$

3.4.2 Calculation method for the regulation price

Knowing the energy price for regulations is a crucial component for enabling the integration of a ventilation system in a flexibility service. It is the needed input for the aggregator, according to which the amount of regulated energy will be compensated to a building owner. A personalized pricing mechanism is used to achieve this, as shown in (3.24). The direction of regulation dictates the ingredients of the final regulation price. It is necessary to compensate for lower IAQ in the zone if up-regulation is activated and the ventilation system's power consumption is reduced. It can be done by considering variable building usage described through the CO_2 generation rate. Regulation-induced amortization of the system must also be addressed to compensate for additional wear (e.g., switching counts for contactors and movement of valves). If down-regulation is activated and the ventilation system's power consumption is increased, then this causes additional energy consumption, which must be compensated.

$$price_t = \begin{cases} \frac{G_t^{co2}}{G_{max}^{co2}} \cdot c_{comf} + \frac{c_{amort}}{\Delta P \cdot \tau_t} + c_{mgn}, & \Delta P < 0 \\ \frac{C_t - C_{t,min}}{C_{limit} - C_{t,min}} \cdot c_{t,el} - c_{t,fees} - \frac{c_{amort}}{\Delta P \cdot \tau_t} - c_{mgn}, & \Delta P > 0 \end{cases} \quad (3.24)$$

where $price_t$ – the calculated regulation price at time *t* (€/kWh),
G_t^{co2} – CO_2 generation rate at time *t* (m^3/s),
G_{max}^{co2} – maximum estimated CO_2 generation rate (m^3/s),
c_{comf} – the regulation cost on comfort (€/kWh),
τ_t – duration of regulation at time *t* (h),
c_{amort} – the regulation cost on amortization (€),
c_{mgn} – margin for regulations (€/kWh),
ΔP – change of power consumption during regulation (kW),
C_t – CO_2 concentration in the return air at time *t* (ppm),
$C_{t,min}$ – minimum CO_2 concentration for maximum airflow rate at time *t* (ppm),
C_{limit} – CO_2 concentration limit value (ppm),
$c_{t,el}$- electricity price including electricity market price and electricity supplier profit margin at time *t* (€/kWh),
$c_{t,fees}$– the sum of all the fees, which include transmission costs and taxes added to consumed energy price at time *t* (€/kWh).

The tendered price for up-regulation depends on the CO_2 generation rate, and the maximum price is achieved at maximum building usage (Figure 3.7 a). Cost on comfort can be selected according to historical balancing energy prices on the market, and in this thesis, the price data for the last two weeks is used. The same approach determines the maximum CO_2 generation rate where the previous two weeks' maximum value is used. Usually, regulations introduce an insignificant amount of additional wear to the system; therefore, amortization costs are neglected in the validation process of developed methods. The margin for regulation is a parameter that is dictated by the building owners, which increases the profitability of the flexibility service. In future studies, this margin can be optimized to maximize regulation activations and income since increasing the regulation price lowers the number of events where the market price is reached. In validating the developed method, the margin is not used, and the difference between the tendered and the market price is split between the building owner and the aggregator. The tendered down-regulation price depends on the CO_2 concentration in the return air (Figure 3.7 b). If the ventilation system's return air CO_2 concentration is higher than the minimum possible CO_2 concentration, the goal is to decrease the CO_2 concentration level by purchasing electricity at a lower price. When the CO_2 concentration is low due to the low occupancy, down-regulation is provided if the additional costs from grid fees and taxes are compensated.

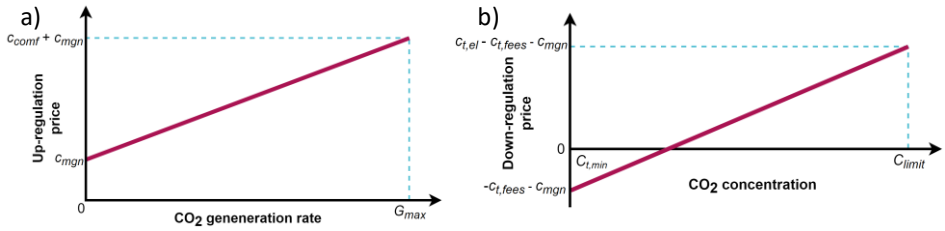

Figure 3.7. Dependence of the regulation price on a) CO_2 generation rate for up-regulation and b) CO_2 concentration for down-regulation.

The estimation of the forced ventilation rate duration dictates the maximum duration for each regulation. The regulation price is calculated for each period separately. Therefore, the duration of each regulation can be derived as follows:

$$\tau_t = \begin{cases} \tau_t^{FVR}, & \tau_t^{FVR} \leq \Delta t \\ \Delta t, & \tau_t^{FVR} > \Delta t \end{cases} \tag{3.25}$$

where τ_t^{FVR} – duration of the forced ventilation rate at time *t* (h),
Δt – duration between two sequent calculation steps (h).

For down-regulations, the minimum possible CO_2 concentration and CO_2 concentration at a specific time must be estimated ahead. It can be derived from the mass balance analysis, as shown in (3.26) and (3.27). Minimum CO_2 concentration depends on the maximum airflow and CO_2 generation rates at selected times. The FVR duration forecasts estimate CO_2 concentration ahead, as discussed in section 3.2.

$$C_{t,min} = \begin{cases} \frac{G_t^{co2}}{Q_{max}} + C_{amb}, & \frac{G_t^{co2}}{Q_{max}} \geq 0 \\ C_{amb}, & \frac{G_t^{co2}}{Q_{max}} < 0 \end{cases} \quad (3.26)$$

where G_t^{co2} – CO_2 generation rate at time t (m^3/s),
Q_{max} – maximum ventilation rate (m^3/s),
C_{amb} – ambient CO_2 concentration (ppm).

$$C_t = \frac{2V \cdot C_{limit} + 2\tau_t^{fvr,co2} \cdot G_t^{co2} - \tau_t^{fvr} \cdot Q_{fvr} \cdot (C_{limit} - 2C_{amb})}{2V - \tau_t^{fvr} \cdot Q_{fvr}} \quad (3.27)$$

where V – zone volume (m^3),
C_{limit} – CO_2 concentration limit value (ppm),
$\tau_t^{fvr,co2}$ – CO_2 concentration based forced ventilation rate duration at time t (s),
G_t^{co2} – CO_2 generation rate at time t (m^3/s),
Q_{fvr} – forced ventilation rate (m^3/s).

3.4.3 Addressing the rebound effect

Regulations can affect the energy consumption of the ventilation system even after activations. After activation of the reserve, the temporary power consumption increase is known as a rebound effect [131]. Power consumption of a CAV type ventilation system will be affected only during regulations, and no rebound effect exists. The reason is that the CAV type system only operates at a set ventilation rate and is not influenced by indoor air conditions. The system's cumulative energy consumption is also reduced if the power consumption is decreased during regulations. The VAV type ventilation system will be affected by regulations. The system controller and system layout influence the magnitude and duration of the rebound effect. If the power consumption of a VAV type ventilation system is decreased and CO_2 concentration-based control is implemented, then after the regulation, there is a temporary increase in power consumption (Figure 3.8). Effects of the regulation on cumulative energy consumption are investigated in simulations.

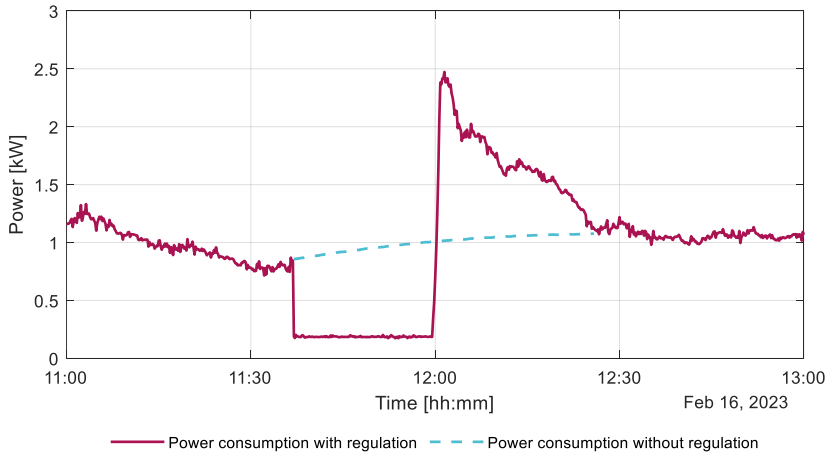

Figure 3.8. Algorithm selection procedure for flexibility management.

After the deactivation of the reserve, the IAQ in the building is disturbed. It creates a need to know the subsequently allowed regulation since consecutive activations can too highly impact the IAQ. In this thesis, the rebound duration is the length of time that it takes for the ventilation system to change a sufficient amount of indoor air with fresh ambient air to reach normal IAQ conditions. The rebound duration can be estimated with the following two equations:

$$C_t^{st} = \frac{G_t^{co2}}{Q_t} + C_{amb} \tag{3.28}$$

$$\tau_t^{rb,CO2} = \frac{V \cdot (C_t^{st} - C_t)}{G_t^{co2} - Q_t \cdot \frac{C_t + C_t^{st} - 2C_{amb}}{2}} \tag{3.29}$$

where C_t^{st} – stable condition CO_2 concentration at timestep *t* (ppm),
$\tau_t^{rb,CO2}$ – CO_2 concentration-based rebound duration at timestep *t* (s).

$$\tau_t^{rb,CO2} = \frac{2V}{Q_t} \tag{3.30}$$

3.4.4 Selection of flexibility management algorithm

Different ventilation system configurations cause the flexibility management algorithm to be combined from the appropriate components described in this thesis. The procedure described in Figure 3.8 can be followed to ease the algorithm selection. First of all, a power consumption forecasting method must be selected. ARMA(p, q) model is suitable for this with the AIC method to tune it. For FVR duration estimations, available IAQ sensors and their locations must be made clear. If there is a CO_2 sensor that gives an adequate overview of CO_2 concentration in a zone, then FVR duration can be calculated accordingly. If sensors are absent, an open-loop approach can be implemented, or another option is to install a CO_2 concentration sensor. These can also be applied to FVR duration estimations if temperature and humidity sensors are available. If one zone includes multiple rooms, then it is necessary to have measurements or estimations from each room separately. A different approach is needed if there are no IAQ sensors in each room. The IAQ parameter limit value must be corrected to avoid exceeding the limit when only one sensor is installed in the return air duct. FVR durations must be adjusted to consider the variable usage of the building. The regulation price must be calculated to enable transactions with an aggregator. After each reserve activation, rebound duration must be calculated to avoid concurrent activations jeopardizing IAQ.

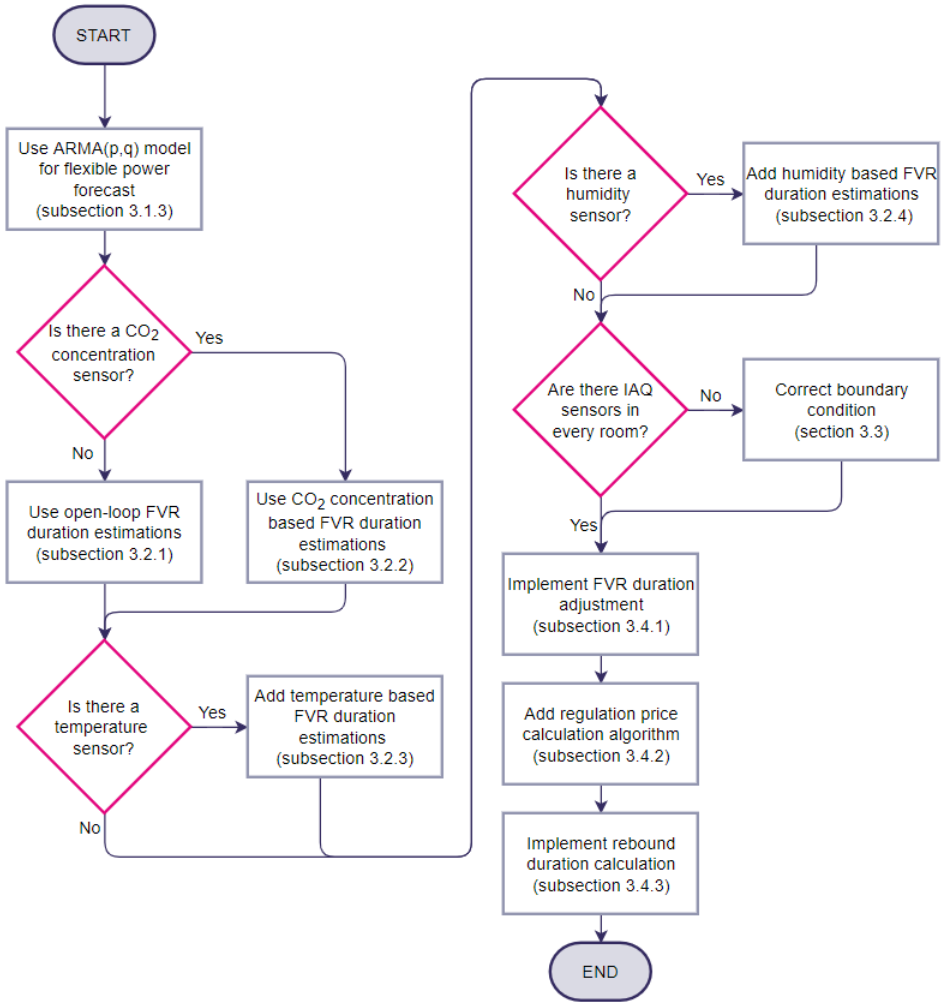

Figure 3.9. Algorithm selection procedure for flexibility management.

3.4.5 Applying flexibility management methods

Flexibility management methods can be applied using a flexibility management system that embeds all needed algorithms (Figure 3.10). The flexibility management system consists of modules, each having its purpose. The regulation activation module aims to listen for activation reserve activation signals, check if the ventilation system is available for regulation, and send commands to the ventilation system to force a defined ventilation rate. The flexible power forecasting module is responsible for acquiring power consumption measurement data and forecasting available power for up- and down-regulations. The pollutant generation calculation module aims to estimate building usage needed for FVR duration calculation. The FVR duration calculation algorithm acquires building usage data and calculates FVR durations based on the data gathered from sensors and building design documentation. The regulation price calculation module is responsible for putting together tendered prices for regulations based on the costs and building IAQ conditions. After calculating everything, the tender is sent to an aggregator of available flexible power, FVR duration, and price for each timestep.

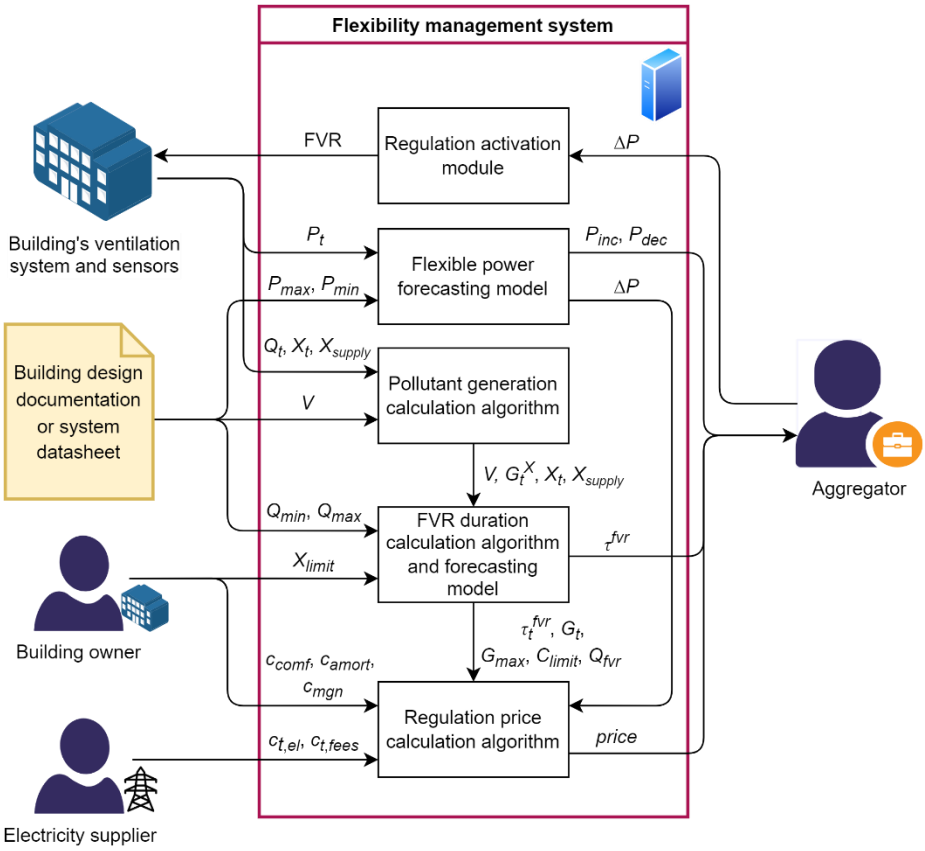

Figure 3.10. Implementation of the flexibility management methods [Paper I].

3.5 Ventilation system as a virtual energy storage

Ventilation systems can be considered a virtual energy storage (VES), which can behave similar to a battery energy storage (BES). Its characteristics and calculation methods must be understood to use a ventilation system as a VES. In this section, the following aspects are discussed:

- Power capacity,
- Energy capacity,
- State of Charge (SoC),
- Self-discharge rate.

3.5.1 Power capacity of virtual energy storage

The power capacity of a ventilation system is defined through its maximum and minimum power consumption, as discussed in section 3.1. The available power capacity depends on the power consumption of a ventilation system at a selected instance (Figure 3.11). The available power capacity for flexible power can be calculated and forecasted using the methods described in section 3.1.

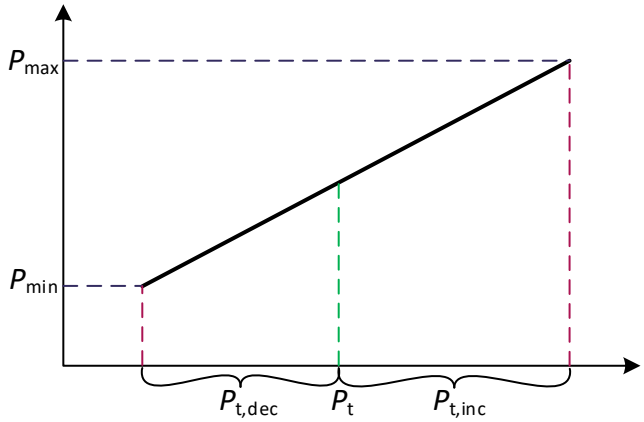

Figure 3.11. Available flexible power of a ventilation system at time t.

3.5.2 Energy capacity of virtual energy storage

A ventilation system differs from a BES by its energy capacity. A ventilation system can exceed its boundary conditions without causing irreversible damage to the system. During charging, the ventilation system consumes more power to increase the percentage of fresh air in the building, lowering the CO_2 concentration. From the IAQ viewpoint, the ventilation system can consume an infinite amount of energy during the charging cycle, but CO_2 concentration cannot decrease beyond the minimum concentration level, as shown in (3.26). The energy to reach the minimum CO_2 concentration level can be calculated with (3.31). During discharging, the power consumption of a ventilation system is reduced, and the air exchange rate is lowered, which causes CO_2 concentration to rise. During the discharging cycle, the ventilation system can operate at a lower power consumption level for a limited time, which is dictated by IAQ conditions in a building. Therefore, the energy capacity for up-regulation is limited, as shown in (3.32). IAQ parameter value at a specific timestep can be calculated according to the forced ventilation rate duration forecast, as shown in (3.27).

$$E_{t,\,inc} = P_{t,inc} \cdot \frac{V \cdot (C_{limit} - C_t)}{G_t^{co2} - Q_{max} \cdot \sqrt[3]{\frac{P_t + P_{t,inc} - P_{bias}}{P_{max} - P_{bias}}} \cdot \frac{C_t + C_{t,min} - 2C_{amb}}{2}} \tag{3.31}$$

$$E_{t,\,dec} = P_{t,dec} \cdot \frac{V \cdot (C_{limit} - C_t)}{G_t^{co2} - Q_{max} \cdot \sqrt[3]{\frac{P_t - P_{t,dec} - P_{bias}}{P_{max} - P_{bias}}} \cdot \frac{C_t + C_{limit} - 2C_{amb}}{2}} \tag{3.32}$$

where V – zone volume (m^3),
C_{limit} – CO_2 concentration limit value (ppm),
C_t – CO_2 concentration value at time *t* (ppm),
C_{supply} – CO_2 concentration value in supply air (ppm),
G_t^{co2} – CO_2 generation rate at time *t* (m^3/s),
Q_{max} – maximum ventilation rate (m^3/s),
P_{bias} – ventilation system power consumption bias (W).

Energy capacity during discharging is non-linearly dependent on the CO_2 concentration (Figure 3.12). Maximum energy capacity is achieved when the CO_2 concentration in the building is at the ambient level. When charging before discharging the VES is planned, it is reasonable not to attempt to lower the CO2 concentration close to the ambient level. The region close to the ambient level does not increase the capacity significantly but increases the self-discharge, as discussed in the following subsections.

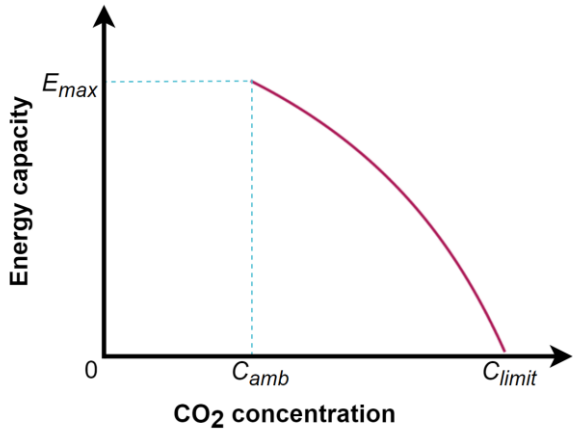

Figure 3.12. Energy capacity dependence on CO_2 concentration in a building.

During regulation, the flexible power can be in the range of current power consumption up or down to the limit. The more the power consumption changes, the more IAQ in a building is affected. Since the energy capacity has a nonlinear dependence on power consumption, there is a possibility to optimize the amount of power to maximize the total energy capacity for one regulation. A regulation duration can be a fixed length, which means that changing the power consumption less than possible will cause the effect where the CO_2 concentration limit is not reached before the regulation is ended. The consequence of this is the unused potential of the ventilation system. Decreasing power consumption to more than the optimal amount causes the situation where the CO_2 concentration limit is reached before the regulation is ended, which also causes lower energy capacity of the VES (Figure 3.13).

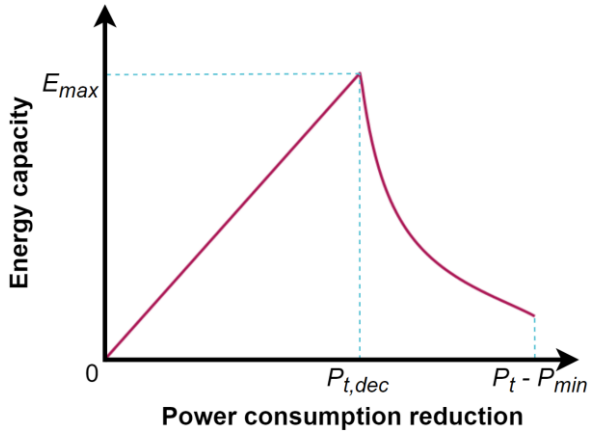

Figure 3.13. Energy capacity dependence on the reduction of power consumption.

If the length of regulation duration is known or estimated ahead, then the power consumption increase or decrease can be calculated as shown in (3.33) and (3.34), respectively. Before the power level can be computed, the CO_2 generation rate must be known. The method to estimate this is given in section 3.2. Power consumption at a specific time is also an important parameter that can be estimated using the method described in section 3.1.

$$P_{t,\,inc} = \left[\frac{\tau_t \cdot G_t^{co2} - V \cdot (C_{limit} - C_t)}{\tau_t \cdot Q_{max} \cdot \frac{C_t + C_{limit} - 2C_{supply}}{2}}\right]^3 \cdot (P_{max} - P_{bias}) - P_t + P_{bias} \qquad (3.33)$$

$$P_{t,\,dec} = \left[\frac{\tau_t \cdot G_t^{co2} - V \cdot (C_{limit} - C_t)}{\tau_t \cdot Q_{max} \cdot \frac{C_t + C_{limit} - 2C_{supply}}{2}}\right]^3 \cdot (P_{bias} - P_{max}) + P_t - P_{bias} \qquad (3.34)$$

where τ_t – regulation duration (s).

3.5.3 Virtual energy storage state of charge

A VES SoC can be described through CO_2 concentration in a building because this parameter is directly connected to building usage and is affected by the people inside. The VES's SoC can fluctuate throughout the day depending on the system type and building usage. When SoC is at 100%, the CO_2 concentration is at a minimum level, which can be calculated through the maximum ventilation rate and the CO_2 generation at the selected timestep, as shown in (3.26). Since the building usage changes throughout the day, the minimum CO_2 concentration also changes accordingly (Figure 3.14). The actual SoC is the CO_2 concentration in a building at each timestep, which can be calculated as shown in (3.27). When SoC is at 0%, the CO_2 concentration has reached its limit. The maximum CO_2 concentration limit does not change, except for a multi-zone ventilation system where the correction of the boundary condition is needed, which is discussed under section 3.3.

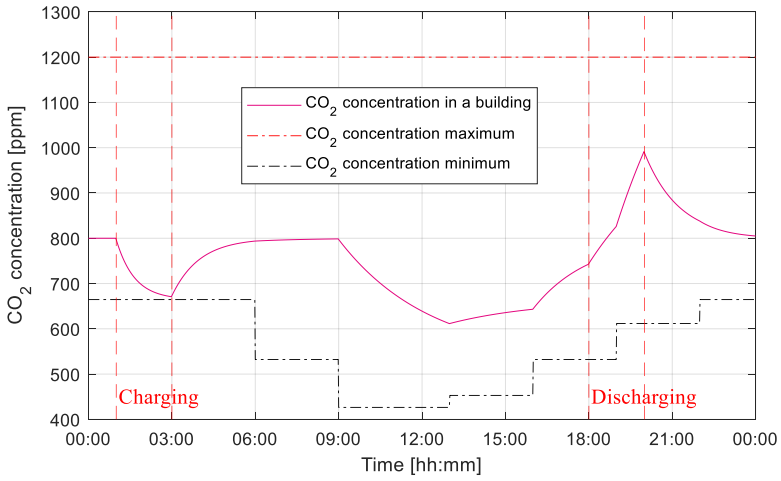

Figure 3.14. CO_2 concentration-based SoC estimation for a ventilation system.

3.5.4 Self-discharge rate of virtual energy storage

CO_2 concentration has always some stable level, which depends on the CO_2 generation and ventilation rates. If the VAV type system is used, the stable condition is around the setpoint C_{set}. This steady-state level causes the effect of self-discharge or self-charge of the VES. Self-discharge occurs when the CO_2 concentration level is lower than the stable level, and self-charge happens when the CO_2 concentration level is higher than the stable level. The self-discharge or self-charge rate can be calculated as follows:

$$k_t^{self} = \left[(P_{t-1} - P_{min}) \cdot \frac{V \cdot (C_{limit} - C_{t-1})}{G_{t-1}^{co2} - Q_{min} \cdot \frac{C_{t-1} + C_{limit} - 2C_{amb}}{2}} - (P_t - P_{min}) \cdot \frac{V \cdot (C_{limit} - C_t)}{G_t^{co2} - Q_{min} \cdot \frac{C_t + C_{limit} - 2C_{amb}}{2}} \right] \cdot \frac{1}{\Delta t} \quad (3.35)$$

where k_t^{self} – the self-discharge or self-charge rate at time t (Ws/s),
P_{min} – ventilation system minimum power consumption (W),
P_{t-1} – ventilation system power consumption at time $t-1$ (W),
C_{t-1} – CO_2 concentration at time $t-1$ (ppm),
Q_{min} – minimum ventilation rate (m^3/s),
Δt – duration between two sequent timesteps (s),
G_{t-1}^{co2} – CO_2 generation rate at time t (m^3/s).

When constant ventilation rate and building usage are considered, the maximum self-discharge rate is near ambient concentration (Figure 3.15). The self-discharge rate is zero when the stable CO_2 concentration level is reached, which can be the CO_2 concentration setpoint for the VAV type of system. The minimum self-discharge rate is present near the limit or maximum CO_2 concentration where the self-discharge is negative, meaning that the VES is charging and CO_2 concentration decreases. The self-discharge rate in the same CO_2 concentration range is lower than the self-charge rate. Therefore, the VES is prone to self-charge better than self-discharge.

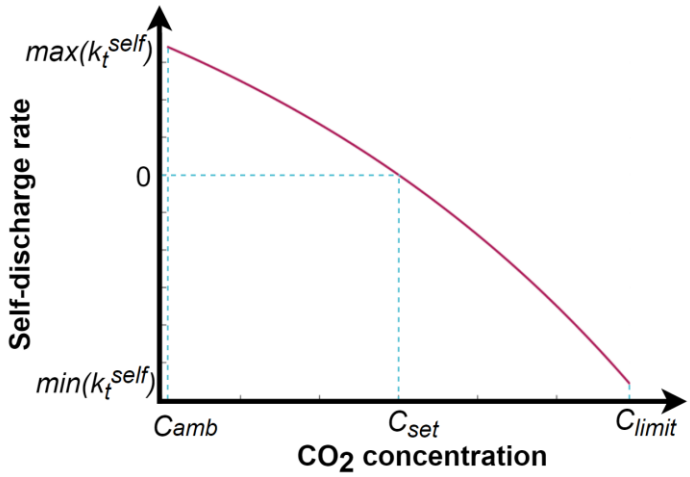

Figure 3.15. Dependence of the self-discharge rate on the CO_2 concentration.

3.6 Conclusions

This chapter described the development of the methods of ventilation system flexibility management. The methods were developed by the definitions of flexibility and the needed input data for an aggregator discussed in Chapter 2. Based on the provided data and estimation, the aggregator can manage each ventilation system or building separately to achieve optimum results.

The ventilation system management methods include flexible power, FVR duration estimation algorithms, and a pricing model. Since there are different types of ventilation systems with specific features, there is no single approach for every system. The following methods are used for the flexibility estimation of a ventilation system:

- Estimations of ventilation system flexible power are based on the measured data, and forecasts for specified horizons are done using the ARMA model.
- CO_2 concentration based FVR duration estimations are based on building usage data. If the CO_2 sensor is present, then through mass balance analysis, CO_2 generation is calculated.
- Temperature-based FVR duration estimations are based on temperature sensor readings, and by using the first law of thermodynamics, a heat generation rate is calculated.
- Humidity-based FVR duration estimations use a similar approach to the CO_2 concentration-based estimation, and estimations rely entirely on sensor data.
- FVR duration adjustment is done by shortening estimations based on the following time steps forecasted durations. It enables the capability to consider the variable usage of a building.
- The price for each regulation is calculated through a personalized pricing mechanism, which the building owner can adjust. The pricing model takes into account the building usage and IAQ conditions.
- A boundary condition correction algorithm is used when there are not enough sensors installed in crucial rooms where regulations affect IAQ the most. The range where the measured parameter can be is narrowed to lessen the regulation effect on the IAQ in high-usage rooms.
- After each reserve activation, the rebound is calculated to stabilize IAQ in a building.

A selection algorithm is described, and guidelines are given to implement the developed flexibility management methods. The flexibility management system to use all the described methods is also brought out to make the implementations as state-forward as possible. Finally, characteristics through which a ventilation system can be described as virtual energy storage are discussed, giving aggregators tools to use ventilation systems as battery energy storage. The assessment and verification of the developed methods will be provided in Chapter 4 and tested in case studies in Chapter 5. The development of the ventilation system flexibility management method showed that the first hypothesis is correct, as mass and energy balance analysis combined with sensor data enables the estimation of forced ventilation rate duration.

4 Validation of the developed flexibility management method

In this chapter, the developed flexibility methods are validated through MATLAB and IDA ICE simulations. First, technical and economic constraints are given as inputs to object models. Technical limitations parameterize inputs for building models in IDA ICE. Economic constraints define the parameters essential for the validation. Object models are described, which are composed in the IDA ICE building simulation tool. Simulations and calculations regarding the flexibility forecast and control are carried out in MATLAB, a programming and numeric computing platform. This chapter also describes control scenarios of a ventilation system to assess the performance of the developed flexibility management method. It includes the results of all the simulations and the evaluation of the effectiveness of the method.

The simulation process can be divided into steps, each conducted in one of the simulation tools (Figure 4.1). Each step can be described as follows:

I. The building model is configured, and the occupancy schedule is generated in MATLAB. All the data between MATLAB and IDA ICE is transferred using PRN files.
II. IDA ICE uses the building model and all the necessary information to run a year-long simulation. Each room and the AHU's measured data are logged into output files.
III. Flexibility management methods are used after importing the IDA ICE output files into MATLAB. It includes measuring and forecasting the energy flexibility of the ventilation system. The day-ahead price, mFRR activations, and the balancing energy price for 2022 are used to schedule activations.
IV. With activations of the reserve, a simulation lasting a year is repeated.
V. Data is collected from IDA ICE, and estimates of previously calculated flexibility are compared with the data acquired in step IV. The dataset is examined in MATLAB, and the conclusions are drawn.

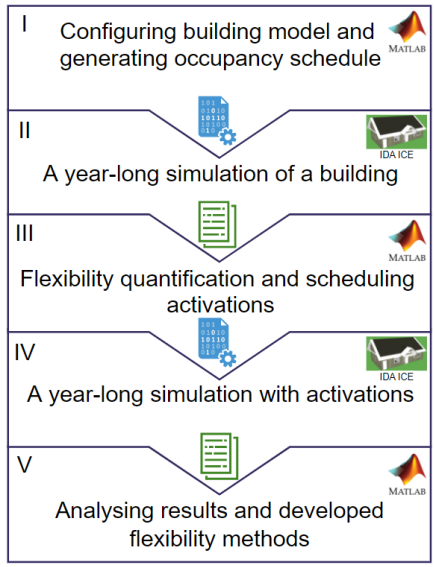

Figure 4.1. MATLAB and IDA ICE co-simulation process [Paper I].

4.1 Technical and economic constraints

This section discusses all the technical and economic constraints that are important to consider when assessing the developed flexibility method. Also, these constraints are essential to set up the object models in IDA ICE.

4.1.1 Determination of ventilation system parameters

For method validation, two main parameters for simulations are needed. These are ventilation rate and power consumption. The ventilation rate can be calculated according to the standard EN 16798-1:2019, which states that design parameters for IAQ shall be derived using one or more of the following methods:

1. Based on perceived air quality
2. By using limit values for substance concentration
3. Based on predefined ventilation air flow rates

The first method calculates the ventilation rate based on perceived air quality. The total ventilation rate is found by combining the ventilation rate for people and a building, as shown in (4.1). These specific ventilation rates are selected according to the building pollution level and IAQ category. For normal conditions, low-polluting buildings and IAQ category II are selected (Table 4.1). The first method is used to prepare models for the validation of the flexibility management method.

$$Q_{tot} = K_{design} \cdot Q_p + A_R \cdot Q_B \tag{4.1}$$

where Q_{tot} – total ventilation rate for the zone (l/s),
K_{design} – design value for the number of persons in a zone,
Q_p – ventilation rate for the number of persons in the zone (l/s),
A_R – zone floor area (m^2),
Q_B – ventilation rate for emissions from the zone (l/[s·m^2]).

Table 4.1. IAQ categories and values for calculating the ventilation rate [127].

Category		I	II	III	IV
Level of expectation		High	Medium	Moderate	Low
Low-polluting building, l/(s·m²)		1.0	0.7	0.4	0.3
Airflow per non-adapted person, l/(s·pers)		10	7	4	2.5
CO_2 concentration above outdoors for non-adapted persons, ppm		550	800	1350	1350
Total design ventilation rate for the zone or room	**l/(s·pers)**	20	14	8	5.5
	l/(s·m²)	2	1.4	0.8	0.55

The second method is using criteria for individual substances. The ventilation rate required to dilute a specific substance can be calculated as shown in (4.2). Typically, CO_2 is used for calculations, the limit values of which can be found in Table 4.1. Default values for ε_v can be found in the standard EN 16798-3. For complete mixing, the ventilation effectiveness equals 1.

$$Q_h = \frac{G_h}{C_{h,i} - C_{h,o}} \cdot \frac{1}{\varepsilon_v} \tag{4.2}$$

where Q_h – the ventilation rate required for dilution (m³/s),
G_h – the generation rate of the substance (µg/s),
$C_{h,i}$ – the guideline value of the substance (µg/m³),
$C_{h,o}$ – the concentration of the substance in the supply air (µg/m³),
ε_v – effectiveness of ventilation.

The third method uses a predefined total designed ventilation rate for the zone or room given in Table 4.1. If the ventilation rate is calculated using per-person and per-floor area approaches, then the highest ventilation rate should be used.

The CO_2 concentration in the return air is used to manage VAV system. Proportional control described in the Trane Engineers newsletter [132] is applied in simulations to control the VAV-type ventilation system. The following procedure is applied to calculate parameters for proportional control:

1. The required ventilation rate for the design zone population is calculated, as shown in (4.1).
2. The minimum ventilation rate is found using (4.1), where the number of persons in a zone is 0, and the rate is calculated only based on the zone floor area.
3. The target CO_2 concentration is found according to the design parameters, as shown in (4.3). This method uses minimum occupancy for the zone to calculate the CO_2 concentration setpoint. Minimum occupancy must be a reasonable non-zero value, which can be acquired from the occupancy schedule discussed in section 4.2. The minimum occupancy value calculates the minimum ventilation rate for the VAV system using equation (4.1). The acquired minimum ventilation rate is used to calculate the design CO_2 concentration for a zone, which can be expressed as follows:

$$C_{design} = C_{amb} + \frac{G_{pers}^{co2} \cdot K_{design}}{Q_{tot}} \tag{4.3}$$

where C_{amb} – ambient CO_2 concentration (ppm),
G_{pers}^{co2} – one person's CO_2 generation rate (m³/(s·pers)),
K_{design} – design value for the number of persons in a zone,
Q_{tot} – total ventilation rate for the zone (l/s).

4. The ventilation rate for the timestep *t* is calculated proportionally based on the CO_2 concentration, and the calculated ventilation rates, which can be expressed as follows:

$$Q_t = \frac{C_t - C_{amb}}{C_{design} - C_{amb}} \cdot \left(Q_{tot} - Q_{tot,min}\right) + Q_{tot,min} \tag{4.4}$$

where C_t – CO_2 concentration at timestep *t* (ppm),
$Q_{tot,min}$ – total minimum ventilation rate for the zone with zero occupancy (l/s).

The standard EN 16798-1:2019:2019 gives guidelines for controlling the ventilation system during unoccupied periods. If the ventilation system is shut off, the minimum air must be delivered to a zone before occupation. This minimum amount is 1 volume of the

zone that must be ventilated within 2 hours. If the ventilation rate is lowered during the unoccupied period, the total airflow for diluting emissions from the building must be at least 0.15 l/(s·m^2) in all rooms. The ventilation rate of 0.15 l/(s·m^2) is also used during regulations when the power consumption of the ventilation system is lowered.

The power consumption of a ventilation system can be calculated through SFP. On average, SFP ranges from 2.0 to 2.7 kW/(m^3/s) [20]. According to Estonian legislation [7], the SFP can be at a maximum of 2.0 kW/(m^3/s) for renovated and new dwellings. In nZEB, the SFP is 1.5 kW/(m^3/s) and even lower [133].

4.1.2 Determination of building usage and internal gains

Building usage and internal gains depend on the building type. Building usage is defined by the number of occupants, which can be calculated using values given by the standard EN 16798-1:2019 (Table 4.2). Building internal gains are heat sources that emit additional heat into a room. These internal gains are caused by occupants who dissipate body heat, lighting, and appliances. All the power consumed by the lighting and appliances is assumed to be converted into heat.

IAQ parameter setpoint can differ for every building or room. Minimum and maximum temperature setpoint values for heating and cooling are used in simulations. These values are given in the standard EN 16798-1:2019. The CO_2 setpoint is selected according to the maximum allowable CO_2 concentration setpoint value. IAQ parameters' limit values are discussed in section 3.2.

Table 4.2. Building parameters for simulations [127].

Building type	Office	Dwelling
Occupants, pers/m^2	0.0588	0.0353
Activity level, MET	1.2	1.2
Lights, W/m^2	10	8
Appliances, W/m^2	12	3
Minimum heating setpoint, °C	21	21
Maximum cooling setpoint, °C	25	27

4.1.3 Determination of economic constraints for the flexibility service

Four main parameters dictate activations in the flexibility service:

- **Available flexible power** – ventilation system is used in regulations only when it provides enough power to be altered. Suppose that there is a need to lower the power consumption and the ventilation system is already operating close to its minimum rate. In that case, this ventilation system will be ignored in regulations. A regulation is rejected in simulations if the available flexible power is less than half the maximum power consumption.
- **Regulation duration** – a ventilation system can operate at FVR for a given time until the IAQ parameter boundary condition is reached. If the allowed duration is already short, selecting a given ventilation system for regulations is not reasonable. It will be ignored until a longer duration is allowed. According to Baltic TSOs [81] the minimum duration of the delivery period is 5 min, which is used in simulations.
- **Regulation price** – each ventilation system operator or owner dictates its regulation price, which can be calculated as discussed in section 3.4.2. If the requested price for regulation is higher than the aggregator is willing to pay, then the given

ventilation system is ignored in regulations. The year 2022 balancing energy price is used to calculate the revenue generated for activations. The tendered price is paid to the ventilation system owner, and the difference between the balancing energy price and the tendered price is split between the system owner and the aggregator. Nord Pool Spot day-ahead prices for Estonia are used to calculate the cost of consumed energy during normal conditions, for which a 20% value-added tax (VAT) is added. Additional charges, such as a fixed tariff grid fee of 86.5 €/MWh, a renewable energy fee of 13.56 €/MWh, and an electricity excise duty of 1.2 €/MWh were added to the day-ahead prices. The energy that was not used was multiplied by the entire cost of power during up-regulation and deducted from the total energy cost used during the simulated period.

- **Activation** – marks the event when the reserve is activated (i.e., ventilation system power consumption is altered). The year 2022 mFRR standard product activations are used in simulations where the available flexible power, regulation duration, and price are checked.

4.2 Description of object models

Two object models are used in simulations to verify the performance of the developed method. The first object is a room in a building, which can be an apartment or an office. The second object is a single-family house. In this section, these two objects are described with building usage profiles used in simulations. Also, the air handling unit (AHU) for these two objects is described. These models are constructed in IDA Indoor Climate and Energy (IDA ICE), a specialized application to imitate building behavior. IDA ICE has been validated according to EN 15255:2007, EN 15265:2007, EN 13791, and ASHRAE 140-2004. EQUA AB website [134] provides reports about the test results of these validations.

4.2.1 Object 1: Small room in a building

The first object is a room that is part of a single-story building (Figure 4.2). This room has an independent ventilation system that was used in simulations. The room's floor area is 13.84 m^2, and the height is 2.7 m. The building with the room is located in Tallinn, Estonia, so weather data for Estonia is used. This room has three internal walls with a thickness of 0.1 m and one external with a thickness of 0.405 m. The floor is lifted 1 m above the ground, with a thickness of 0.293 m. The thickness of the ceiling, which is also a roof, is 0.713 m. The building has light-frame construction with thermal insulation in between wall panels. During winter, the temperature in the room is held with a wall-mounted radiator.

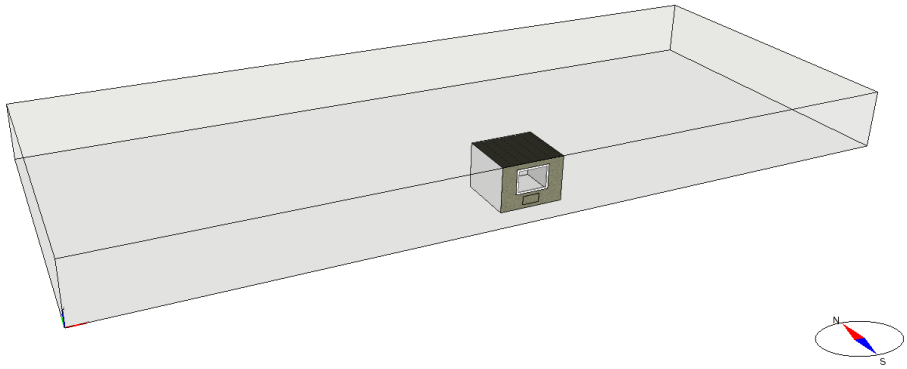

Figure 4.2. The room of a building used in simulations [Paper II].

This room can be an office or an apartment. The room type is changed through changes in occupancy, ventilation system operation schedule, and building-specific parameters discussed in the previous section. The occupancy schedule depends on the weekday and time. According to the standard EN 16798-1:2019, offices are not used during weekends and nighttime, which means that building usage at that time equals 0 (Table 4.3). Apartments have the highest usage during the night and the lowest during the daytime. All the presented data will be used in simulations, and schedules will be selected according to the building type.

Table 4.3. Occupancy schedule according to a room type.

Start time	End time	Office	Apartment
00:00	06:00	0	1
06:00	07:00	0	0.5
07:00	08:00	0.2	0.5
08:00	09:00	0.6	0.5
09:00	10:00	0.6	0.1
10:00	11:00	0.7	0.1
12:00	13:00	0.4	0.1
13:00	14:00	0.6	0.2
14:00	15:00	0.7	0.2
16:00	17:00	0.6	0.5
17:00	18:00	0.2	0.5
18:00	19:00	0	0.5
19:00	22:00	0	0.8
22:00	00:00	0	1

The room AHU power consumption is dependent on the room type. Office's AHU maximum power consumption is around 18% more than for an apartment due to higher occupancy (Table 4.4). Both room types have the same minimum ventilation rate since during up-regulation, a ventilation rate of 0.15 l/(s·m^2) is held.

Table 4.4. Parameters of the room ventilation system for simulations.

Parameter	Office	Apartment
AHU maximum power consumption	25.4 W	21.6 W
AHU minimum power consumption	0.9 W	0.9 W
Maximum ventilation rate	15.3 l/s	13.0 l/s
Minimum ventilation rate	2.0 l/s	2.0 l/s

4.2.2 Object 2: Single-family house

The second object is a single-family, single-story house (Figure 4.3). The house is divided into eleven rooms: utility room, bathroom, technical room, kitchen, main bedroom, living room, hall, vestibule, toilet, office, and bedroom (Figure 4.4). The total floor area of the building is 100.2 m^2, and the room height is 2.7 m. The building is located in Tallinn, Estonia, so weather data for Estonia is used. The internal walls of the building have a thickness of 0.126 m, and external walls - 0.366 m. The floor is placed at ground level with a thickness of 0.347 m. The ceiling thickness is 0.413 m, with an attic above. The building has light-frame construction with thermal insulation in between wall panels. During winter, room temperature is held with central heating using wall-mounted radiators with a total heating power of 9.65 kW. The building has a central AHU responsible for exchanging air from the room and outdoors but also provides cooling when needed. AHU has integrated a 2 kW electrical air heater to warm the supply air with a heating setpoint of 18 °C. This air heater is only used when the heat recovery is insufficient.

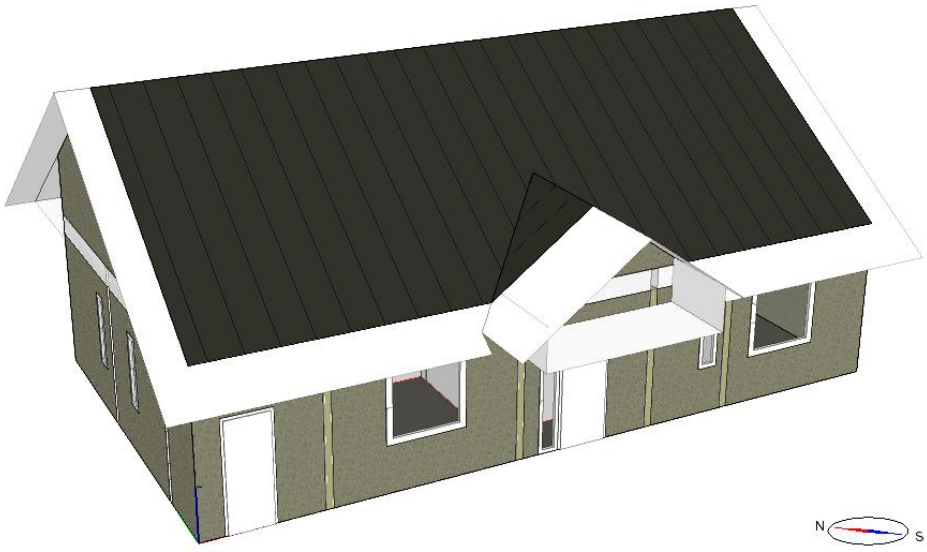

Figure 4.3. The single-family house used in simulations.

Figure 4.4. Floor plan of the single-family house [Paper I].

The building model is based on a small single-family home that serves as a model for redefining the cost-optimality threshold for new nearly zero-energy dwellings in Estonia [135]. The relevant documentation is provided, and the model has been validated in a related project [136]–[140]. According to statistics [141], a single-floor level building with a total floor size of 100 m^2 can be considered a typical single-family dwelling in Estonia. The study in [142] discusses the application of a neural network to construct a thermal model of the same building and includes a more comprehensive description of this model.

The building is used by a three-person family with two adults and one child. An occupancy simulation tool [143] generated a building occupancy schedule for each room (Figure 4.5). As a result, bedrooms have the highest usage at night and the lowest during the day when there are few or no residents at home. The rest of the rooms have a volatile usage profile dependent on the residents' daytime activities. The technical room, utility room, and vestibule are expected to have very low usage if used only for short durations. It is the reason why they are not included in the occupancy schedule. The occupancy simulation tool was used twice to generate profiles for the toilet and office using second-run bathroom and living room profiles. As a result, the building can accommodate a maximum of five people, which can be reasonable when guests are considered. The metabolic equivalent of task (MET) of 1.2 was chosen for the building object.

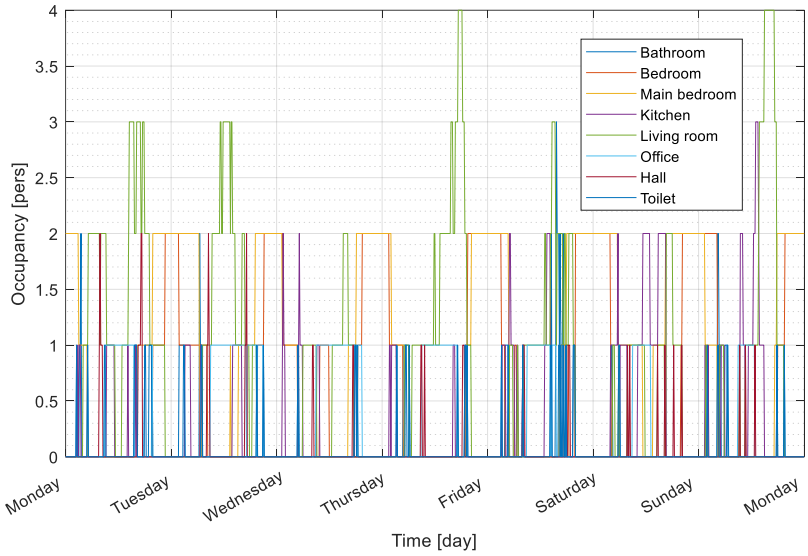

Figure 4.5. Room-specific occupancy schedule.

4.2.3 Air handling unit

An energy recovery type of a ventilation system was used for simulations. Estonian legislation [136] requires that this ventilation system must be used in low-energy buildings and nZEB. This requirement is not mandatory if one of the following statements is true:

1) The heat source is the extract air heat pump.
2) There is no constructional possibility to install an energy recovery ventilation system.
3) The extracted air contains pollutants that must not be introduced into the heat recovery.
4) The planned operating time of the AHU is less than four hours a day.
5) During significant reconstruction, installing ventilation ducts in the building is not technically possible.
6) A different ventilation system ensures the required energy efficiency of the building, IAQ, and thermal comfort.

None of these statements are true for objects used in the simulations. This means that the AHU has heat recovery and air ducts for supplying fresh air and extracting polluted air from the building (Figure 4.6). In total, two fans are used for air exchange. The supply air is also heated or cooled depending on the ambient conditions. The supply air temperature setpoint is defined to be 18 °C. In total, six sensors are placed into air ducts. The flexibility method developed in the previous chapter requires CO_2 concentration, humidity, and temperature data in the extracted air to estimate the FVR duration. Temperature and humidity are measured in the supply air, which is also needed for FVR duration estimations. An airflow rate sensor is required to measure the ventilation rate; this can be done indirectly using fan laws, but direct measurements are taken in simulations.

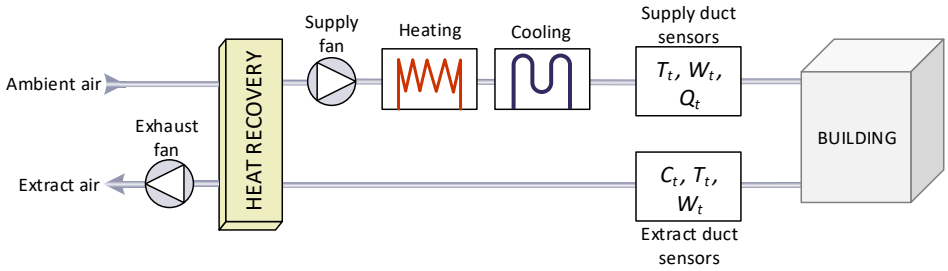

Figure 4.6. System layout of the air handling unit [Paper I].

As described in subsection 4.1.1, an AHU can be shut off during unoccupied hours. Office and educational buildings are not used 24 hours a day and seven days a week; an AHU is not always operational. In simulations, office building ventilation works from 06:00 to 18:00 and in educational buildings, from 07:00 to 16:00 (Table 4.5). This operation schedule is defined by an occupancy schedule where one-hour ventilation is used before the building is occupied. The AHU is off on weekends when the building is not used. An AHU in dwellings is constantly operational since dwellings can always be occupied.

Table 4.5. Operation schedule of the air handling unit during workdays.

Start time	End time	Office	Apartment	Dwelling
00:00	06:00	0	1	1
06:00	07:00	1	1	1
07:00	16:00	1	1	1
16:00	18:00	1	1	1
18:00	00:00	0	1	1

4.2.4 Description of simulation scenarios

Simulation scenarios are created to validate the methods of the developed ventilation system flexibility management. The object 1 model can have two use cases: office or apartment (Table 4.6). There may be no sensors in the room, only one to measure CO_2 concentration, or all three relevant IAQ parameters (CO_2 concentration, temperature, and relative humidity) may be monitored. The different sensor configurations are used to compare open-loop estimations with those based on measurements. The ventilation system airflow rate is always constant when turned on. Object 2 has one use case and will be used as a dwelling. The ventilation system can have two operation types: CAV or VAV. CO_2 concentration-based proportional control is applied for the VAV type system. Also, different feedback configurations are used where there can be one IAQ sensor in the return air duct and three IAQ sensors in every room. Under three IAQ sensors, three different IAQ parameters are measured: CO_2 concentration, temperature, and relative humidity.

Simulations are conducted on one-year data. Activations are generated according to 2022 mFRR service activation and balancing electricity price data. The simulation is run twice. The first iteration generates the baseline, and the second iteration generates data to validate the accuracy and performance of the developed flexibility management method. A ventilation system operates at its minimum or maximum rate during regulation, depending on the regulation direction.

Table 4.6. Scenarios for ventilation system flexible control.

Scenario no	Object 1		Object 2	
	Room type	IAQ sensors in the room	System type	Sensors' location
1	Office	None	CAV	IAQ sensors in the return air
2	Office	CO_2 sensor	CAV	IAQ sensors in every room
3	Office	All three	VAV	IAQ sensors in the return air
4	Apartment	None	VAV	IAQ sensors in every room
5	Apartment	CO_2 sensor		
6	Apartment	All three		

4.3 Analysis of simulation results

Two different objects are considered, and six scenarios for simulation are implemented. Simulation results show the accuracy of each method, described through the root mean square error (RMSE) and mean absolute percentage error (MAPE).

4.3.1 Object 1: Small room in a building

A ventilation system operates during occupied hours in offices, enabling down-regulations when needed. However, the number of down-regulations activated with sensor feedback is relatively low, with only four during a year-long simulation period (Table 4.7). The open-loop approach expects higher than reality CO_2 concentration; therefore, there are fewer up-regulations and more down-regulations than in scenarios with sensor feedback. Only using CO_2 concentration sensors in estimations will result in around 35% of cases where the temperature limit will be exceeded. Measuring all three IAQ parameters is the best approach where the temperature limit was reached in 4% of cases. However, it caused a reduction in the number of total up-regulations due to temperature boundaries. In around 34% of cases, three IAQ parameter limit conditions were reached during a maximum hour-long regulation.

Table 4.7. Simulation parameters for office.

Parameter	No sensors	CO_2 sensor	All three sensors
Total number of up-regulations	297	301	152
Total number of down-regulation	106	4	4
Number of up-regulations where CO_2 concentration limit was reached	47	90	46
Number of up-regulations where temperature limit was reached	104	105	6
Number of up-regulations where relative humidity limit was reached	0	0	0
Number of up-regulations where at least one of three IAQ parameter limits was reached	132	150	51

A typical ventilation system operates throughout the day in apartment buildings, providing no down-regulations. It enables using an apartment ventilation system at least twice more for up-regulations than for offices (Table 4.8). The open-loop approach again expects higher than reality CO_2 concentration; therefore, there are fewer up-regulations compared to scenarios with CO_2 sensor feedback. Only using CO_2 concentration sensors in estimations will result in around 33% of cases where the temperature limit will be exceeded. Measuring all three IAQ parameters is the best approach, where the temperature limit was reached in around 14% of cases. However, it caused a reduction in the number of total up-regulations due to temperature limits. The relative humidity did not influence the regulations for either the office or the apartment. In around 20% of cases, three IAQ parameter limit conditions were reached during a maximum hour-long regulation.

Table 4.8. Simulation parameters for an apartment.

Parameter	**No sensors**	**CO_2 sensor**	**All three sensors**
Total number of up-regulations	628	635	503
Total number of down-regulation	0	0	0
Number of up-regulations where CO_2 concentration limit was reached	38	40	31
Number of up-regulations where temperature limit was reached	211	208	71
Number of up-regulations where relative humidity limit was reached	0	0	0
Number of up-regulations where at least one of three IAQ parameter limits was reached	235	238	101

4.3.1.1 Power consumption forecast

Power consumption is forecasted using the ARMA(0, 5) model for the office and the ARMA(0, 4) model for the apartment. ARMA model terms are calculated by using the AIC method. The forecast horizon is selected to be 24 hours. Previous week's measurement data forecast the next day's power consumption. Power consumption measurements and the forecast are divided into 5-minute timeslots to have a fast response between ventilation system startups and shutdowns, where the same slot data of the previous week is used to forecast power consumption in the following 24 hours. The 24th-hour forecast with the highest uncertainty is compared with the measured data to calculate the accuracy of the forecast model. One year RMSE is around 0.35 W for the office and 0.17 W for the apartment. The mean absolute percentage error (MAPE) is about 1.2% for the office and approximately 0.6% for the apartment. Figure 4.16 is an example of measured and forecasted power consumption during the first week of November 2022, where regulations can also be seen. There are noticeable differences in the number of regulations in each room type, where the apartment provides more flexibility than the office.

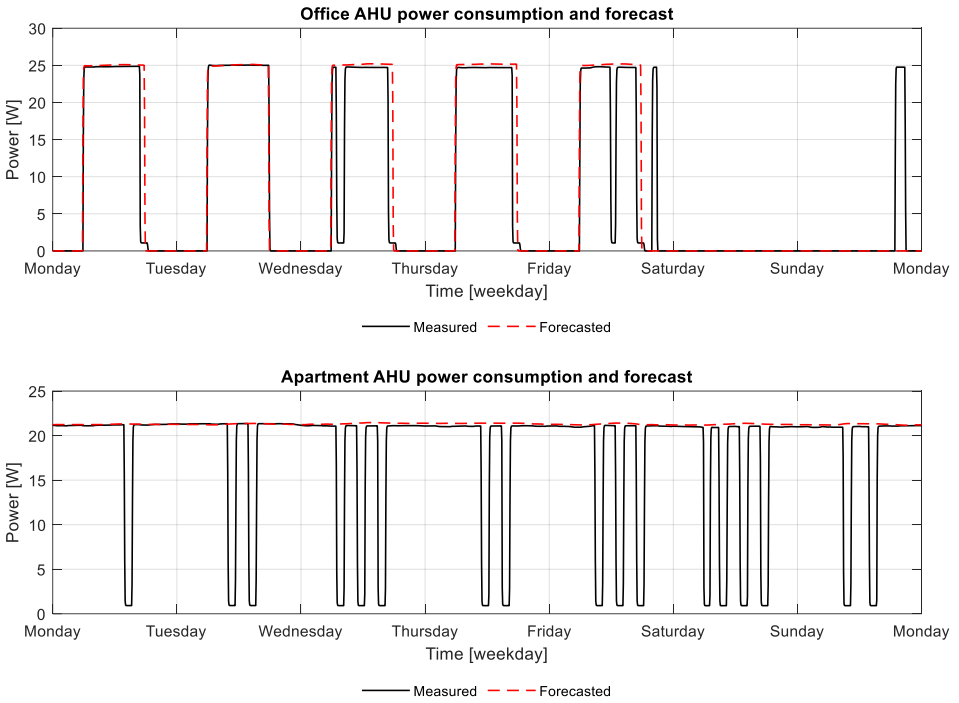

Figure 4.7. Power consumption of office and apartment AHU with regulations.

4.3.1.2 FVR duration estimation

Simulation results show that the temperature has the highest impact on the flexibility for object 1, a small room in a building. It can be seen in Figure 4.8, where an example of one-week FVR duration estimations is shown for the first week of November. The system FVR duration is dictated by CO_2 concentration and temperature. The parameter with short FVR dictates the whole system duration. FVR duration estimations are done for both room types. In the office, the FVR duration is longer during outside working hours since no occupants are in the room. In the apartment, this effect is less noticeable. These results show that depending on the system configuration and if a ventilation system is used to cool a space, the temperature can be more important than CO_2 concentration to estimate ventilation system flexibility. The FVR duration estimations are limited to 60 min as it is the most prolonged delivery period for simulation.

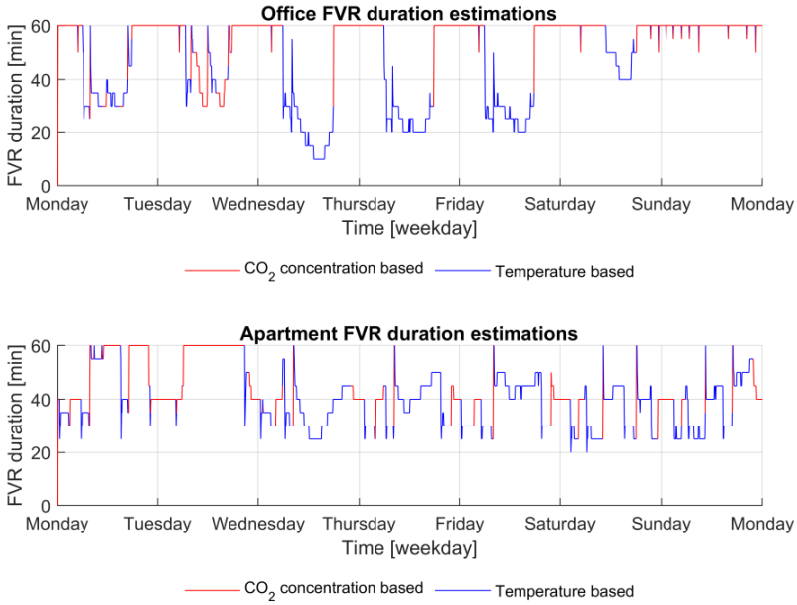

Figure 4.8. FVR duration estimations for office and apartment ventilation systems.

FVR duration estimation residuals for the open-loop approach with no sensors are biased (Figure 4.9) since estimated durations are shorter than the ventilation system can provide. The drawback of this approach is that the actual indoor environment conditions are not known, and it can estimate higher CO_2 concentration levels than in reality. CO_2 concentration based FVR duration estimation residuals are on the positive side for both room types, which is the consequence of using the FVR duration adjustment method. The adjustment method will shorten the estimations based on the consecutive time steps, giving more conservative results. It is good from the occupants' standpoint as an IAQ parameter limit is less likely to be exceeded during a regulation. The temperature has some restrictive effect when all three IAQ sensors are used, which has a negligible effect on CO_2 concentration-based FVR duration estimations. Temperature-based FVR duration estimation residuals are positive, meaning that the temperature boundary is less likely to be exceeded during regulations by implementing the developed method.

The highest inaccuracy in FVR duration estimations was observed with the open-loop approach, where no IAQ sensors are used (Table 4.9). CO_2 concentration-based FVR duration estimations are more accurate for the office than the apartment, which is the effect of the consecutive regulations and different room usage. It can be expected that in actual application, the methods can have even better performance since changes in the IAQ can be included in the estimations. Temperature-based FVR duration estimations show lower accuracy than CO_2 concentration-based estimations since temperature is highly dependent on outdoor conditions. However, the method gives more conservative estimations to avoid exceeding temperature limits during regulations. IAQ parameter limit exceeded for negligible cases when the reserve was activated. It means that during these cases, the FVR duration was estimated to be longer than the ventilation system could provide, causing the IAQ parameter limit to be exceeded during activation. In the office, the CO_2 concentration limit was exceeded for more cases than for the apartment, which is caused by the effect where the reserves were mainly activated during working hours when the office had high occupancy.

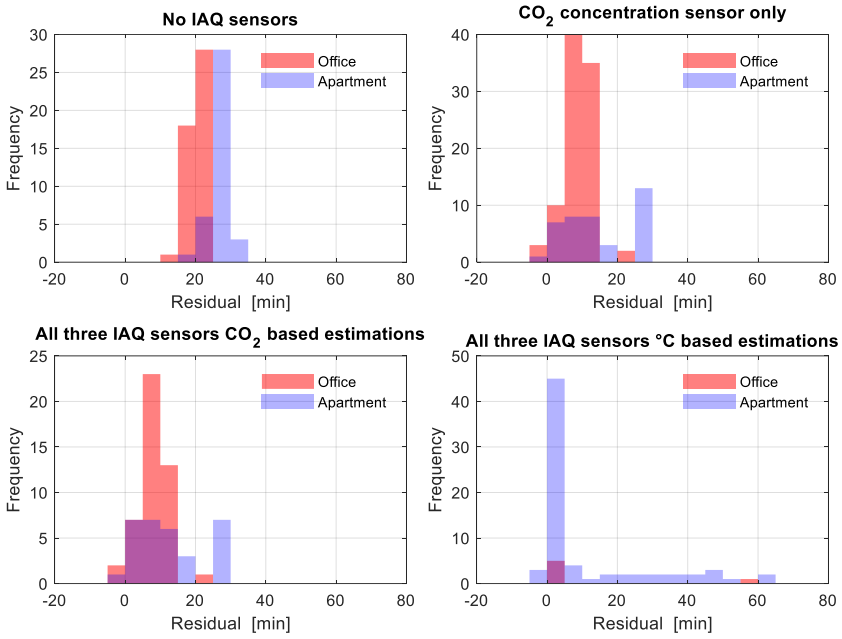

Figure 4.9. Residuals of the FVR duration estimations for object 1.

Table 4.9. Performance of FVR duration estimation methods with object 1.

IAQ sensors in the room		None	CO_2 sensor	All three	
Parameter		CO_2 concentration	CO_2 concentration	CO_2 concentration	Temperature
Office	**RMSE**	18.1 min	7.7 min	7.1 min	22.4 min
	MAPE	38.2%	11.1%	10%	14.1%
	IAQ limit exceeded	0%	1.2%	1.4%	0%
Apartment	**RMSE**	24.5 min	15.7 min	13.7 min	19.1 min
	MAPE	35.8%	15.9%	13.7%	27.1%
	IAQ limit exceeded	0%	0.2%	0.2%	0.6%

4.3.1.3 The ventilation system as a virtual energy storage

Methods to consider a ventilation system as a virtual energy storage (VES) are discussed in section 3.5. These methods were applied to object 1 to analyze the performance of the method and compare to the approach which considers the ventilation system as a typical load that operates at minimum or maximum power consumption level during activation. Unlike conventional energy storage systems, the VES can have SoC higher than 1 (Figure 4.10). It is caused by volatile building usage, where the CO_2 concentration can be at the ambient level during unoccupied hours, causing the SoC to be higher than 1. The SoC for the VES can also be lower than 0, which can occur when the CO_2 concentration boundary is exceeded. SoC below 0 is not the recommended state, but compared to conventional battery energy storage, it does not damage the system. The SoC of the VES is heavily dependent on room usage and fluctuates accordingly. During the weekend, the office is unoccupied, causing the SoC to stabilize around 1 since there is some air

exchange even when the ventilation system is shut down. The selected system is CAV type, where the ventilation rate is at the maximum level. Therefore, SoC is permanently stabilizing around 1.

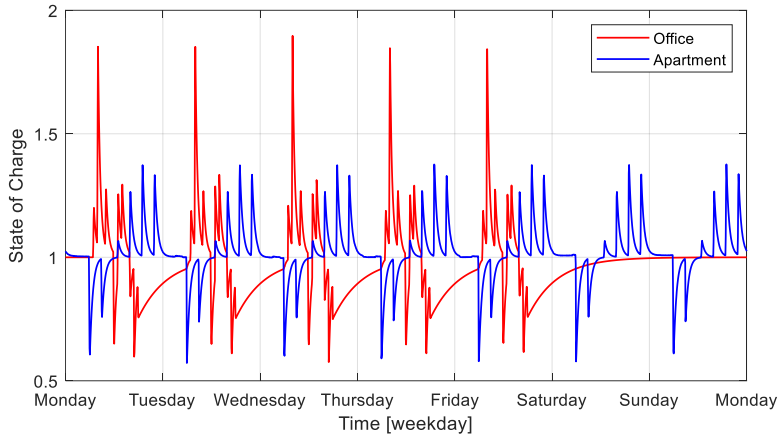

Figure 4.10. Example of a VES state of charge during a week [Paper II].

ARMA(0, 5) model was used to forecast ventilation system power consumption for the office, and ARMA(0, 4) model was used for forecasting in the apartment. The forecasting MAPE is around 1.2% for the office and about 0.6% for the apartment. The forecasting RMSE is approximately 0.4 W for the office and around 0.2 W for the apartment. Down-regulations are only possible for the office (Figure 4.11), where the ventilation system is scheduled to shut down during unoccupied hours. During maximum occupancy hours, there is a slight decrease in the available discharge power caused by the method to provide a higher than minimum ventilation rate to support a 60-minute regulation duration. The apartment can only provide discharge power since the ventilation system is designed to work at its maximum level throughout the day (Figure 4.12). For the apartment, the reduction in available discharge power occurs during night hours when the room usage is the highest.

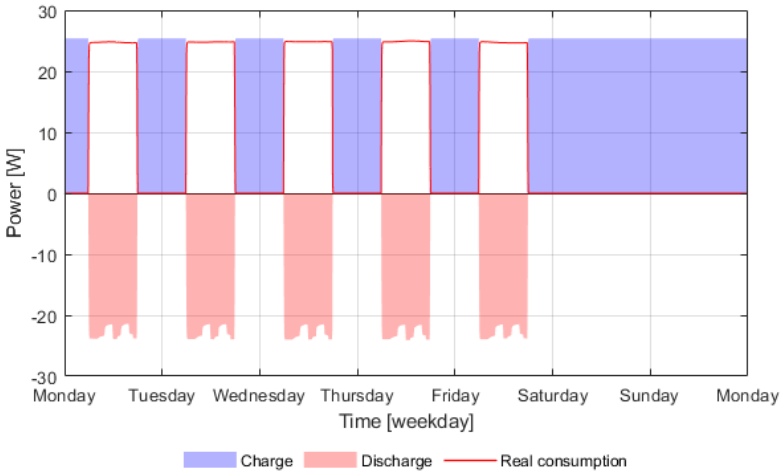

Figure 4.11. Example of VES power consumption, charge, and discharge power of the office during a week [Paper II].

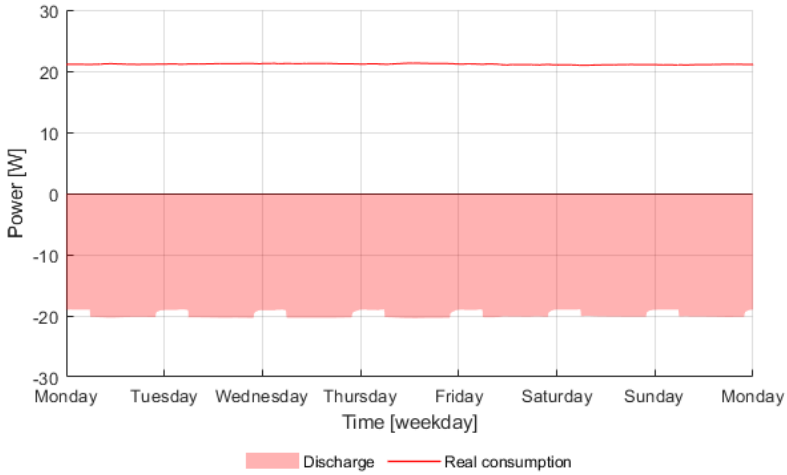

Figure 4.12. Example of VES power consumption and discharge power of the apartment during a week [Paper II].

Residuals of energy capacity estimations are only calculated for regulations where the CO_2 concentration reached its limit, which is less than the total number of regulations conducted during the simulation. Only residuals for up-regulation could be calculated (Figure 4.13) since the minimum CO_2 concentration was not achieved during down-regulations. The energy capacity estimation MAPE is around 15.7% for the office and about 8.3% for the apartment. The energy capacity RMSE is approximately 4.6 Wh for the office and 2.2 Wh for the apartment. For the office, more over-optimistic estimations can be caused by consecutive regulations where the CO_2 concentration cannot recover. There is a problem with thet kind of simulation where estimations cannot be adjusted when the subsequent regulation is activated. Therefore, it can be expected that the accuracy of the VES energy capacity estimation method can be improved with real applications.

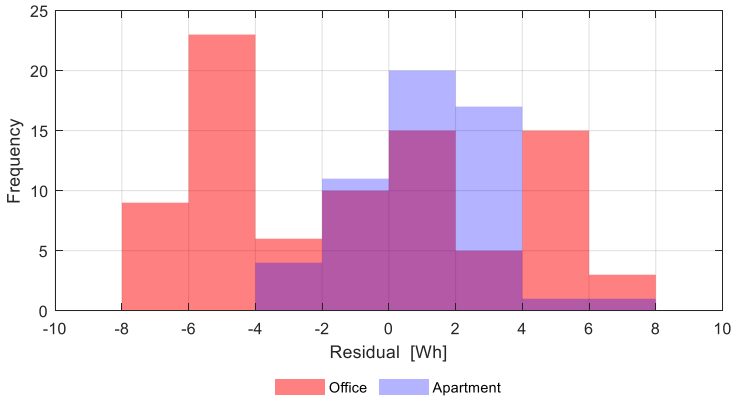

Figure 4.13. Residuals of VES energy capacity estimations for up-regulations [Paper II].

4.3.1.4 Flexibility service activations and pricing

Each hour's price for the flexibility service is calculated based on the CO_2 concentration measurements and costs. For example, upward regulations for the first week of November 2022 are shown in Figure 4.14. The tendered price was calculated using equation (3.24), where comfort cost was derived from the last two weeks' maximum balancing energy price. The reserve was only activated if the tendered price was lower than the balance energy market price. There was mFRR activation and the available capacity for the regulation was more than 10 W. More activations occurred for the apartment than for the office because an apartment ventilation system is running throughout a day. In the office, the ventilation system is shut down during weekend and night hours, which restricts availability for up-regulations, and the tendered price for up-regulations will also drop to 0. A separate figure for down-regulations is not shown since these were rare for the selected object.

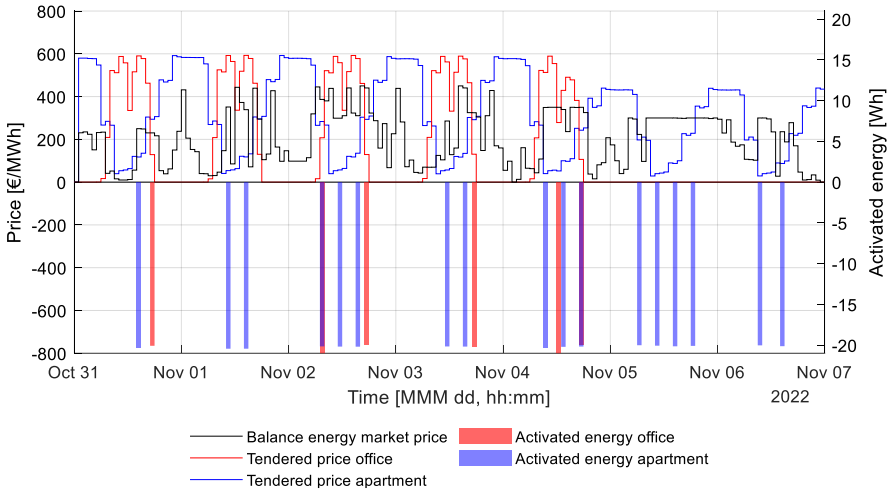

Figure 4.14. Example of flexibility service prices and activation during a week for up-regulations.

Before the financial impact of the regulations can be analyzed, the baseline must be found. It is achieved by measuring ventilation system energy consumption throughout the year without regulations for each room type. In the apartment, the ventilation system's total energy consumption and cost for consumed energy are over two times higher than for the office (Table 4.10).

Table 4.10. Baseline values of energy consumption and cost of energy.

Parameter	Office	Apartment
Energy consumption without regulations	77.8 kWh	186.5 kWh
The total cost of energy without regulations	29.82 €	62.16 €

With the open-loop approach, the energy consumption for the office does not have a significant difference from the baseline (Table 4.11). The reason is a high number of down-regulations as compared to the sensor-based approach. Nevertheless, with the open-loop approach, the total energy cost for a year was reduced by 9.7% for the office and 14.6% for the apartment. With sensors, the total energy consumption was decreased even more since more potential of the ventilation system could be exploited for the

flexibility service. In the office, adding sensors reduced the total energy cost by 1.1% from the baseline. The total energy cost in the apartment was increased by 1% by adding all three IAQ sensors. It is caused by the reduction in the total number of up-regulations due to temperature restrictions. The ventilation system as a VES approach showed the best results in the energy consumption and cost savings' viewpoint. Total energy consumption was reduced by 9.4% for the office and 8.9% for the apartment compared to the baseline. Total energy cost was reduced by 27.3% for the office and 28.9% for the apartment compared to the baseline. The VES approach gave better results since the energy capacity of the ventilation system for regulation is maximized.

Table 4.11. Regulation effect on the energy consumption and cost of energy.

Room type	Scenario	Energy consumption	The total cost of energy
Office	No sensors	77.2 kWh	26.92 €
	CO_2 sensor	74.8 kWh	26.64 €
	All three sensors	74.8 kWh	26.64 €
	As a VES	70.5 kWh	21.67 €
Apartment	No sensors	174.2 kWh	53.06 €
	CO_2 sensor	173.7 kWh	53.04 €
	All three sensors	173.7 kWh	53.69 €
	As a VES	169.9 kWh	44.17 €

4.3.2 Object 2: Single-family house

In the single-family house, the ventilation system runs continuously under normal conditions. It creates the possibility of exploiting the system more for up-regulations than for down-regulations. In total, 374 up-regulations for the CAV type system were conducted; the same value for the VAV type was 257 (Table 4.7). There were zero down-regulations since the capacity for this was insufficient, and the price for regulation was not suitable. The most restrictive IAQ parameter was CO_2 concentration, whose boundary condition reached 82% of cases for the CAV type system and 83% for the VAV type system. In comparison, the temperature limit reached 38% and 31% of cases for the CAV and VAV type system, respectively. Relative humidity had no restrictive effect on regulations with the applied simulation setup.

The same ventilation system is used for CAV and VAV systems with the same maximum and minimum power consumption. It also applies to the ventilation rate. The only difference is in the way the ventilation rate is controlled. The ventilation rate under normal conditions is close to the maximum for the CAV type system. However, for the VAV type system, the ventilation rate depends on the CO_2 concentration in the return air. CO_2 concentration causes a proportional increase in the ventilation rate.

With a maximum of one-hour regulation length, the limit for at least one IAQ parameter was reached for around 78% of cases for the CAV type system and 79% for the VAV. The majority of FVR durations were within 10 minutes. At least 30 minutes of maximum power reduction during up-regulation was provided for 35% of cases for the CAV type system and 37% for the VAV type system. The FVR duration is heavily dependent on the system configuration and building usage. Rooms with higher usage dictate an overall flexibility, and it is reasonable to provide more fresh air to these rooms to increase the FVR duration for the whole system. In dwellings, critical rooms are bedrooms and living rooms.

Table 4.12. Simulation parameters and counts.

Parameter	System type	
	CAV	VAV
Total number of up-regulations	374	257
Total number of down-regulation	0	0
Number of up-regulations where CO_2 concentration limit was reached	280	195
Number of up-regulations where temperature limit was reached	70	45
Number of up-regulations where relative humidity limit was reached	0	0
Number of up-regulations where at least one of three IAQ parameter limits was reached	293	204
AHU maximum power consumption	134 W	134 W
AHU minimum power consumption	6 W	6 W
Maximum ventilation rate	89.9 l/s	89.9 l/s
Minimum ventilation rate	14.4 l/s	14.4 l/s

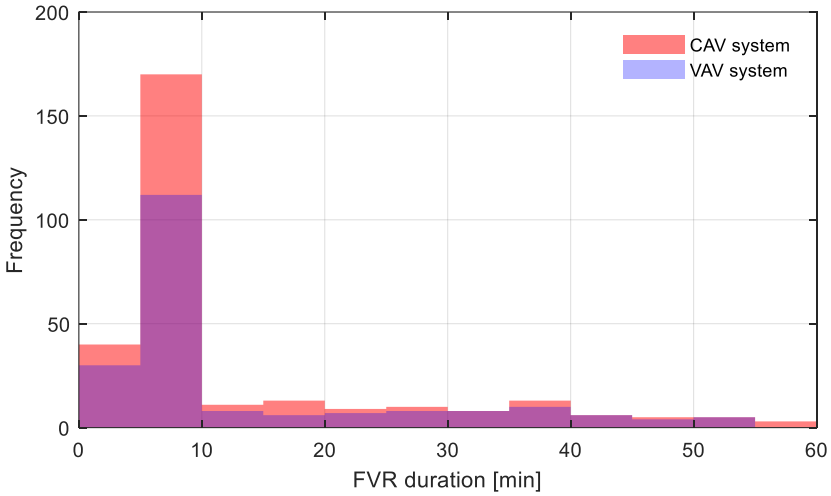

Figure 4.15. Distribution of FVR durations where an IAQ parameter limit was reached.

4.3.2.1 Power consumption forecast

The ARMA(0, 5) model was used to forecast power consumption for both system types. The AIC approach was used to calculate the terms of the ARMA model. 24 hours were chosen as the forecast horizon. The power consumption for the following day was forecasted using measurement data from previous days. For the quick reaction between the ventilation system starting and shutdown, one day was divided into 5-minute timeslots. The forecasts were done for each timeslot separately. The accuracy of the method was determined through the 24th-hour forecast with the most significant uncertainty compared with the observed data. For the CAV and VAV, the RMSE of the annual power consumption forecasts was roughly 1.3 W and 10 W, respectively. For the CAV and VAV, respectively, the MAPE was roughly 0.8% and 6.5%. The inclusion of

stochastic occupancy data hampered the accuracy of the VAV system power consumption forecasts. An illustration of measured and forecasted power consumption for the first week of November is shown in Figure 4.16.

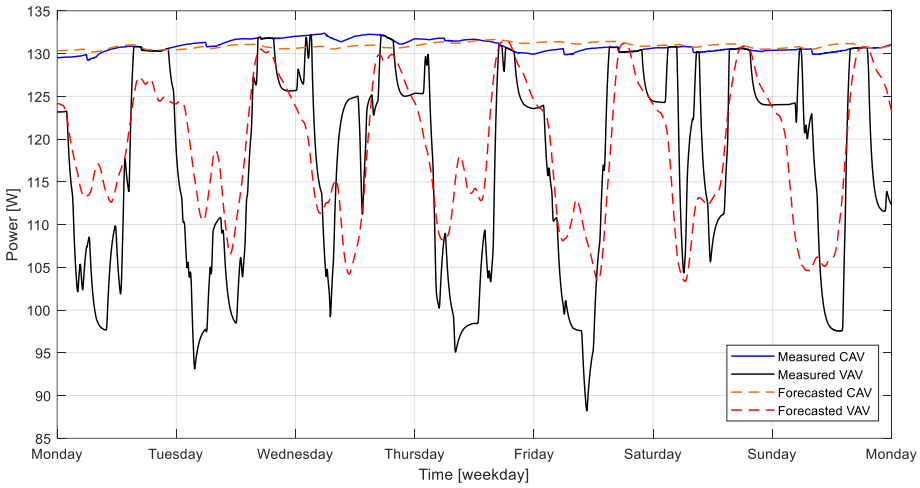

Figure 4.16. Measured and forecasted power consumption of the ventilation system [Paper I].

4.3.2.2 Estimation of FVR duration

Boundary conditions and pollutant generation are both essential for determining the FVR duration. It is necessary to make corrections in boundary conditions in advance if all IAQ sensors are installed in the AHU. The corrections based on data gathered during the second week of January are shown in Figure 4.17. Based on the data from one week, where the 5-minute average is calculated for each timestep within a day, the boundary conditions are adjusted. The occupancy of a room and how uniformly the pollutant concentration is distributed among the rooms are critical factors in the corrections of boundary conditions. The boundary conditions of the two ventilation system types differ slightly.

The simulation results showed that CO_2 concentrations had the most significant impact on flexibility. The first week of November is depicted in Figure 4.18 as an example of a one-week CAV type of ventilation system with estimated FVR durations, where the FVR duration was mainly determined by CO_2 concentration. On the other hand, FVR duration is less affected by temperature. The duration of the entire system is determined by the parameter with the shortest FVR. Since the occupancy profile is the same for both CAV and VAV types of ventilation systems, the FVR durations (Figures 4.18 and 4.19) are comparable. The availability of flexibility is reduced by demand-controlled ventilation, though, as FVR durations are marginally lower. For each system type, two methods – room-based estimations and AHU-based estimations – were used. Room-based estimations used the room with the shortest FVR duration and considered the IAQ sensors in each room. Sensors placed only in the AHU were considered in AHU-based calculations, which also used corrected boundary conditions. The FVR duration profile produced by AHU-based estimations is comparable to that of room-based estimations. However, notable variances can be brought out at stochastic occupancy and created boundary conditions.

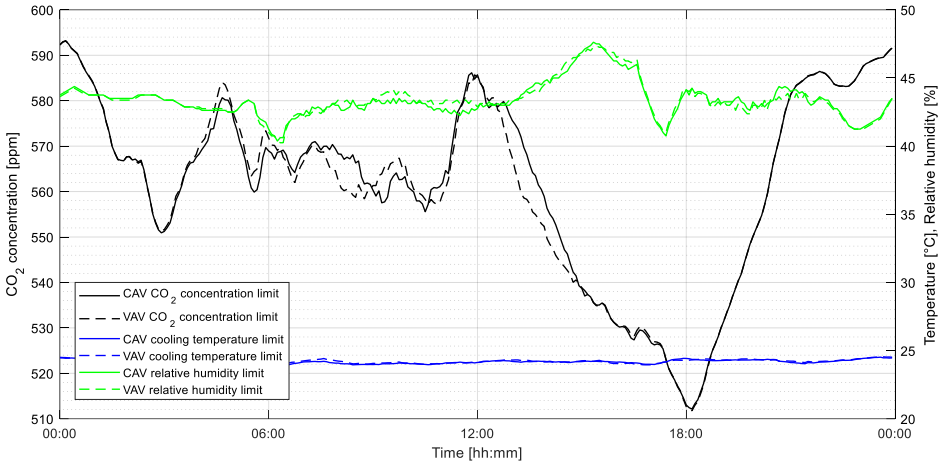

Figure 4.17. Daily IAQ parameter limits after the correction of the boundary condition [Paper I].

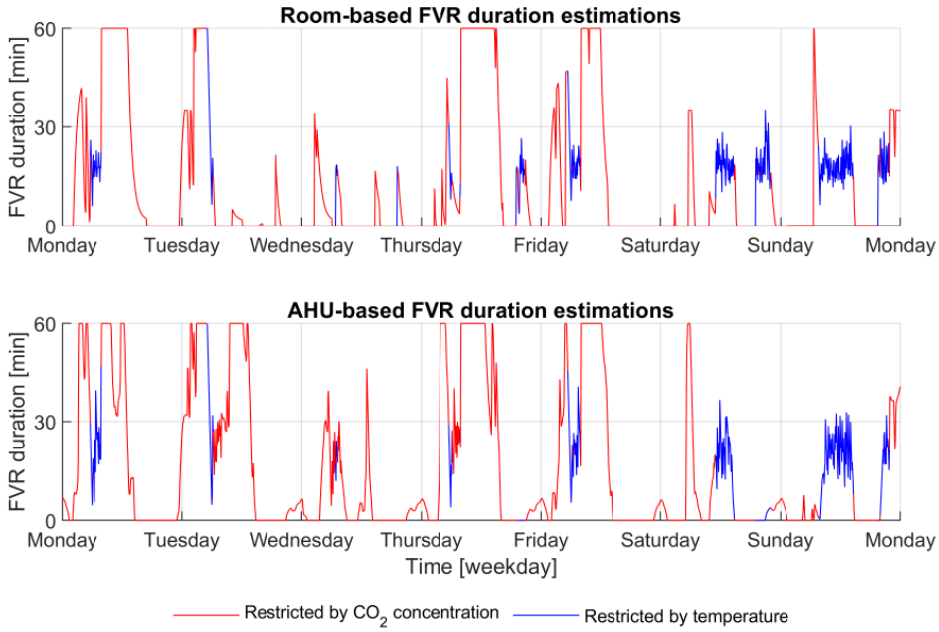

Figure 4.18. Example of one-week FVR duration estimations for a CAV type ventilation system.

The room-based technique was the most accurate way to estimate FVR duration according to residual analysis (Figure 4.20). Room-based approach residuals had a positive bias and provided more conservative FVR durations. It was the reason for applying the FVR duration adjustment method, which reduced the specified timestep estimation according to the following time-step forecasts.

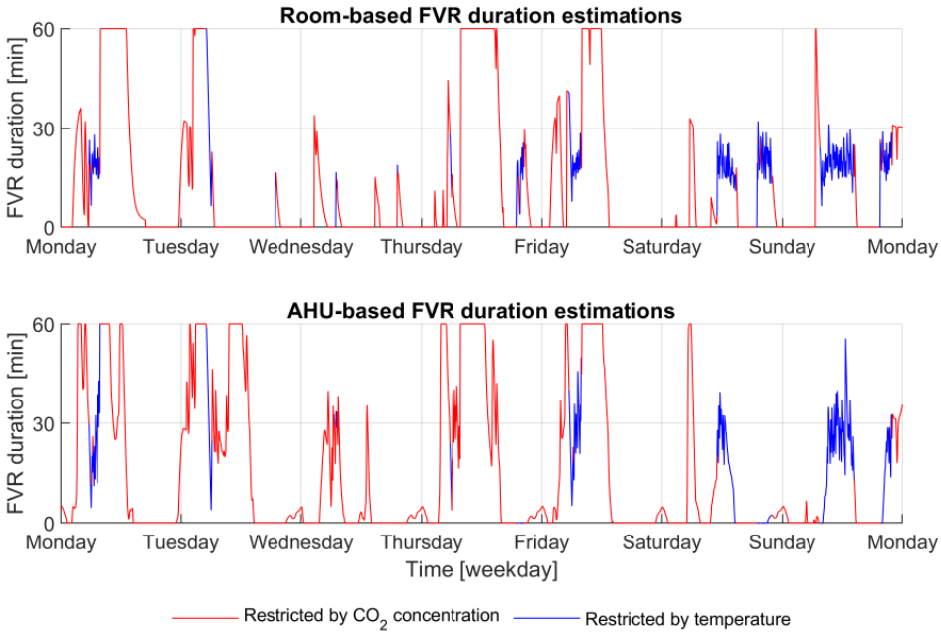

Figure 4.19. Example of one-week FVR duration estimations for a VAV type ventilation system.

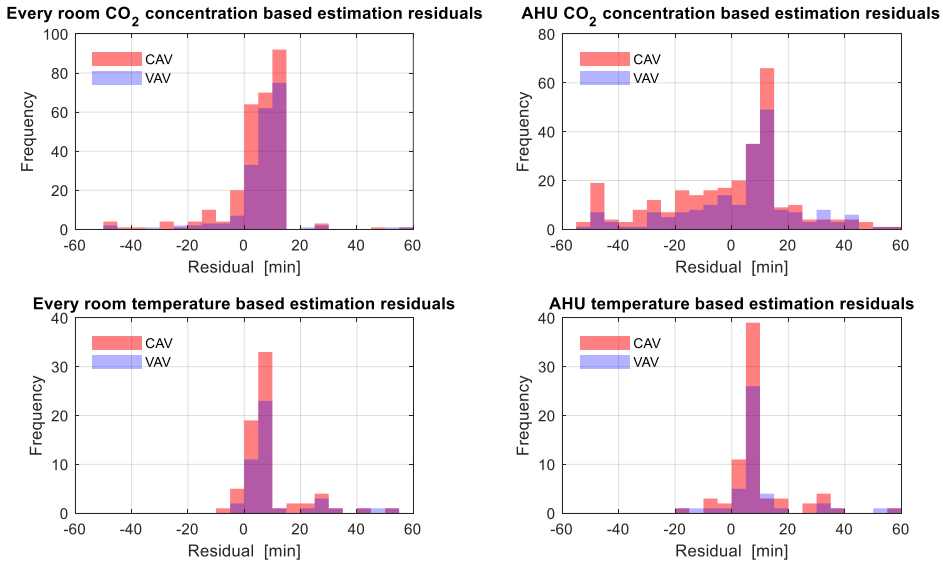

Figure 4.20. Residuals of the FVR duration forecasting.

The highest inaccuracy in FVR duration estimations was observed with the approach where the IAQ sensors were located in the AHU (Table 4.9). CO_2 concentration-based FVR duration estimations are more accurate for the VAV than for the CAV, resulting from fluctuating CO_2 concentration. It can be expected that in actual application, the methods can have even better performance since changes in the IAQ can be included in the estimations. Temperature-based FVR duration estimations showed higher MAPE error

than CO_2 concentration-based estimations since the temperature is highly dependent on outdoor conditions. However, the method gives more conservative estimations to avoid exceeding temperature limits during regulations.

Table 4.13. Performance of FVR duration estimation methods with object 2.

IAQ sensors location		In every room		In the AHU	
Parameter		CO_2 concentration	Temperature	CO_2 concentration	Temperature
Constant Air Volume	**RMSE**	12 min	11 min	23 min	14 min
	MAPE	69%	71%	149%	97%
	IAQ limit exceeded	13.1%	1.6%	31.8%	1.6%
Variable Air Volume	**RMSE**	11 min	14 min	21 min	16 min
	MAPE	67%	74%	122%	89%
	IAQ limit exceeded	7.8%	0.8%	24.9%	1.6%

4.3.2.3 Flexibility service activations and pricing

The cost of operating the ventilation system and the CO_2 concentration measurements were used to determine the cost of providing flexibility. For instance, upward regulations are depicted in Figure 4.21, where the tendered price was computed using equation (3.24), and comfort cost was obtained from the maximum balanced energy price for the previous two weeks. Calculations also considered the highest rate of CO_2 generated during the last two weeks. The reserve was only activated when the tendered price was less than the balance energy market price, the mFRR was activated, and there was more than 10 W of available flexible power for the regulation. The VAV type system was demand-controlled, which resulted in less power that can be used for up-regulations.

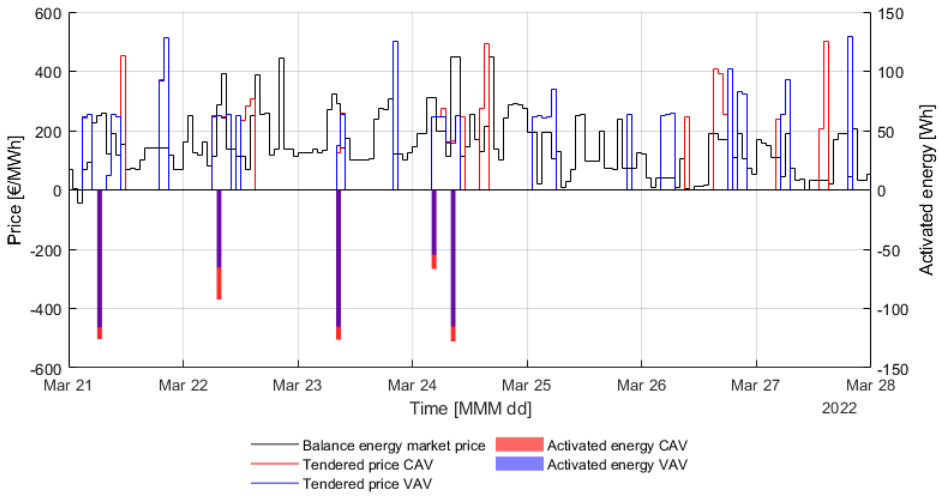

Figure 4.21. Flexibility service prices and activations.

Regulations have little impact on overall energy use in residential buildings because the ventilation system runs continuously (Table 4.14). The total energy used by fans was decreased throughout the simulation period by 1.2% for the CAV system but only by 0.8% for the VAV system. The cost of energy was lowered by 4% for the CAV type system, and for the VAV type system, a decrease of about 2.2% was reached. These percentages can be raised when the profit margins are adjusted for a good balance between system availability to provide service and exploitation, where the ventilation system is used more extensively for flexibility service.

Table 4.14. Regulation effect on energy consumption and cost of energy.

Parameter	**System type**	
	CAV	**VAV**
Energy consumption without regulations	1.152 MWh	1.034 MWh
Energy consumption with regulations	1.138 MWh	1.026 MWh
Total cost of energy without regulations	384.11 €	344.82 €
Total cost of energy with regulations	368.78 €	337.23 €

4.4 Conclusions

This chapter described the validation process of the ventilation system flexibility management methods developed in Chapter 3, based on the state-of-art analysis discussed in Chapter 2. The validation process started with constructing object models: a small room in a building and a single-family house. A year-long simulation was conducted on these objects where the first iteration was done to acquire a baseline, and the second iteration was for testing the performance of the methods. The results addressed power consumption, FVR duration, and economic parameters, where the main observations were:

- ARMA(p, q) model is sufficient to forecast the power consumption of the ventilation system. The forecast MAPE was around 1% for the CAV type systems, and for the VAV type system with a stochastic occupancy profile, the MAPE was 6.5%. According to the Estonian TSO Elering AS [144] up to ± 10% steady-state error is allowed for the mFRR capacity or 0.1 MW, whichever is larger.
- The open-loop approach to estimate FVR duration is used when no IAQ sensors are available, and the goal is to minimize initial investment costs. However, this will result in higher inaccuracies in estimations. From the results of the small room, the variance of residuals is low, but there is a bias that can be removed if parameters are adjusted to actual conditions.
- Placing sensors only in the AHU approach is used when the aim is to lower the initial investment costs while having minimum sensor data. The residual analysis showed higher variability and lower accuracy than placing sensors in each room. Portable sensors are recommended to improve the performance of this approach to tune the corrected boundaries.
- FVR duration estimations based on CO_2 concentration showed an RMSE of 7 min up to 16 min when the fixed occupancy profile was selected and about 12 min when the stochastic occupancy profile was used. Considering that the delivery period is typically not longer than 30 minutes instead of 1 hour,

which was considered in the simulation, it can be assumed that this error is even less in the actual application.

- FVR duration estimations based on temperature showed a RMSE of around 20 min for most scenarios. Therefore, temperature-based FVR duration is more difficult to estimate accurately, but it can be expected that the estimations will also become more accurate with shorter delivery periods.
- The results showed that cost savings are achievable when a ventilation system is integrated into the flexibility service. In the apartment, up to 10% of cost savings were achieved; in the office, up to 15%, and in the single-family house, up to 4%. The cost savings heavily depend on how much the flexibility service exploits the ventilation system. In the single-family house, the CO_2 concentration was already close to the limit, seen from the share of regulations where the CO_2 concentration limit was reached.
- A ventilation system as virtual energy storage is an approach to maximize the energy capacity used for flexibility service. Based on the results, the VES approach increases the total cost savings by twofold compared to operating a ventilation system at a minimum ventilation rate during the activation of the reserve.

The results acquired in this chapter make it possible to implement the developed flexibility management methods on real systems. The experiments conducted in the case studies will be discussed in Chapter 5. In this chapter, two hypotheses were tested. For most cases, the FVR duration is estimated to be shorter than the ventilation system can provide to avoid exceeding limits for IAQ. The second hypothesis is mostly correct since for most cases, the IAQ limits were not exceeded in more than 5% of situations when the reserve was activated. The limit is exceeded more with stochastic occupancy. The third hypothesis is mostly correct since most studied ventilation systems could provide more than half of the cases when the reserve is activated for at least 30 minutes, the maximum amount of power. The exception is the single-family house, where at least 30 minutes of FVR duration was achieved for around 35% of cases. The high pollutant concentration caused this during normal conditions.

5 Case studies with the developed flexibility management methods

In this chapter, developed flexibility methods are experimentally validated on an actual building. First, experimental setups and the experiments are described. Second, the results of the experiments are analyzed, and the performance of the methods is addressed. The aim of the experiments is to discover details that influence the implementation of the developed methods in an actual building that otherwise simulations cannot identify.

Experiments were conducted in the Tallinn University of Technology (TalTech) educational building with a code "SOC" (Figure 4.1), used by the School of Business and Governance. The building is located in Akadeemia tee 3, Tallinn. It is a four-story building with an underground parking area. The total floor area of the building is 10 346 m^2. The installed power of the building is 1.63 MW, and the calculated power consumption is 1.3 MW. The building accommodates lecture rooms, offices, a cafeteria, recreational areas, underground parking, and technical rooms. The SOC building was selected for experiments as it has a wide selection of different ventilation systems and is one of the most modern buildings on the TalTech campus.

Figure 5.1. TalTech SOC educational building.

5.1 Description of the building ventilation systems and experimental setups

Ventilation systems of the TalTech SOC educational building were used to validate the developed flexibility management method. Power consumption of ten ventilation systems was monitored (Table 5.1). The rest of the ventilation systems installed in the building were shut down during the measurement period or had power consumption close to zero. Measurements started on the 16th of June 2021 and ended on the 31st of January 2022. Measurements were taken with a multi-channel energy meter SATEC

BFM136. This energy meter complies with the requirements for accuracy class 0.5S in the standard IEC 62053-21. Most of the systems installed in the SOC building are CAV type, and only two are VAV type. Ventilation systems are also classified as single or multi-zone systems. According to the building design documentation, the total rated power of ventilation systems is 98 kW. The design values differ in actual measurements, and there can be various reasons behind it, such as changes in the equipment, configuration, aging of the system, and leakage through construction.

Table 5.1. Ventilation systems in the TalTech SOC building and the design values.

Code	System type	Multi or single-zone	Fans' rated power, kW	Airflow rate, m^3/s
302SV	CAV	Multi	26.0	6.6
303SV	CAV	Multi	9.5	3.2
304SV	CAV	Multi	16.5	5.7
305SV	VAV	Multi	30.0	8.6
306SV	VAV	Single	9.0	1.8
307S	CAV	Multi	4.0	2.0
307.1V	CAV	Single	1.2	1.3
308V	CAV	Multi	1.2	1.4
309V	CAV	Multi	0.3	0.3
310V	CAV	Single	0.3	0.3

Ventilation systems in the SOC building operate according to a schedule (Figure 5.2). During the daytime, a ventilation system operates at a higher ventilation rate, and during nighttime, a ventilation system operates at a minimum rate or is shut down. The maximum total power consumption of ventilation systems is roughly 35 kW, and the minimum is around 4 kW. Thus, around 31 kW of power can be reduced during the daytime.

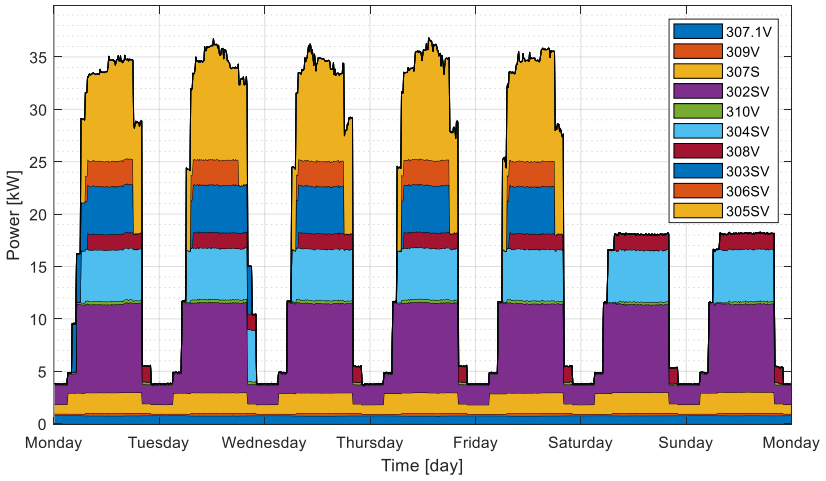

Figure 5.2. Power consumption of SOC building ventilation systems.

5.1.1 Case study 1: Ventilation system 306SV and auditorium room

TalTech auditorium served as the site for the case study. A ventilation system that was mainly servicing one auditorium was used in the study. The chosen auditorium has a floor size of 224.5 m^2, and its estimated indoor air volume is 1122.5 m^3. The auditorium can hold 200 people at a time and has a 1.76 m^3/s designed ventilation rate. The fan rotational frequency of 17 Hz, with around 0.48 m^3/s ventilation rate, was used to determine the lowest permitted airflow rate.

A CO_2 cylinder with attachments to measure and control gas flow was placed in the middle of the auditorium as a source of pollution. The CO_2 cylinder was weighed before and after the experiment to calculate the average CO_2 generation rate. To provide a vertical component to CO_2 pollution and help mix the air, an air mixing fan was positioned close to the CO_2 gas exit nozzle (Figure 5.3). Due to the low temperature of the injected CO_2 gas, which does not mix well with interior air while the air exhaled by people is warmer and has superior mixing capabilities, a mixing fan was necessary. Multiple fresh air inlets bring clean air into the auditorium from below the floor, and one air duct removes polluted air from above, located in Figure 5.3 on the right side of the room.

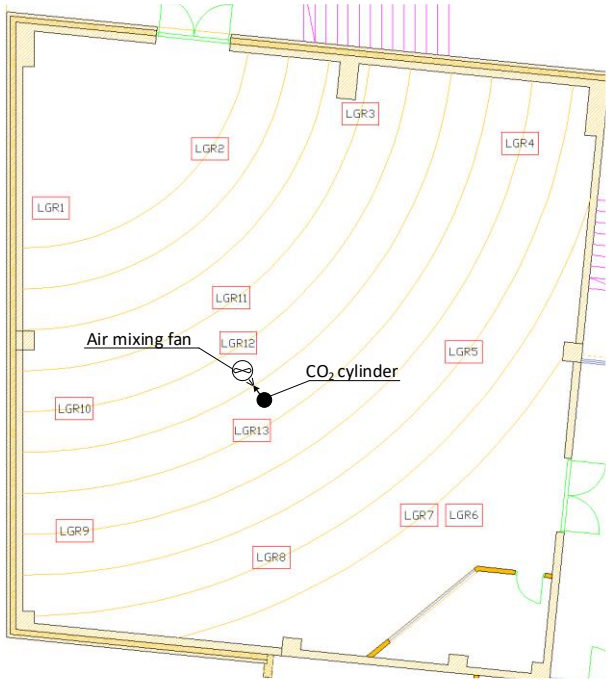

Figure 5.3. The auditorium and measurement equipment layout [Paper III].

IAQ loggers were put in the auditorium, marked LGR1 through LGR13, all of which were placed around 0.8 m, except for LGR6, which was mounted on the extract air orifice at a height of about 3 m. The Evikon E6226 measurement unit (CO_2 level 0 to 10000 ppm) was used to determine the CO_2 concentration. These loggers were placed in the room to provide a clearer picture of the CO_2 distribution inside the auditorium, but their usage to calculate the ventilation system's flexibility was excluded. Only measurements in the extract air duct, suitable for such sensors in most ventilation systems, were used in

flexibility estimations. With little expenditure, the stated flexibility estimation methods can be used for most ventilation systems.

Two fans bring fresh air and remove polluted air from the auditorium as part of a mechanical ventilation system (Figure 5.4). Additionally, the system has an enthalpy heat exchanger configured to run at maximum rotational speed. Air filters, heating, and cooling of the supplied air are additional components of the ventilation system not shown in Figure 5.4.

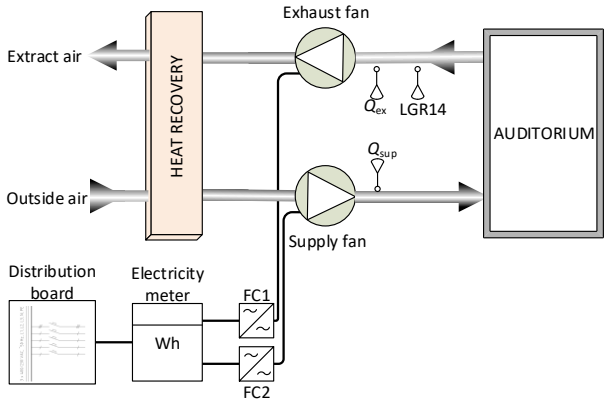

Figure 5.4. Ventilation system 306SV layout and placement of measurement equipment [Paper III].

A timestep of 1 min was used to measure extract and supply airflow rates. A multipurpose indoor air quality meter, Testo 435-4, with a differential pressure range of 0 to 250 Pa and an accuracy of 1 Pa, was used to measure the airflow. A single IAQ logger with a 1-minute timestep was inserted into the extract air duct to measure the CO_2 concentration in the return air. Each fan drive was powered from the HVAC distribution board, and frequency converters FC1 and FC2 were used to control each fan's speed. One electricity meter, model BFM136, was used to measure the individual power consumption of each fan. Measurements logging interval of electricity consumption was 2 min, and average power was saved for each timestep.

5.1.2 Case study 2: Ventilation system 303SV and lecture rooms

Ventilation system 303SV servicing multiple lecture rooms is the point of interest in the second case study. The total floor area connected to the selected ventilation system is 664.1 $m^{2,}$ with a total air volume of around 2324 m^3 (Table 5.2). The ventilation system provides air exchange for the rooms on the second, third, and fourth floors. These rooms are used for lectures, except on the second floor, where there is a recreational area with a floor size of 190.3 m^2. The total airflow rate is 3.36 m^3/s, and the ventilation system power consumption at this rate is approximately 6.2 kW. The minimum rotational frequency of the fan is 15 Hz, with around 1.0 m^3/s ventilation rate and 0.24 kW power consumption. The fan drives have frequency converters that can be operated in the range of 15 to 50 Hz. However, in flexibility estimations, it is considered that the ventilation systems are shut down completely. It is due to complications where the case study used measurements from the lecture rooms, and the ventilation system's operation was not altered since it was not allowed by the system's administrator.

IAQ loggers were installed in each of the 12 lecture rooms connected to the ventilation system. Loggers were placed on the lecturer table with a height of around 0.8 m (Figure 5.5). One of the loggers was placed inside the AHU return air duct to monitor the CO_2 concentration of the extracted air. Lecturers were given pre-filled forms to mark down the number of people inside the lecture room. Since the method calculated the pollutant generation rate, it is possible to derive the number of people from the measurements and compare this data to the written number.

Table 5.2. Rooms connected to ventilation system 303 [145].

Floor	Room number	Floor area, m^2	Room height, m	Airflow rate, m^3/s
II	216	190.3	3.5	0.34
	217	35	3.5	0.21
	218	34.1	3.5	0.26
	219	34.1	3.5	0.24
	220	35	3.5	0.25
	221	35	3.5	0.21
	222	37.2	3.5	0.23
III	315	44	3.5	0.17
	316	44	3.5	0.24
	317	43.7	3.5	0.33
IV	416	44	3.5	0.27
	417	44	3.5	0.34
	418	43.7	3.5	0.27
Total		**664.1**		**3.36**

Figure 5.5. IAQ logger location in a lecture room [145].

IAQ measurements were taken during six weeks, from 7th February 2022 to 17th April 2022. A cap was in between measurements where the loggers were removed from the rooms from 21st March 2022 to 18th April 2022. IAQ was measured with HOBO MX1102A, which measures CO_2 concentration, temperature, and relative humidity (Table 5.3). A timestep of 5 min was used to measure IAQ conditions inside each room, and the AHU return extract air duct. Each fan drive of the ventilation system 303SV was powered from the HVAC distribution board, and frequency converters were used to control each fan's speed. One electricity meter, model BFM136, was used to measure the individual power consumption of each fan. A logging interval of 10 min was selected to measure electricity consumption and average power during each timestep.

Table 5.3. HOBO MX1102A CO_2 logger specification [146].

Parameter	Value
Temperature range	0…50 °C
Temperature measurement accuracy	±0.21 °C
Temperature measurement resolution	0.024 °C at 25 °C
Relative humidity range	1…90%
Relative humidity measurement accuracy	±2% in the range 20…80% ±4.5% in the range 80…90%
Relative humidity measurement resolution	0.01%
CO_2 concentration range	0…5000 ppm
CO_2 concentration measurement accuracy	±(50 ppm + 5% from the reading)
CO_2 concentration measurement resolution	1 ppm

5.2 Analysis of case study results

Two case studies were conducted in the building, and flexibility management methods were tested based on the acquired data. The focus of these studies was on power consumption and FVR duration. The accuracy of each method is described through the root mean square error (RMSE) and mean absolute percentage error (MAPE). Economic aspects are considered for case study 2, where more data was generated for an extended period.

5.2.1 Case study 1: Ventilation system 306SV and auditorium room

On October 9th, 2020, a case study was initiated in the ventilation system servicing an auditorium of an educational building. During the experiment, the regular ventilation rate of the system was changed to minimal (Figure 5.6). The goal was to decrease the system's energy usage and estimate flexibility. The case study was separated into events where something happened or changed during the experiment (Table 5.4). One disturbance was also added where the mixing fan was shortly shut off.

Before being set to the lowest rate, the average power usage of the ventilation system was around 2.43 kW, equivalent to an airflow rate of roughly 1.79 m^3/s. The calculated specific fan power (SFP) was around 1.36 $kW/(m^3/s)$. The system power consumption at the FVR was around 0.17 kW, equivalent to an airflow rate of about 0.48 m^3/s. At the FVR, the calculated SFP was around 0,35 $kW/(m^3/s)$. According to the standard EN 13779, SFP should be less than 2.0 $kW/(m^3/s)$, which the ventilation system complies with. It took around 90 s for the ventilation system to transition from one power level to the next. Therefore, the rate of power change was roughly 25 W/s.

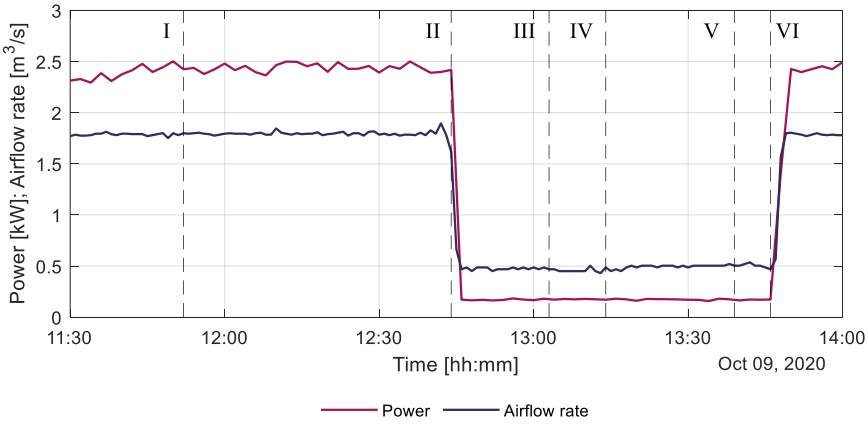

Figure 5.6. The power consumption of the ventilation system and the airflow rate during the experiment [Paper III].

Table 5.4. Events of the case study and schedule [Paper III].

Event	Description	Time
I	Start of the experiment, CO2 gas injection into the auditorium	11:52
II	The ventilation system is switched to the minimum rate	12:44
III	At the start of the disturbance, the CO2 gas mixing fan is switched off	13:03
IV	End of the disturbance, the CO2 gas mixing fan is switched on	13:14
V	The maximum allowable CO2 concentration of 1100 ppm reached	13:39
VI	End of the experiment, the ventilation system returned to regular operation	13:46

5.2.1.1 Power consumption forecast

The ventilation system 306SV was observed for approximately one week, from November 23rd to November 30th, 2020 (Figure 5.7). Results indicate that the ventilation system runs according to schedule, including on weekends. Between 7:00 and 22:00, when the ventilation system is set to operate at the maximum rate, the power consumption can only be reduced during this time window. Between 22:00 and 7:00, the ventilation system is working at its lowest power level, which implies that during that period, the power consumption can only be increased.

The ARMA(0, 2) model was used to forecast power consumption. The AIC approach was used to calculate the terms of the ARMA model. 24 hours were chosen as the forecast horizon. The power consumption for the following day was forecasted using measurement data from previous days. Data for the first two days were used to initialize the forecasting model, and the rest was used to test the model performance. For the quick reaction between the ventilation system starting and shutdown, one day was divided into 2-minute timeslots. The forecasts were done for each timeslot separately. The accuracy of the method was determined through the 24th-hour forecast with the most significant uncertainty compared with the observed data. The RMSE of the power consumption forecasts was roughly 0.04 kW. The MAPE was roughly 2.2%.

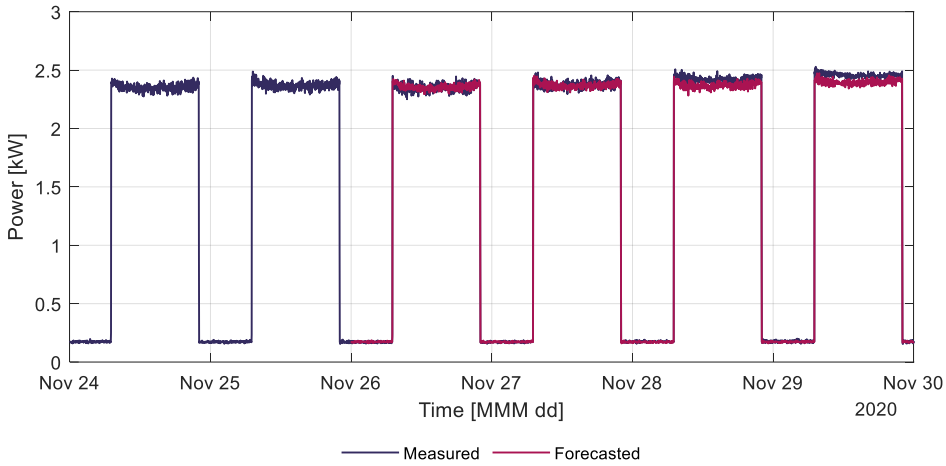

Figure 5.7. Measured and forecasted power consumption of the ventilation system.

5.2.1.2 FVR duration estimation

The valve of the CO_2 cylinder was opened to begin the experiment at 11:52 (Figure 5.8). Throughout the experiment, the CO_2 gas flow rate in the auditorium was maintained at around 22 l/min, equivalent to the CO_2 produced by 66 people, or 33% of the room's occupancy. The ventilation system was forced to operate at the minimum rate from 12:44. The period before this action was utilized to stabilize the CO_2 concentration level in the auditorium and determine how long it could continue operating at its lowest rate. The CO_2 gas mixing fan was turned off at 13:03 and turned back on at 13:14. As a result of inadequate CO_2 gas mixing in the auditorium, this temporarily decreased the concentration of CO_2 in the extract air. The flexibility estimation algorithm recognized this as an unexpectedly low CO_2 generation rate and began calculating the CO_2 concentration in the auditorium using the CO_2 generation data from the preceding five minutes. Only when the ventilation system is forced to work at a rate lower than expected operating conditions to reduce power consumption is this portion of the algorithm active.

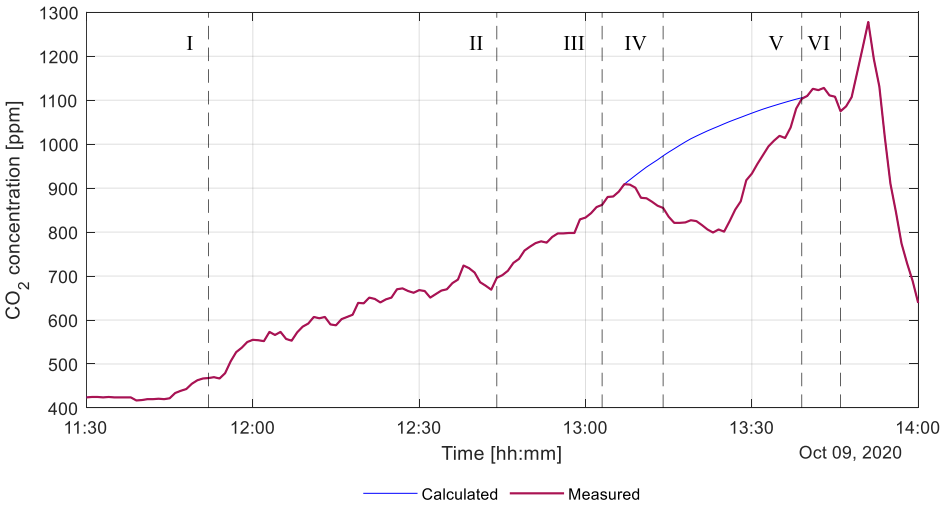

Figure 5.8. CO_2 concentration in extract air during the experiment [Paper III].

It took around 55 minfor the CO_2 concentration to reach and surpass boundary conditions. The estimated FVR duration was 53 min, calculated before the ventilation system was forced to operate at the minimum rate at 12:44. Therefore, the estimation error was 2 min, 4% off from the measured duration. A moving-average filter was used since the initial estimation approach for a shorter operation period generated high fluctuations (Figure 5.9). The filter's window duration was adjusted to 3 min to smooth out more significant oscillations without having too high a lag from the initial estimation. The measured duration indicates the time elapsed after the FVR began until the CO_2 concentration limit was reached. The CO_2 concentration level was estimated from 13:07 as the algorithm detected a negative CO_2 generation rate. The estimated CO_2 concentration reached the boundary of 1100 ppm before it was measured, which is why the estimations are lower than the measured results.

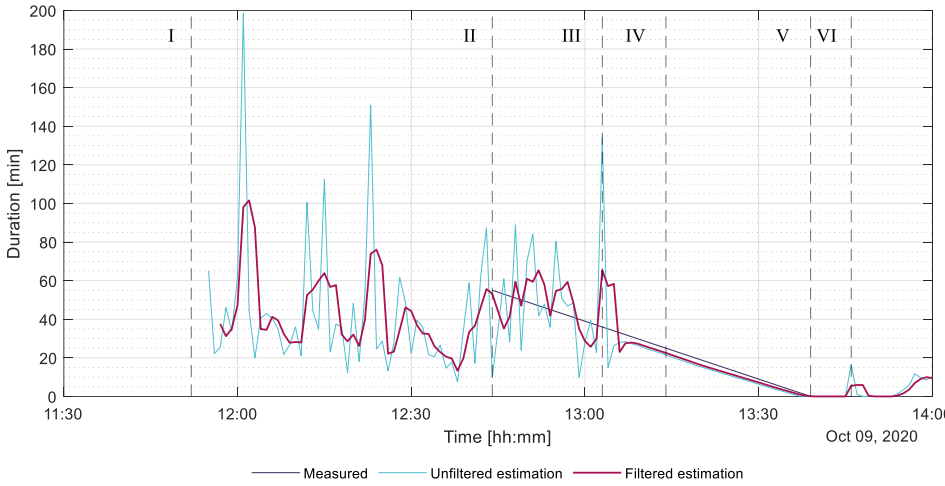

Figure 5.9. Measured and estimated FVR durations [Paper III].

5.2.1.3 IAQ conditions inside the auditorium room

IAQ loggers placed within the lecture room were employed in the case study to get a general outline of the pollutant distribution and overall conditions during the experiment. The average CO_2 concentration inside the auditorium and the CO_2 concentration measured in the extract air duct had a weakly positive correlation during regular operation with a coefficient of about 0.48. Figure 5.10 shows that at normal functioning of the ventilation system, the CO_2 concentration in the extract air was within the range of the CO_2 concentration in the auditorium measured at multiple points. The average CO_2 concentration within the auditorium and CO_2 concentration during the FVR measured inside the extract air duct did not correlate, as shown in Figure 5.10. The reason may be a lack of proper CO_2 gas mixing inside the auditorium or inertia existing between the extracted air and the auditorium's CO_2 concentration change. This experiment should be repeated with persons to understand better the reasons where thorough planning and ethical reasons should be addressed.

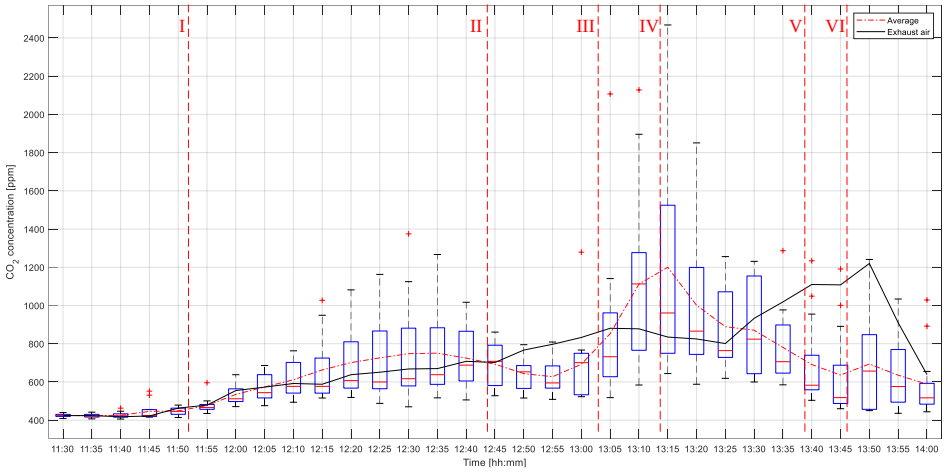

Figure 5.10. Flexibility service prices and activations [Paper III].

5.2.2 Case study 2: Ventilation system 303SV and lecture rooms

In total, 12 lecture rooms are connected to the ventilation system 303SV. The ventilation system runs according to a schedule where it is shut down during unoccupied hours. On Mondays, the ventilation system starts at 4:00 and is shut down at 18:00. On Tuesdays, the ventilation system is started at 7:00 and shut down at 22:00. On all other working days, the ventilation system is started at 7:00 and shut down at 18:00. The ventilation system is shut down during the whole weekend. It allows both up- and down-regulations. However, based on the data acquired during the measurement period, no down-regulations would be conducted on the system. The reason is that the balancing energy price to activate the reserve was unsuitable for the system. There could have been 55 up-regulations during the period starting from 21st March 2022 to 18th April 2022. CO_2 concentration limit would have been reached during 31 regulations or 56% of all the cases. However, in 41 cases, the FVR duration was longer than 30 min, meaning that the ventilation system could support up to 30-minute activations for around 75% of the time.

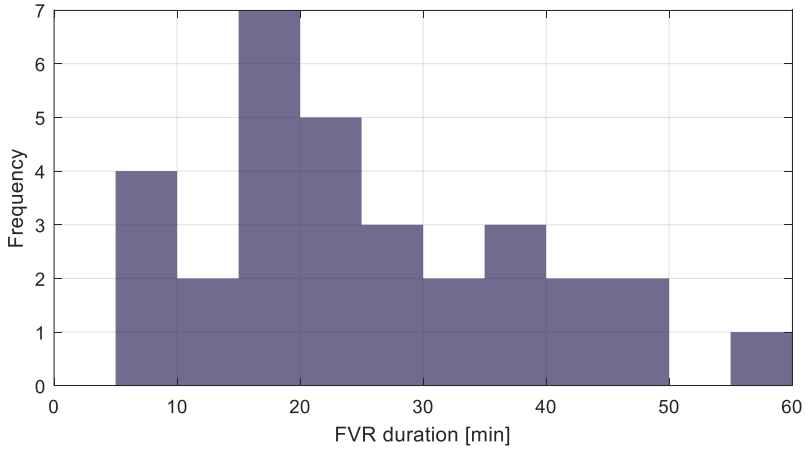

Figure 5.11. Distribution of CO_2 concentration based FVR duration estimates shorter than 60 minutes.

5.2.2.1 Power consumption forecast

The ARMA(0, 2) model was used to forecast the power consumption of the ventilation system 303SV. The AIC approach was used to calculate the terms of the ARMA model. 24 hours were chosen as the forecast horizon. The power consumption for the following day was forecasted using measurement data from previous days. Data from the first two weeks were used to initialize the forecasting model, and the rest was used to test the model's performance. For quick reaction between the ventilation system start and shutdown, one day was divided into 10-minute timeslots. The forecasts were done for each timeslot separately. The accuracy of the method was determined through the 24th-hour forecast, with the most significant uncertainty compared with the observed data. The RMSE of the model during the measurement period was roughly 0.11 kW. The MAPE was roughly 4.3%.

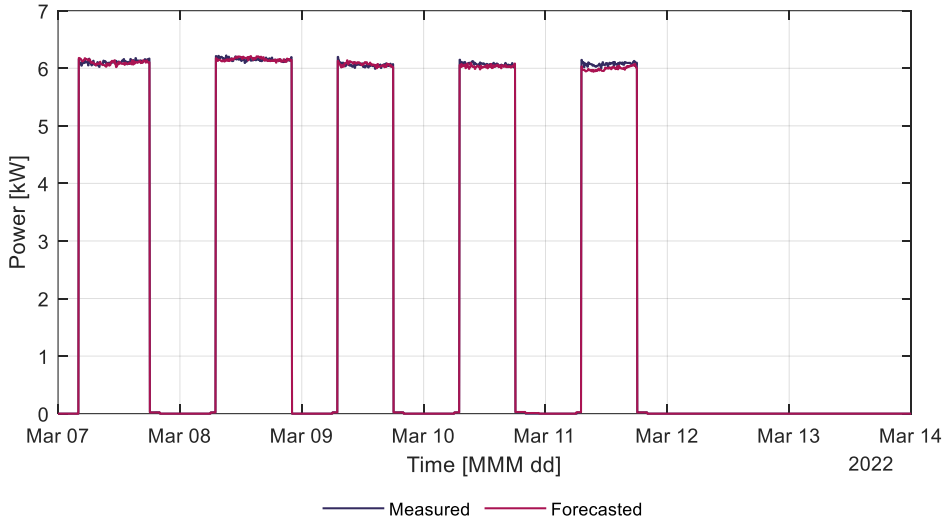

Figure 5.12. Example of measured and forecasted power consumption of the ventilation system.

5.2.2.2 FVR duration estimation

The last week of the monitoring week is depicted in Figure 5.13 as an example of one-week FVR duration estimations. The FVR duration was only determined by the CO_2 concentration. It is due to the reason that inadequate information was acquired on the conditions of the supply air. The temperature and humidity FVR duration method relies on the supply and return air values. Without that, the estimations are inaccurate and cannot be used for flexibility estimations. The the usage profile of the lecture rooms was not the same every week; there were changes in the number of people inside the room, and the time of the lectures changed. However, it can be seen from Figure 5.13 that from Monday to Thursday, rooms were used during working hours, causing a decrease in the FVR duration. There is also a slight decrease on Friday, but it is too small to influence the ventilation system availability for flexibility service significantly.

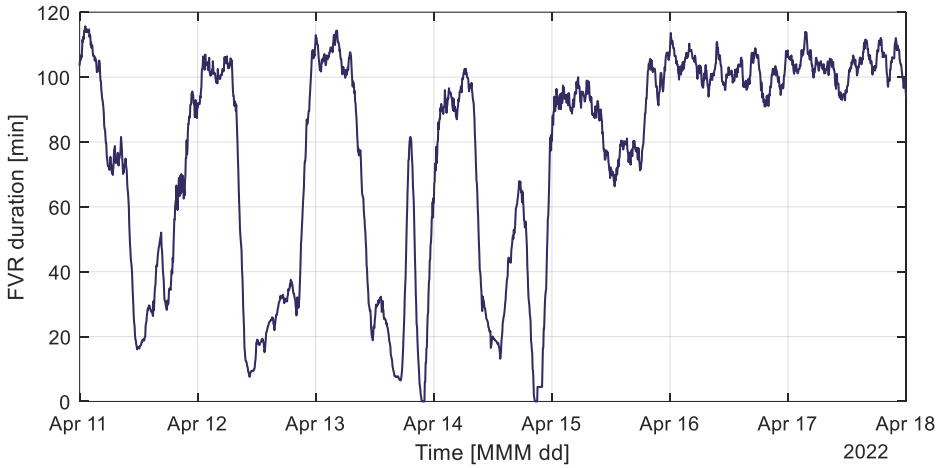

Figure 5.13. Example of one-week FVR duration estimations.

5.2.2.3 Flexibility service activations and pricing

The cost of operating the ventilation system and the CO_2 concentration measurements were used to determine the reduction of cost that it would generate to provide flexibility. For instance, upward regulations are depicted in Figure 5.14, where the tendered price was computed using equation (3.24), and comfort cost was obtained from the maximum balanced energy price for the previous two weeks. Calculations also considered the highest rate of CO_2 generated over the previous two weeks. The reserve was only activated when the tendered price was less than the balance energy market price, the mFRR was activated, and there was more than 100 W of available flexible power for the regulation. It can be seen that during high occupancy hours, the activated energy is lower since the CO_2 concentration will reach its limit faster compared to low occupancy hours, where the ventilation system can be exploited the most. Tendered price also shows the building usage, where the price increases when more people are inside rooms.

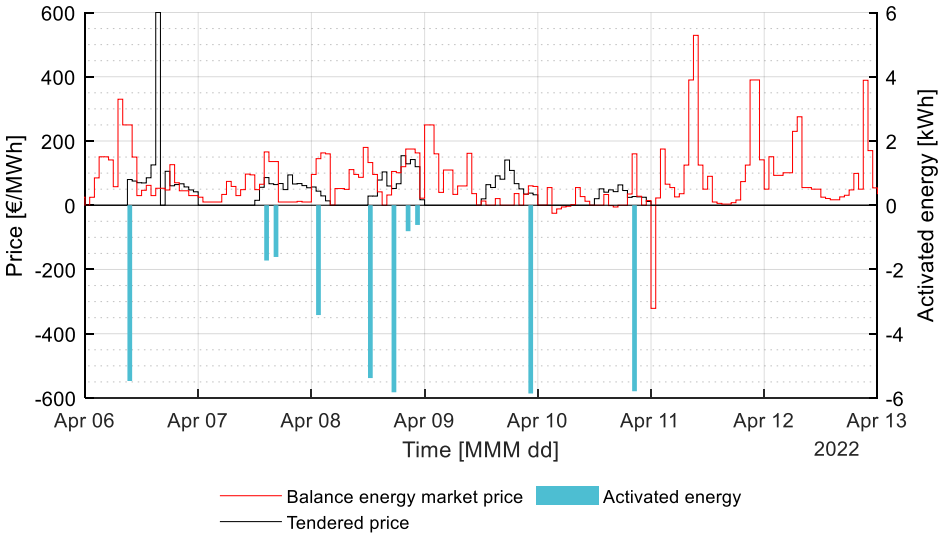

Figure 5.14. Prices and activations of the flexibility service.

With the ventilation system 303SV, no actual regulations were made. The measured power consumption was compared with the calculations done in Matlab. According to the calculations, the total energy of the fans used could decrease throughout the measurement period by 12.5%. The cost of energy could be lowered by 37%. These percentages are prone to changes if the building usage or electricity price changes. During four weeks, the total operation cost of the ventilation system could be reduced by 157 euros, meaning that the annual cost savings could be up to 2000 euros. It is not the only ventilation system in the building, meaning that annual cost savings could be increased even more while providing more flexibility to the grid.

Table 5.5. Regulation effect on energy consumption and cost of energy.

Parameter	**Value**
Energy consumption without regulations	1.68 MWh
Energy consumption with regulations	1.47 MWh
The total cost of energy without regulations	419.48 €
The total cost of energy with regulations	262.85 €

5.3 Conclusions

This chapter described case studies of the flexibility management methods of the developed ventilation system in a building discussed in Chapter 3. The case studies continued the validation process described in Chapter 4, which aimed to test the performance of the management methods in actual usage. Two case studies were performed in one of TalTech educational buildings. The first case study considered a single activation where the room usage was around 1/3. The focus of the second case study was on a multi-zone ventilation system that was monitored for six weeks. The measurement results were used to estimate the flexibility potential of the system. The outcomes addressed power consumption, FVR duration, and economic parameters where the main observations were:

- ARMA(p, q) model is suitable to forecast ventilation system power consumption. The forecast MAPE was around 2.2% for the system in the first case study and 4.3% for the second case study.
- The second case study showed that the ventilation system could provide, in around 75% of cases, the maximum power for up-regulations for at least 30 minutes.
- CO_2 concentration based FVR duration estimation error was 2 min for the first case study at the activation time.
- According to the results acquired from the second case study, it is possible to reduce the total cost of energy by at least 30%.

With the results acquired from this chapter, it is possible to implement the developed flexibility management methods on real systems. Furthermore, the economic findings of this chapter enable the assessment and feasibility studies of integrating ventilation systems in the flexibility service. The fourth hypothesis is correct for most cases where at least 5% of the total cost reduction was noted with the flexibility service. However, in some cases, it can be challenging to achieve. If the system is already operating at the limit, then there are fewer cost savings, but for the case study where the actual ventilation system was monitored, the cost savings could be up to 37%.

6 Conclusions and future work

This doctoral thesis provides novel flexibility management methods for ventilation systems. The developed methods enable the integration of ventilation systems in a flexibility service, thus providing more flexible power to TSOs and other balancing authorities. The findings and results of this thesis are also valuable for building owners who can now reduce energy costs by providing flexibility service with their ventilation systems. In a broader sense, these methods will aid the deployment of renewable energy sources. Besides conventional flexibility sources (e.g., energy storage, power plants), demand-side flexibility where ventilation systems are exploited now has more potential to balance the electric power system.

The developed management methods are created from an aggregator's viewpoint. The flexibility of a ventilation system is described mainly through three parameters: flexible power, FVR duration, and price for the regulation. Flexible power is the amount of power consumption that can be altered. Calculations of the flexible power are based on historical data by implementing the ARMA forecasting model. FVR duration estimations are based on the mass and energy balance analysis. It is achieved by considering the zone size, supply air, return air, and measurement data. The price for the service is calculated for up- and down-regulations separately. During up-regulations, it is crucial to consider buildings with higher usage. The regulation effect is more noticeable, thus causing it to be more expensive. During down-regulations, additional energy consumption is caused by increasing power consumption. It is compensated through a CO_2 concentration level where a higher concentration level provides lower regulation prices.

Flexibility management methods are needed to integrate loads like ventilation systems of different buildings (e.g., residential and commercial) into the flexibility service. However, the available methods described in research papers require further development for implementation in practice. Heating and cooling systems have received much attention from researchers, but the potential of ventilation systems has been left out of focus. Methods described in research papers lack robustness or do not give the building owners or aggregators clear guidelines on implementing these in their systems.

Validation of the developed methods was done with simulations and two case studies. Simulations used data generated with validated building models constructed in IDA ICE. All calculations were done, and the algorithm was written in Matlab. The primary outcomes of the validation process are:

- ARMA(p, q) model is sufficient to forecast ventilation system power consumption. The maximum forecast MAPE of 6.5% was observed with a single-family building with a stochastic occupancy profile. Also, the VAV type system was used for this case, which decreases the accuracy of the forecast.
- The open-loop approach to estimate FVR duration can be a viable option if the occupancy profile does not change over time and the aim is to minimize initial investment costs. From the results of the small room, the variance of residuals is low, but there is a bias that can be removed if parameters are adjusted to actual conditions.
- Placing sensors only in the AHU is also a viable option if the aim is to lower the initial investment costs. The residual analysis showed higher variability and lower accuracy than placing sensors in each room. Portable sensors could be used to improve the performance of this approach to tune the corrected boundaries.

- FVR duration estimations based on CO_2 concentration showed an RMSE of around 8 min when the fixed occupancy profile was selected and around 12 min when the stochastic occupancy profile was used. FVR duration estimations based on temperature showed an RMSE around 20 min for most scenarios. Therefore, temperature-based FVR duration is more difficult to estimate accurately, but it can be expected that the estimations will also become more accurate with shorter delivery periods. Relative humidity had no significant impact on the ventilation system's flexibility.
- The results showed that cost savings are achievable when a ventilation system is integrated into a flexibility service. In the apartment, up to 11% of cost savings were achieved; in the office, up to 15%; in the single-family house, up to 4%; and in the educational building, up to 37%. The cost savings heavily depend on how much the ventilation system can be exploited in the flexibility service. If the IAQ parameters are already near the limit, then there is less possibility to exploit the system in the flexibility service.
- A ventilation system as virtual energy storage is a viable approach to maximize energy capacity and revenue. VES approach can increase the total cost savings twofold compared to operating a ventilation system at a minimum ventilation rate during activation of the reserve.

At the beginning of this research, five main hypotheses were made. Therefore, based on the results discussed in this thesis, the following conclusions and remarks can be made:

1. The development of the ventilation system flexibility management method showed that the hypothesis is correct, as mass and energy balance analysis combined with sensor data enables the estimation of forced ventilation rate duration.
2. For most cases, the IAQ limits were not exceeded in more than 95% of situations when the reserve was activated. High CO_2 concentration in rooms and stochastic occupancy increase the probability that the IAQ limit will be exceeded during a regulation.
3. Most of the studied ventilation systems could provide more than half of the cases when the reserve is activated for at least 30 min, the maximum amount of power. The exception is the single-family house, where at least 30 min of FVR duration was achieved for around 35% of the cases. The high pollutant concentration caused this during normal conditions.
4. ARMA(p, q) models that forecast power consumption 24 h ahead had the MAPE less than 10% for all cases. FVR duration estimation errors of CO_2 concentration were mostly within 10 min, except for a single-family house where the RMSE was 13 minutes. However, temperature-based FVR durations are more challenging to estimate, and the RMSE of 20 min was observed.
5. At least 5% of the total cost reduction is possible with the flexibility service, but in some cases, it can be challenging to achieve. If the system is already operating at the limit, then there are fewer cost savings, but for the case study where the actual ventilation system was monitored, the cost savings could be up to 37%.

6.1 Future work

Future challenges in managing the flexibility of ventilation systems lie in improving and adapting the methods. Due to the complex nature of the problem and the urge to maximize the potential of ventilation systems in the flexibility service, the author has identified the following directions for further research on this topic:

- Identification of the zone volume should be achieved without measuring it separately. In some cases, the actual volume of the zone is difficult to measure due to furniture. Fluctuations in the CO_2 concentration can be used to achieve it.
- Using portable sensors and acquiring environment measurement data from smart devices can be a potential alternative to a dedicated sensor or can be employed to improve the accuracy of the calculations.
- Machine learning approaches can assist and improve the accuracy of the management methods addressed in this thesis. The more data is generated, the more accurate the estimations will be.
- While the methods have been validated in simulations and two case studies, it is crucial to implement this in a real system to further the investigation of the performance of the methods in different conditions.
- The developed pricing model to calculate the price for each activation needs to be further investigated and improved. One improvement is optimizing the profit margins to achieve an optimum between ventilation system exploitation and revenue generation.
- The focus is mainly on industrial and commercial consumers that can provide flexibility. However, methods and products to include households with smaller capacities to the flexibility service are needed.

List of figures

List of tables

References

[1] European Commission, “Renewable energy directive.” Accessed: May 20, 2021. [Online]. Available: https://ec.europa.eu/energy/topics/renewable-energy/renewable-energy-directive/overview_en

[2] European Commission. Statistical Office of the European Union., “Shedding light on energy in the EU : 2023 interactive publication.,” 2023.

[3] S. Kerscher and P. Arboleya, “The key role of aggregators in the energy transition under the latest European regulatory framework,” *International Journal of Electrical Power and Energy Systems*, vol. 134, no. July 2021, p. 107361, 2022, doi: 10.1016/j.ijepes.2021.107361.

[4] Elering AS, “Sünkroniseerimine Mandri-Euroopaga.” Accessed: May 20, 2021. [Online]. Available: https://elering.ee/sunkroniseerimine

[5] European Commission, “Energy performance of buildings directive.” Accessed: May 20, 2021. [Online]. Available: https://ec.europa.eu/energy/topics/energy-efficiency/energy-efficient-buildings/energy-performance-buildings-directive

[6] Estonian Government, “Minimum requirements for energy performance,” Riigi Teataja. Accessed: May 20, 2021. [Online]. Available: https://www.riigiteataja.ee/en/eli/520102014001

[7] Eurelectric, “Flexibility and aggregation - requirements for their interaction in the market,” 2014.

[8] J. Song, Y. Lee, and E. Hwang, “Time-Frequency Mask Estimation Based on Deep Neural Network for Flexible Load Disaggregation in Buildings,” *IEEE Trans Smart Grid*, vol. 12, no. 4, pp. 3242–3251, Jul. 2021, doi: 10.1109/TSG.2021.3066547.

[9] Z. Li, S. Su, X. Jin, H. Chen, Y. Li, and R. Zhang, “A hierarchical scheduling method of active distribution network considering flexible loads in office buildings,” *International Journal of Electrical Power & Energy Systems*, vol. 131, p. 106768, Oct. 2021, doi: 10.1016/J.IJEPES.2021.106768.

[10] F. Mancini, G. lo Basso, and L. de Santoli, “Energy Use in Residential Buildings: Characterisation for Identifying Flexible Loads by Means of a Questionnaire Survey,” *Energies 2019, Vol. 12, Page 2055*, vol. 12, no. 11, p. 2055, May 2019, doi: 10.3390/EN12112055.

[11] I. Drovtar, J. Niitsoo, A. Rosin, J. Kilter, and I. Palu, “Electricity consumption analysis and power quality monitoring in commercial buildings,” *PQ 2012: 8th International Conference - 2012 Electric Power Quality and Supply Reliability, Conference Proceedings*, pp. 107–112, 2012.

[12] M. Gil-Baez, Á. Barrios-Padura, M. Molina-Huelva, and R. Chacartegui, “Natural ventilation systems in 21st-century for near zero energy school buildings,” *Energy*, vol. 137, pp. 1186–1200, Oct. 2017, doi: 10.1016/J.ENERGY.2017.05.188.

[13] U.S. Department of Energy, “Whole-House Ventilation.” Accessed: Dec. 01, 2021. [Online]. Available: https://www.energy.gov/energysaver/whole-house-ventilation

[14] D. Burmester, R. Rayudu, W. Seah, and D. Akinyele, “A review of nanogrid topologies and technologies,” *Renewable and Sustainable Energy Reviews*, vol. 67, pp. 760–775, Jan. 2017, doi: 10.1016/J.RSER.2016.09.073.

[15] A. Burgio, D. Menniti, N. Sorrentino, A. Pinnarelli, and M. Motta, “A compact nanogrid for home applications with a behaviour-tree-based central controller,” *Appl Energy*, vol. 225, pp. 14–26, Sep. 2018, doi: 10.1016/J.APENERGY.2018.04.082.

[16] Y. Han, X. Xie, H. Deng, and W. Ma, “Central energy management method for photovoltaic DC micro-grid system based on power tracking control,” *IET Renewable Power Generation*, vol. 11, no. 8, pp. 1138–1147, Jun. 2017, doi: 10.1049/IET-RPG.2016.0351.

[17] M. Movahednia, H. Karimi, and S. Jadid, “Optimal hierarchical energy management scheme for networked microgrids considering uncertainties, demand response, and adjustable power,” *IET Generation, Transmission & Distribution*, vol. 14, no. 20, pp. 4352–4362, Oct. 2020, doi: 10.1049/IET-GTD.2020.0287.

[18] Statistics Estonia, “Granted building permits and completed buildings.”

[19] Ettevõtlus- ja infotehnoloogiaminister, “Hoone energiatõhususe miinimumnõuded,” Riigi Teataja. Accessed: Jan. 03, 2022. [Online]. Available: https://www.riigiteataja.ee/akt/113122018014?leiaKehtiv

[20] H. Kuivjõgi, A. Uutar, K. Kuusk, M. Thalfeldt, and J. Kurnitski, “Market based renovation solutions in non-residential buildings – Why commercial buildings are not renovated to NZEB,” *Energy Build*, vol. 248, Oct. 2021, doi: 10.1016/J.ENBUILD.2021.111169.

[21] H. Hao, Y. Lin, A. S. Kowli, P. Barooah, and S. Meyn, “Ancillary Service to the grid through control of fans in commercial Building HVAC systems,” *IEEE Trans Smart Grid*, vol. 5, no. 4, pp. 2066–2074, 2014.

[22] Elering AS, Augstsprieguma tīkls AS, and Litgrid AB, “Baltic Transparency Dashboard.” Accessed: May 22, 2023. [Online]. Available: https://baltic.transparency-dashboard.eu/

[23] Elering AS, “Elering Live.” Accessed: May 22, 2023. [Online]. Available: https://dashboard.elering.ee/en

[24] T. Freire-Barceló, F. Martín-Martínez, and Á. Sánchez-Miralles, “A literature review of Explicit Demand Flexibility providing energy services,” *Electric Power Systems Research*, vol. 209, p. 107953, Aug. 2022, doi: 10.1016/J.EPSR.2022.107953.

[25] I. Mamounakis, D. J. Vergados, P. Makris, E. Varvarigos, and T. Mavridis, “A Virtual MicroGrid platform for the efficient orchestration of multiple energy prosumers,” *ACM International Conference Proceeding Series*, vol. 01-03-October-2015, pp. 191–196, Oct. 2015, doi: 10.1145/2801948.2802012.

[26] A. F. Meyabadi and M. H. Deihimi, “A review of demand-side management: Reconsidering theoretical framework,” *Renewable and Sustainable Energy Reviews*, vol. 80, pp. 367–379, Dec. 2017, doi: 10.1016/J.RSER.2017.05.207.

[27] Pöyry and Imperial College London, “Roadmap for flexibility services to 2030 - A report to the Committee on Climate Change,” 2017.

[28] E. Ercan and E. Kentel, “Optimum daily operation of a wind-hydro hybrid system,” *J Energy Storage*, vol. 50, Jun. 2022, doi: 10.1016/J.EST.2022.104540.

[29] M. M. Bertsiou and E. Baltas, “Management of energy and water resources by minimizing the rejected renewable energy,” *Sustainable Energy Technologies and Assessments*, vol. 52, Aug. 2022, doi: 10.1016/J.SETA.2022.102002.

[30] J. H. Halleraker, M. S. Kenawi, J. H. L’Abée-Lund, T. H. Bakken, and K. Alfredsen, “Assessment of flow ramping in water bodies impacted by hydropower operation in Norway – Is hydropower with environmental restrictions more sustainable?,” *Science of The Total Environment*, vol. 832, p. 154776, Aug. 2022, doi: 10.1016/J.SCITOTENV.2022.154776.

[31] Y. Qiu and F. Jiang, “A review on passive and active strategies of enhancing the safety of lithium-ion batteries,” *Int J Heat Mass Transf*, vol. 184, Mar. 2022, doi: 10.1016/J.IJHEATMASSTRANSFER.2021.122288.

[32] K. W. See *et al.*, “Critical review and functional safety of a battery management system for large-scale lithium-ion battery pack technologies,” *Int J Coal Sci Technol*, vol. 9, no. 1, Dec. 2022, doi: 10.1007/S40789-022-00494-0.

[33] IEA, “World electricity final consumption by sector, 1974-2019, IEA, Paris.” Accessed: Sep. 10, 2021. [Online]. Available: https://www.iea.org/data-and-statistics/charts/world-electricity-final-consumption-by-sector-1974-2019

[34] Global Alliance for Buildings and Construction, “2020 global status report for buildings and construction - towards a zero-emissions, efficient and resilient buildings and construction sector,” 2020. Accessed: Sep. 09, 2022. [Online]. Available: www.globalabc.org.

[35] European Commission, “EU Buildings Factsheets.” Accessed: Sep. 11, 2021. [Online]. Available: https://ec.europa.eu/energy/eu-buildings-factsheets_en

[36] A. R. Coffman, Z. Guo, and P. Barooah, “Characterizing Capacity of Flexible Loads for Providing Grid Support,” *IEEE Transactions on Power Systems*, vol. 36, no. 3, pp. 2428–2437, May 2021, doi: 10.1109/TPWRS.2020.3033380.

[37] H. Tang, S. Wang, and H. Li, “Flexibility categorization, sources, capabilities and technologies for energy-flexible and grid-responsive buildings: State-of-the-art and future perspective,” *Energy*, vol. 219, Mar. 2021, doi: 10.1016/j.energy.2020.119598.

[38] T. Kaschub, P. Jochem, and W. Fichtner, “Solar energy storage in German households: profitability, load changes and flexibility,” *Energy Policy*, vol. 98, pp. 520–532, Nov. 2016, doi: 10.1016/J.ENPOL.2016.09.017.

[39] R. Luthander, J. Widén, D. Nilsson, and J. Palm, “Photovoltaic self-consumption in buildings: A review,” *Appl Energy*, vol. 142, pp. 80–94, Mar. 2015, doi: 10.1016/J.APENERGY.2014.12.028.

[40] R. Kempener, “Clean Energy Solutions Center | Battery Storage for Renewables: Market Status and Technology Outlook,” Abu Dhabi, 2015. Accessed: Aug. 26, 2022. [Online]. Available: https://cleanenergysolutions.org/resources/battery-storage-renewables-market-status-technology-outlook

[41] M. A. López, S. de La Torre, S. Martín, and J. A. Aguado, “Demand-side management in smart grid operation considering electric vehicles load shifting and vehicle-to-grid support,” *International Journal of Electrical Power & Energy Systems*, vol. 64, pp. 689–698, Jan. 2015, doi: 10.1016/J.IJEPES.2014.07.065.

[42] X. Han, T. Ji, Z. Zhao, and H. Zhang, “Economic evaluation of batteries planning in energy storage power stations for load shifting,” *Renew Energy*, vol. 78, pp. 643–647, Jun. 2015, doi: 10.1016/J.RENENE.2015.01.056.

[43] Q. A. Phan, T. Scully, M. Breen, and M. D. Murphy, “Determination of optimal battery utilization to minimize operating costs for a grid-connected building with renewable energy sources,” *Energy Convers Manag*, vol. 174, pp. 157–174, Oct. 2018, doi: 10.1016/J.ENCONMAN.2018.07.081.

[44] G. He, Q. Chen, C. Kang, Q. Xia, and K. Poolla, “Cooperation of Wind Power and Battery Storage to Provide Frequency Regulation in Power Markets,” *IEEE Transactions on Power Systems*, vol. 32, no. 5, pp. 3559–3568, Sep. 2017, doi: 10.1109/TPWRS.2016.2644642.

[45] I. H. Yang and E. J. Nam, “Economic analysis of the daylight-linked lighting control system in office buildings,” *Solar Energy*, vol. 84, no. 8, pp. 1513–1525, Aug. 2010, doi: 10.1016/J.SOLENER.2010.05.014.

[46] F. Rubinstein, L. Xiaolei, and D. S. Watson, “Using Dimmable Lighting for Regulation Capacity and Contingency Reserves in the Ancillary Services Market. A Feasibility Study,” 2010. Accessed: Sep. 01, 2022. [Online]. Available: https://www.osti.gov/servlets/purl/1004218

[47] A. Arteconi *et al.*, “Thermal energy storage coupled with PV panels for demand side management of industrial building cooling loads,” *Appl Energy*, vol. 185, pp. 1984–1993, Jan. 2017, doi: 10.1016/J.APENERGY.2016.01.025.

[48] S. H. Kim, “An evaluation of robust controls for passive building thermal mass and mechanical thermal energy storage under uncertainty,” *Appl Energy*, vol. 111, pp. 602–623, Nov. 2013, doi: 10.1016/J.APENERGY.2013.05.030.

[49] E. Nyholm, S. Puranik, É. Mata, M. Odenberger, and F. Johnsson, “Demand response potential of electrical space heating in Swedish single-family dwellings,” *Build Environ*, vol. 96, pp. 270–282, Feb. 2016, doi: 10.1016/J.BUILDENV.2015.11.019.

[50] B. Kirby, J. Kueck, T. Laughner, and K. Morris, “Spinning Reserve from Hotel Load Response,” *The Electricity Journal*, vol. 21, no. 10, pp. 59–66, Dec. 2008, doi: 10.1016/J.TEJ.2008.11.004.

[51] J. Bode, M. Sullivan, and J. H. Eto, “Measuring Short-term Air Conditioner Demand Reductions for Operations and Settlement | Electricity Markets and Policy Group,” Berkeley, 2012. Accessed: Sep. 02, 2022. [Online]. Available: https://emp.lbl.gov/publications/measuring-short-term-air-conditioner

[52] J. Cai and J. E. Braun, “A regulation capacity reset strategy for HVAC frequency regulation control,” *Energy Build*, vol. 185, pp. 272–286, Feb. 2019, doi: 10.1016/J.ENBUILD.2018.12.018.

[53] H. Hao, Y. Lin, A. S. Kowli, P. Barooah, and S. Meyn, “Ancillary Service to the grid through control of fans in commercial Building HVAC systems,” *IEEE Trans Smart Grid*, vol. 5, no. 4, pp. 2066–2074, 2014, doi: 10.1109/TSG.2014.2322604.

[54] R. D’hulst, W. Labeeuw, B. Beusen, S. Claessens, G. Deconinck, and K. Vanthournout, “Demand response flexibility and flexibility potential of residential smart appliances: Experiences from large pilot test in Belgium,” *Appl Energy*, vol. 155, pp. 79–90, Oct. 2015, doi: 10.1016/J.APENERGY.2015.05.101.

[55] D. Setlhaolo, X. Xia, and J. Zhang, “Optimal scheduling of household appliances for demand response,” *Electric Power Systems Research*, vol. 116, pp. 24–28, Nov. 2014, doi: 10.1016/J.EPSR.2014.04.012.

[56] European Smart Grids Task Force Expert Group 3, “Demand Side Flexibility Perceived barriers and proposed recommendations,” 2019.

[57] R. Kucęba, “Dimensions and Factors that Determine Integration of Small-Scale Sources in the Structures of Virtual Power Plants,” *Production Engineering Archives*, vol. 28, no. 2, pp. 185–192, Jun. 2022, doi: 10.30657/PEA.2022.28.22.

[58] S. Awerbuch and A. Preston, *The Virtual Utility*. Springer US, 1997. doi: 10.1007/978-1-4615-6167-5.

[59] M. Ferrara, A. Violi, P. Beraldi, G. Carrozzino, and T. Ciano, “An integrated decision approach for energy procurement and tariff definition for prosumers aggregations,” *Energy Econ*, vol. 97, p. 105034, May 2021, doi: 10.1016/J.ENECO.2020.105034.

[60] T. Freire-Barceló, F. Martín-Martínez, and Á. Sánchez-Miralles, "A literature review of Explicit Demand Flexibility providing energy services," *Electric Power Systems Research*, vol. 209, Aug. 2022, doi: 10.1016/J.EPSR.2022.107953.

[61] M. Kubli and P. Canzi, "Business strategies for flexibility aggregators to steer clear of being 'too small to bid,'" *Renewable and Sustainable Energy Reviews*, vol. 143, p. 110908, Jun. 2021, doi: 10.1016/J.RSER.2021.110908.

[62] "USEF: WORK STREAM ON AGGREGATOR IMPLEMENTATION MODELS Recommended practices and key considerations for a regulatory framework and market design on explicit Demand Response A solid foundation for smart energy futures".

[63] "Demand Response Activation by Independent Aggregators As Proposed in the Draft Electricity Directive On behalf of EURELECTRIC", Accessed: Sep. 08, 2022. [Online]. Available: www.dnvgl.com

[64] P. Barooah, "Smart Grid Control: Overview and Research Opportunities," J. Stoustrup, A. Annaswamy, A. Chakrabortty, and Z. Qu, Eds., in Power Electronics and Power Systems. Cham: Springer International Publishing, 2019. doi: 10.1007/978-3-319-98310-3.

[65] G. Parkinson, "UBS: closures coal and gas fired power plants in Europe accelerating." Accessed: Sep. 05, 2020. [Online]. Available: https://energypost.eu/ubs-closures-coal-gas-fired-power-plants-europe-accelerating/

[66] T. Kim *et al.*, "An Overview of Cyber-Physical Security of Battery Management Systems and Adoption of Blockchain Technology," *IEEE J Emerg Sel Top Power Electron*, vol. 10, no. 1, pp. 1270–1281, Feb. 2022, doi: 10.1109/JESTPE.2020.2968490.

[67] X. Lai *et al.*, "Critical review of life cycle assessment of lithium-ion batteries for electric vehicles: A lifespan perspective," *eTransportation*, vol. 12, May 2022, doi: 10.1016/J.ETRAN.2022.100169.

[68] T. Raj *et al.*, "Recycling of cathode material from spent lithium-ion batteries: Challenges and future perspectives," *J Hazard Mater*, vol. 429, p. 128312, May 2022, doi: 10.1016/J.JHAZMAT.2022.128312.

[69] L. Meng *et al.*, "Large-Scale Li-Ion Battery Research and Application in Mining Industry," *Energies 2022, Vol. 15, Page 3884*, vol. 15, no. 11, p. 3884, May 2022, doi: 10.3390/EN15113884.

[70] K. W. See *et al.*, "Critical review and functional safety of a battery management system for large-scale lithium-ion battery pack technologies," *Int J Coal Sci Technol*, vol. 9, no. 3, p. 36, 2022, doi: 10.1007/s40789-022-00494-0.

[71] S. Meyn, P. Barooah, A. Bušić, and J. Ehren, "Ancillary service to the grid from deferrable loads: The case for intelligent pool pumps in Florida," *Proceedings of the IEEE Conference on Decision and Control*, pp. 6946–6953, 2013, doi: 10.1109/CDC.2013.6760990.

[72] A. Nayyar, M. Negrete-Pincetic, K. Poolla, and P. Varaiya, "Duration-Differentiated Energy Services with a Continuum of Loads," *IEEE Trans Control Netw Syst*, vol. 3, no. 2, pp. 182–191, Jun. 2016, doi: 10.1109/TCNS.2015.2428491.

[73] A. R. Coffman, Z. Guo, and P. Barooah, "Capacity of flexible loads for grid support: Statistical characterization for long term planning," *Proceedings of the American Control Conference*, vol. 2020-July, pp. 533–538, Jul. 2020, doi: 10.23919/ACC45564.2020.9147252.

[74] H. Hao, B. M. Sanandaji, K. Poolla, and T. L. Vincent, “Aggregate flexibility of thermostatically controlled loads,” *IEEE Transactions on Power Systems*, vol. 30, no. 1, pp. 189–198, Jan. 2015, doi: 10.1109/TPWRS.2014.2328865.

[75] A. R. Coffman, A. Busic, and P. Barooah, “Aggregate capacity for TCLs providing virtual energy storage with cycling constraints,” *Proceedings of the IEEE Conference on Decision and Control*, vol. 2019-December, pp. 4208–4215, Dec. 2019, doi: 10.1109/CDC40024.2019.9028939.

[76] S. Kundu, K. Kalsi, and S. Backhaus, “Approximating flexibility in distributed energy resources: A geometric approach,” *20th Power Systems Computation Conference, PSCC 2018*, Aug. 2018, doi: 10.23919/PSCC.2018.8442600.

[77] F. Lin and V. Adetola, “Flexibility characterization of multi-zone buildings via distributed optimization,” *Proceedings of the American Control Conference*, vol. 2018-June, pp. 5412–5417, Aug. 2018, doi: 10.23919/ACC.2018.8431400.

[78] “EUR-Lex - 32017R2195 - EN - EUR-Lex.” Accessed: Sep. 08, 2022. [Online]. Available: https://eur-lex.europa.eu/legal-content/EN/TXT/?uri=CELEX%3A32017R2195

[79] A. Uk, “DEMAND RESPONSE PARTICIPATION IN DIFFERENT MARKETS IN EUROPE CORE View metadata, citation and similar papers at core,” 2019.

[80] “ACER’s Final Assessment of the EU Wholesale Electricity Market Design,” 2022.

[81] AS “Augstsprieguma tīkls,” E. AS, and L. AB, “Baltic Load-Frequency Control block concept document,” p. 69, 2020, [Online]. Available: https://www.ast.lv/sites/default/files/editor/Baltic_Load_Frequency_Control_concept_document.pdf

[82] “PICASSO.” Accessed: Sep. 08, 2022. [Online]. Available: https://www.entsoe.eu/network_codes/eb/picasso/

[83] “Manually Activated Reserves Initiative.” Accessed: Sep. 08, 2022. [Online]. Available: https://www.entsoe.eu/network_codes/eb/mari/

[84] “TERRE.” Accessed: Sep. 08, 2022. [Online]. Available: https://www.entsoe.eu/network_codes/eb/terre/

[85] Elering AS, AS “Augstsprieguma tīkls,” and LITGRID AB, “Baltic balancing market rules,” 2020.

[86] F. Plaum, R. Ahmadiahangar, A. Rosin, and J. Kilter, “Aggregated demand-side energy flexibility: A comprehensive review on characterization, forecasting and market prospects,” *Energy Reports*, vol. 8, pp. 9344–9362, Nov. 2022, doi: 10.1016/J.EGYR.2022.07.038.

[87] F. Amara *et al.*, “Comparison and Simulation of Building Thermal Models for Effective Energy Management,” *Smart Grid and Renewable Energy*, vol. 6, no. 4, pp. 95–112, Apr. 2015, doi: 10.4236/SGRE.2015.64009.

[88] B. Lehmann, D. Gyalistras, M. Gwerder, K. Wirth, and S. Carl, “Intermediate complexity model for Model Predictive Control of Integrated Room Automation,” *Energy Build*, vol. 58, pp. 250–262, Mar. 2013, doi: 10.1016/J.ENBUILD.2012.12.007.

[89] A. Mirakhorli and B. Dong, “Model predictive control for building loads connected with a residential distribution grid,” *Appl Energy*, vol. 230, pp. 627–642, Nov. 2018, doi: 10.1016/J.APENERGY.2018.08.051.

[90] E. Vrettos, F. Oldewurtel, M. Vasirani, and G. Andersson, “Centralized and decentralized balance group optimization in electricity markets with demand response,” *2013 IEEE Grenoble Conference PowerTech, POWERTECH 2013*, 2013, doi: 10.1109/PTC.2013.6652519.

[91] X. Li, J. Wen, and E. W. Bai, “Building energy forecasting using system identification based on system characteristics test,” *2015 Workshop on Modeling and Simulation of Cyber-Physical Energy Systems, MSCPES 2015 - Held as Part of CPS Week, Proceedings*, May 2015, doi: 10.1109/MSCPES.2015.7115401.

[92] X. Li and J. Wen, “Review of building energy modeling for control and operation,” *Renewable and Sustainable Energy Reviews*, vol. 37, pp. 517–537, Sep. 2014, doi: 10.1016/J.RSER.2014.05.056.

[93] A. Kathirgamanathan, M. De Rosa, E. Mangina, and D. P. Finn, “Feature Assessment in Data-driven Models for unlocking Building Energy Flexibility”, doi: 10.26868/25222708.2019.210591.

[94] R. Yin *et al.*, “Quantifying flexibility of commercial and residential loads for demand response using setpoint changes,” *Appl Energy*, vol. 177, pp. 149–164, Sep. 2016, doi: 10.1016/J.APENERGY.2016.05.090.

[95] E. C. Kara, M. D. Tabone, J. S. MacDonald, D. S. Callaway, and S. Kiliccote, “Quantifying flexibility of residential thermostatically controlled loads for demand response: A data-driven approach,” *BuildSys 2014 - Proceedings of the 1st ACM Conference on Embedded Systems for Energy-Efficient Buildings*, pp. 140–147, Nov. 2014, doi: 10.1145/2674061.2674082.

[96] M. Behl, F. Smarra, and R. Mangharam, “DR-Advisor: A data-driven demand response recommender system,” *Appl Energy*, vol. 170, pp. 30–46, May 2016, doi: 10.1016/J.APENERGY.2016.02.090.

[97] D. S. Kapetanakis, O. Neu, and D. P. Finn, “Prediction of Residential Building Demand Response Potential Using Data-Driven Techniques,” *Building Simulation Conference Proceedings*, vol. 15, pp. 1656–1666, 2017, doi: 10.26868/25222708.2017.439.

[98] S. Prívara, Z. Váňa, E. Žáčeková, and J. Cigler, “Building modeling: Selection of the most appropriate model for predictive control,” *Energy Build*, vol. 55, pp. 341–350, Dec. 2012, doi: 10.1016/J.ENBUILD.2012.08.040.

[99] S. Prívara, J. Cigler, Z. Váňa, F. Oldewurtel, C. Sagerschnig, and E. Žáčeková, “Building modeling as a crucial part for building predictive control,” *Energy Build*, vol. 56, pp. 8–22, Jan. 2013, doi: 10.1016/J.ENBUILD.2012.10.024.

[100] P. Bacher and H. Madsen, “Identifying suitable models for the heat dynamics of buildings,” *Energy Build*, vol. 43, no. 7, pp. 1511–1522, Jul. 2011, doi: 10.1016/J.ENBUILD.2011.02.005.

[101] Z. Wang and Y. Chen, “Data-driven modeling of building thermal dynamics: Methodology and state of the art,” *Energy Build*, vol. 203, p. 109405, Nov. 2019, doi: 10.1016/J.ENBUILD.2019.109405.

[102] A. Kathirgamanathan, M. De Rosa, E. Mangina, and D. P. Finn, “Data-driven predictive control for unlocking building energy flexibility: A review,” *Renewable and Sustainable Energy Reviews*, vol. 135, Jan. 2021, doi: 10.1016/J.RSER.2020.110120.

[103] L. H. M. Truong *et al.*, “Accurate prediction of hourly energy consumption in a residential building based on the occupancy rate using machine learning approaches,” *Applied Sciences (Switzerland)*, vol. 11, no. 5, pp. 1–19, Mar. 2021, doi: 10.3390/app11052229.

[104] I. Walker, B. Less, D. Lorenzetti, and M. D. Sohn, “Development of Advanced Smart Ventilation Controls for Residential Applications,” *Energies 2021, Vol. 14, Page 5257*, vol. 14, no. 17, p. 5257, Aug. 2021, doi: 10.3390/EN14175257.

[105] J. Li, J. Wall, and G. Platt, “Indoor air quality control of HVAC system,” *Proceedings of the 2010 International Conference on Modelling, Identification and Control*, pp. 756–761, 2010.

[106] European Standard, “UNE-EN 15251:2008. Indoor environmental input parameters for design and assessment of energy performance of buildings addressing indoor air quality, thermal environment, lighting and acoustics,” *Aenor*, pp. 1–52, 2008, doi: 10.1520/E2019-03R13.Copyright.

[107] V. L. Erickson and A. E. Cerpa, “Occupancy based demand response HVAC control strategy,” *2nd ACM Workshop on Embedded Sensing Systems for Energy-Efficiency in Buildings (BuildSys’10)*, pp. 7–12, 2010, doi: 10.1145/1878431.1878434.

[108] Z. Yang, B. Becerik-Gerber, N. Li, and M. Orosz, “A systematic approach to occupancy modeling in ambient sensor-rich buildings,” *Simulation*, vol. 90, no. 8, pp. 960–977, 2014, doi: 10.1177/0037549713489918.

[109] Z. Shi, X. Li, and S. Hu, “Direct feedback linearization based control of CO2 demand controlled ventilation,” *ICCET 2010 - 2010 International Conference on Computer Engineering and Technology, Proceedings*, vol. 2, pp. 571–574, 2010, doi: 10.1109/ICCET.2010.5485621.

[110] L. Yu, D. Xie, C. Huang, T. Jiang, and Y. Zou, “Energy Optimization of HVAC Systems in Commercial Buildings Considering Indoor Air Quality Management,” *IEEE Trans Smart Grid*, vol. 10, no. 5, pp. 5103–5113, Sep. 2019, doi: 10.1109/TSG.2018.2875727.

[111] C. Luppe and A. Shabani, “Towards reliable intelligent occupancy detection for smart building applications,” *Canadian Conference on Electrical and Computer Engineering*, pp. 0–3, 2017, doi: 10.1109/CCECE.2017.7946831.

[112] Ettevõtlus- ja infotehnoloogiaminister, “Hoone energiatõhususe miinimumnõuded,” Riigi Teataja. Accessed: Aug. 16, 2023. [Online]. Available: https://www.riigiteataja.ee/akt/113122018014

[113] S. Rauf, A. R. Kalair, and N. Khan, “Variable Load Demand Scheme for Hybrid AC/DC Nanogrid,” *International Journal of Photoenergy*, vol. 2020, 2020, doi: 10.1155/2020/3646423.

[114] I. Roasto, T. Jalakas, and A. Rosin, “Bidirectional Operation of the Power Electronic Interface for Nearly-Zero Energy Buildings,” *2018 20th European Conference on Power Electronics and Applications, EPE 2018 ECCE Europe*, p. 2021, 2018.

[115] L. Martirano, E. Habib, A. Giuseppi, and A. di Giorgio, “Nearly zero energy building model predictive control for efficient heating,” *2018 IEEE Industry Applications Society Annual Meeting, IAS 2018*, pp. 6–11, 2018, doi: 10.1109/IAS.2018.8544632.

[116] E. Hamatwi, I. E. Davidson, J. Agee, and G. Venayagamoorthy, “Model of a hybrid distributed generation system for a DC nano-grid,” *Clemson University Power Systems Conference, PSC 2016*, Apr. 2016, doi: 10.1109/PSC.2016.7462851.

[117] S. Teleke, L. Oehlerking, and M. Hong, “Nanogrids with energy storage for future electricity grids,” *Proceedings of the IEEE Power Engineering Society Transmission and Distribution Conference*, p. 2021, 2014, doi: 10.1109/tdc.2014.6863235.

[118] M. Najafzadeh, I. Roasto, and T. Jalakas, “Energy Router Based Energy Management System for Nearly Zero Energy Buildings,” *2019 IEEE 60th Annual International Scientific Conference on Power and Electrical Engineering of Riga Technical University, RTUCON 2019 - Proceedings*, no. October 2014, pp. 5–10, 2019, doi: 10.1109/RTUCON48111.2019.8982366.

[119] I. Roasto, T. Jalakas, and A. Rosin, “Control of bidirectional grid-forming inverter for nearly zero energy buildings,” *2018 IEEE 59th Annual International Scientific Conference on Power and Electrical Engineering of Riga Technical University, RTUCON 2018 - Proceedings*, 2018, doi: 10.1109/RTUCON.2018.8659848.

[120] I. Roasto, O. Husev, M. Najafzadeh, T. Jalakas, and J. Rodriguez, “Voltage Source Operation of the Energy-Router Based on Model Predictive Control,” *Energies 2019, Vol. 12, Page 1892*, vol. 12, no. 10, p. 1892, May 2019, doi: 10.3390/EN12101892.

[121] I. Cvetkovic *et al.*, “A testbed for experimental validation of a low-voltage DC nanogrid for buildings,” *15th International Power Electronics and Motion Control Conference and Exposition, EPE-PEMC 2012 ECCE Europe*, 2012, doi: 10.1109/EPEPEMC.2012.6397514.

[122] I. Roasto, A. Rosin, and T. Jalakas, “Multiport interface converter with an energy storage for nanogrids,” *Proceedings: IECON 2018 - 44th Annual Conference of the IEEE Industrial Electronics Society*, pp. 6088–6093, Dec. 2018, doi: 10.1109/IECON.2018.8591104.

[123] Y. Chen *et al.*, “Quantification of electricity flexibility in demand response: Office building case study,” *Energy*, vol. 188, Dec. 2019, doi: 10.1016/J.ENERGY.2019.116054.

[124] R. v. Klyuev *et al.*, “Methods of Forecasting Electric Energy Consumption: A Literature Review,” *Energies (Basel)*, vol. 15, no. 23, Dec. 2022, doi: 10.3390/EN15238919.

[125] S. Rotger-Griful, R. H. Jacobsen, D. Nguyen, and G. Sørensen, “Demand response potential of ventilation systems in residential buildings,” *Energy Build*, vol. 121, pp. 1–10, 2016.

[126] A. Nielsen, *Practical Time Series Analysis*. O’Reilly Media, Inc., 2019. Accessed: Jan. 23, 2022. [Online]. Available: https://learning.oreilly.com/library/view/practical-time-series/9781492041641/?ar=

[127] Estonian Centre of Standardisation and Accreditation, “EVS-EN 16798-1:2019+NA:2019 Energy performance of buildings - Ventilation for buildings - Part 1: Indoor environmental input parameters for design and assessment of energy performance of buildings addressing indoor air quality, thermal environment, lighting and acoustics - Module M1-6,” 2019.

[128] ASHRAE, *2013 ASHARE Handbook - Fundamentals*. Atlanta, 2013.

[129] Vaisala, “HUMIDITY CONVERSION FORMULAS - Calculation formulas for humidity,” *Humidity Conversion Formulas*, p. 16, 2013, [Online]. Available: https://www.vaisala.com/sites/default/files/documents/Humidity_Conversion_Formulas_B210973EN-F.pdf

[130] A. Tenwolde and C. L. Pilon, “The Effect of Indoor Humidity on Water Vapor Release in Homes,” *30 Years of Research Proceedings Thermal Performance of the Exterior Envelopes of Whole Buildings X*, pp. 1–9, 2007, [Online]. Available: http://originwww.fpl.fs.fed.us/documnts/pdf2007/fpl_2007_tenwolde001.pdf

[131] P. Lutolf, M. Scherer, O. Megel, M. Geidl, and E. Vrettos, “Rebound effects of demand-response management for frequency restoration,” *2018 IEEE International Energy Conference, ENERGYCON 2018*, pp. 1–6, Jun. 2018, doi: 10.1109/ENERGYCON.2018.8398849.

[132] Trane, “CO2-based demand-controlled ventilation with ASHRAE Standard 62.1-2004,” 2005, [Online]. Available: https://www.trane.com/content/dam/Trane/Commercial/global/products-systems/education-training/engineers-newsletters/standards-codes/admapn017en_1005.pdf
[133] J. Kurnitski, A. Saari, T. Kalamees, M. Vuolle, J. Niemelä, and T. Tark, “Cost optimal and nearly zero (nZEB) energy performance calculations for residential buildings with REHVA definition for nZEB national implementation,” *Energy Build*, vol. 43, no. 11, pp. 3279–3288, Nov. 2011, doi: 10.1016/J.ENBUILD.2011.08.033.
[134] “Validation & certifications - Simulation Software | EQUA.” [Online]. Available: https://www.equa.se/en/ida-ice/validation-certifications
[135] “Liginullenergia eluhooned, väikemajad,” Tallinn, 2017.
[136] RAUSI OÜ and HEVAC OÜ, “Liginullenergia eluhooned, väike eramu. Päikese-elektrisüsteem, tugevvool. Variant 2,” 2017. [Online]. Available: https://kredex.ee/sites/default/files/2019-03/PV_ja_tugevvool_variant_2.pdf
[137] Roofit Solar Energy OÜ, “Liginullenergia eluhooned, väike eramu. Päikese-elektrisüsteem, tugevvool. Variant 1,” 2017. [Online]. Available: https://kredex.ee/sites/default/files/2019-03/PV_ja_tugevvool_variant_1.pdf
[138] Hevac OÜ, “Liginullenergia eluhooned, väike eramu. Soojusvarustus, küte ja ventilatsioon,” 2017. [Online]. Available: https://kredex.ee/sites/default/files/2019-03/Kute_ja_ventilatsioon_3.pdf
[139] TTÜ, “Liginullenergia eluhooned, väike eramu. Energiatõhusus,” 2017. [Online]. Available: https://kredex.ee/sites/default/files/2019-03/Energiatohusus_3.pdf
[140] Tibeco Woodhouse OÜ, “Liginullenergia eluhooned, väike eramu. Arhitektuur,” 2017. [Online]. Available: https://kredex.ee/sites/default/files/2019-03/Arhitektuur_3.pdf
[141] Statistics Estonia, “Dwellings and buildings with dwellings,” Estonia counts 2021. [Online]. Available: https://rahvaloendus.ee/en/results/dwellings-and-buildings-dwellings
[142] T. Häring, T. M. Kull, R. Ahmadiahangar, A. Rosin, M. Thalfeldt, and H. Biechl, “Microgrid Oriented modeling of space heating system based on neural networks,” *Journal of Building Engineering*, vol. 43, p. 103150, Nov. 2021, doi: 10.1016/J.JOBE.2021.103150.
[143] S. Wolf, D. Calì, and M. J. Alonso, “ProccS - An occupancy simulation tool for private households,” 2019. Accessed: Feb. 23, 2022. [Online]. Available: https://www.proccs.org/
[144] Elering AS, “The prequalification process and technical requirements of Manual Frequency Restoration Reserves (mFRR) Service,” 2022. [Online]. Available: https://elering.ee/sites/default/files/2022-07/mFRR%20service_prequalification%20process%20and%20technical%20requirements_20220722.pdf
[145] T. Heinsoo, “Indoor air quality assessment in rooms serviced by a constant air flow ventilation systems,” 2022. Accessed: Aug. 15, 2023. [Online]. Available: https://digikogu.taltech.ee/et/item/d68408fa-c822-4dbb-a22d-18394a4993ed
[146] Onset Computer Corporation, “HOBO MX CO2 Logger (MX1102A) Manual,” 2019. Accessed: Aug. 15, 2023. [Online]. Available: www.onsetcomp.com

Acknowledgements

Primarily, I would like to thank my family for their support and encouragement in my decision to study at Tallinn University of Technology and pursue a doctoral degree. Thank you all my loved family in Võrumaa and friends who have joined and traveled with me on this journey. I thank my parents, Ove and Vaike, who raised me and funded my education. I thank the rest of my family and friends for their support and presence.

I want to thank my supervisors for their counseling and support. I especially want to thank my principal supervisor, Professor Argo Rosin, for guiding and mentoring me. Thank you for seeing the potential in me and showing me the way. Special thanks to my co-supervisor, Senior Researcher Tarmo Korõtko, who assisted me and led me along the way to the details. Many thanks to my co-supervisor from the first years of my Ph.D., Senior Lecturer Indrek Roasto, for mentoring me on academic writing.

I want to thank my colleagues from Tallinn University of Technology for fruitful discussions and meaningful conversations.

This research work has been supported by the European Regional Development Fund (project "Doctoral School of Energy and Geotechnology III"), Estonian Archimedes Foundation (program "Dora Pluss), Estonian Research Council grants (PUT1680 and PSG739), Estonian Centre of Excellence in Zero Energy and Resource Efficient Smart Buildings and Districts ZEBE (grant 2014-2020.4.01.15-0016), European Commission through the H2020 project Finest Twins (grant No. 856602), Estonian Ministry of Education and Research and European Regional Fund (grant 2014-2020.4.01.20-0289). This doctoral thesis was supported by the project "Increasing the knowledge intensity of Ida-Viru entrepreneurship" co-funded by the European Union (2021-2027.6.01.23-0034).

Abstract
Research and development of explicit demand flexibility management methods for ventilation systems

Increasing use of volatile renewable energy sources poses challenges in balancing supply and demand. Therefore, demand-side flexibility is increasingly important for system operators and balancing authorities. Explicit flexibility management methods are needed to integrate loads like ventilation systems of different buildings (e.g., residential and commercial) into the flexibility service. However, the available methods described in research papers require further development for their implementation in practice. Heating and cooling systems have received much attention from researchers, but the potential of ventilation systems has been left out of focus. Therefore, this thesis provides a complete set of novel flexibility management methods for ventilation systems created from an aggregator's viewpoint.

Firstly, the definitions of flexibility and problems to measure it were addressed. It was found that flexible power (how much power consumption can be altered), forced ventilation rate (FVR) duration (how long this forced state can be held), and price for the activation are the main parameters for quantification. Mathematic principles were explained for each parameter, and instructions on implementing these were given.

Secondly, the proposed methods were validated on a building model constructed and simulated in IDA ICE. The data processing and flexibility management methods were applied in MATLAB. It was found that FVR duration estimations based on CO_2 concentration have a mean error of 8 to 12 min. FVR duration estimations based on temperature showed a mean error of around 20 min for most scenarios. The results showed that cost savings are achievable when a ventilation system is integrated into a flexibility service. For example, in the apartment, up to 11% of cost savings were achieved; in the office, up to 15%; and in the single-family house, up to 4%. The cost savings heavily depend on how much the ventilation system can be exploited in the flexibility service.

Finally, the developed methods were tested on a real ventilation system. Two case studies were conducted. It was found that there can be problems in implementing these methods, but all difficulties arising during the validation process were addressed and solved.

In conclusion, the goals set were achieved. From the results obtained from simulations and case studies, the developed management methods are applicable for ventilation system flexibility management. By considering potential cost savings, this topic should raise the attention of building owners and aggregators. Implementing the developed methods was aided with guidelines for system integrators on selecting appropriate methods and where to find the needed data.

Lühikokkuvõte
Ventilatsioonisüsteemidele otsese energiapaindlikkuse juhtimismeetodite uurimine ja arendamine

Suurenev muutlike taastuvenergiaallikate kasutuselevõtt tekitab väljakutseid tootmise ja tarbimise tasakaalustamisel. Seetõttu on koormuse energiapaindlikkusel süsteemi operaatorite ja bilansihaldurite jaoks üha suurem tähtsus. Otsese energiapaindlikkuse juhtimismeetoid on vajalikud integreerimaks koormusi paindlikkusteenusesse nagu erinevate hoonete (näiteks elamute ja äriruumide) ventilatsioonisüsteemid. Siiski nõuavad teaduspublikatsioonides kirjeldatud meetodid praktikas rakendamiseks täiendavat arendamist. Küll on teadlased pööranud palju tähelepanu kütte- ja jahutussüsteemidele, kuid ventilatsioonisüsteemide potentsiaal on jäänud tähelepanuta. Seetõttu pakub see doktoritöö välja uudse paindlikkuse juhtimismeetodite komplekti ventilatsioonisüsteemide jaoks, mis on välja töötatud agregaatori vaatepunktist.

Esmalt käsitleti paindlikkuse mõistet ja selle mõõtmisega seotud probleeme. Teadustööde ülevaatest selgus, et olulised paindlikkuse mõõtmiseks vajalikud parameetrid on paindlik võimsus (kui palju energiatarbimist saab muuta), sunnitud ventileerimise hulga (FVR) kestus (kui kaua seda sunnitud olekut saab hoida) ja teenuse aktiveerimise hind. Iga parameetri jaoks on lahti selgitatud matemaatilised põhimõtted ning lisatud juhised, kuidas neid rakendada.

Teiseks valideeriti väljatöötatud meetodid hoone mudelil, mis oli loodud ja simuleeritud programmis IDA ICE. Andmete töötlemist ja paindlikkuse juhtimise meetodeid rakendati MATLAB-is. Selgus, et FVR kestuse hinnangud, mis põhinesid CO_2 kontsentratsioonil, olid keskmise veaga 8 kuni 12 minutit. FVR kestuse hinnangud, mis põhinesid temperatuuril, olid enamuse stsenaariumide puhul keskmise veaga umbes 20 minutit. Saadud tulemused näitasid, et ventilatsioonisüsteemi integreerimisel paindlikkusteenusesse on võimalik saavutada kulude kokkuhoid. Näiteks korteris saavutati kuni 11% kulude kokkuhoidu, kontoris kuni 15% ja ühepereelamus kuni 4%. Kulude kokkuhoid sõltub suuresti sellest, kui palju ventilatsioonisüsteemi paindlikkusteenuses saab ära kasutada.

Lõpuks testiti väljaarendatud meetodeid reaalsel ventilatsioonisüsteemil. Selleks viidi läbi kaks juhtumiuuringut. Valideerimisprotsessi käigus tuvastati reaalsetel süsteemidel probleemid, millele leiti lahendused.

Kokkuvõtteks võib väita, et seatud eesmärgid on täidetud. Simulatsioonide ja juhtumiuuringutest saadud tulemuste põhjal on võimalik öelda, et välja töötatud juhtimismeetodid on ventilatsioonisüsteemidel rakendatavad. Arvestades potentsiaalset kulude kokkuhoidu, peaks antud teema äratama tähelepanu hoonete omanikes ja agregaatorites. Väljatöötatud meetodite rakendamise toetamiseks on doktritöös välja toodud juhised süsteemi integraatoritele sobivate meetodite valikuks ja vajalike andmete hankimiseks.

Appendix

Publication I

Maask, V., Rosin, A., Korõtko, T., Thalfeldt, M., Syri, S., Ahmadiahangar, R. (2023), "Aggregation ready flexibility management methods for mechanical ventilation systems in buildings," Energy and Buildings, vol. 296, Oct. 2023 doi: https://doi.org/10.1016/j.enbuild.2023.113369.

Publication II

Maask, V., Rosin, A., Korõtko, T. (2023), “Virtual Energy Storage Model of Ventilation System for Flexibility Service,” 17th IEEE International Conference on Compatibility, Power Electronics and Power Engineering, CPE-POWERENG 2023 (1–6). IEEE.

Publication III

Maask, V., Mikola, A., Korõtko, T., Rosin, A., Thalfeldt, M. (2021), “Contributions to ventilation system demand response: a case study of an educational building,” Cold Climate HVAC & Energy 2021 (1–6). E3S Web of Conferences.

Publication IV

Ferrantelli, a., Aljas, H. K., Maask, V., Thalfeldt, M. (2021), “Tenant-based measured electricity use in 4 large office buildings in Tallinn, Estonia,” Cold Climate HVAC & Energy 2021 (1–10). E3S Web of Conferences.

Publication V

Maask, V., Häring, T., Ahmadiahangar, R., Rosin, A., Korõtko, T. (2020), “Analysis of Ventilation Load Flexibility Depending on Indoor Climate Conditions,” 21st International Conference on Industrial Technology, ICIT2020 (1–6). IEEE.

Publication VI

Maask, V., Rosin, A., Roasto, I. (2018), “Development of Experimental Load Management System for Nearly Zero-Energy Building,” 59th International Scientific Conference on Power and Electrical Engineering of Riga Technical University, RTUCON 2018 (1–5). IEEE.

Curriculum vitae

Personal data

Name:	Vahur Maask
Date of birth:	22.09.1993
Place of birth:	Estonia
Citizenship:	Estonian

Contact data

E-mail:	vahur.maask@taltech.ee

Education

2017–2023	Tallinn University of Technology, PhD
2015–2017	Tallinn University of Technology, MSc
2012–2015	Tallinn University of Technology, BSc
2009–2012	Võru Kreutzwaldi Gymnasium, Secondary Education

Language competence

Estonian	Native speaker
English	Fluent
Russian	Basic skills

Professional employment

2018–	Tallinn University of Technology, Junior Researcher
2017–2017	Tallinn University of Technology, Engineer
2015–2015	Ensto Ensek Ltd, development engineer (internship)
2014–2014	Elektrilevi OÜ, protected zone supervision (internship)

Scientific work and Research and Development projects

2021–2023	PSG409, “New generation dynamic sizing methods for heating and cooling systems in intermittently operated buildings”
2021–2022	LEEEE21133, “Providing energy consulting in relation to machine learning models”
2021–2021	LEEAE21059, “Assessment of the reliability of electrical installations with on-site measurements”
2020–2023	EE20107, “Energy flexilibilty service pilot project - Stage 2”
2019–2021	Lep18101, “Proof of concept of an integrated monitoring and diagnostics solution for predictive maintenance of expansion joints”
2017–2021	PUT1680, “Power electronics based energy management systems for net zero energy buildings”
2020–2020	EE20012, “Energy flexilibilty service pilot project - Stage 1”
2018–2018	Lep18038, “Development of a virtual power plant laboratory”
2016–2018	VERT16061, “Strategic Partnership in the field of Mechatronics for innoavative and smart growth of European manufacturing SMEs”
2018–2018	Lep18042, “Composition of a development plan for developing monitoring solutions for compensators in the frame of smart specialisation growth area”
2017–2018	Lep17108, “Preliminary research of the technological solution for monitoring the compensators conditions at site”
2017–2018	Lep17114, “Replacement of electromechanical contactors with semiconductor devices”

Elulookirjeldus

Isikuandmed

Nimi:	Vahur Maask
Sünniaeg:	22.09.1933
Sünnikoht:	Eesti
Kodakondsus:	eestlane

Kontaktandmed

E-post:	vahur.maask@taltech.ee

Hariduskäik

2017–2023	Tallinna Tehnikaülikool, PhD
2015–2017	Tallinna Tehnikaülikool, MSc
2012–2015	Tallinna Tehnikaülikool, BSc
2009–2012	Võru Kreutzwaldi Gümnaasium, reaalsuund

Keelteoskus

Eesti	Emakeel
Inglise	Kõrgtase
Vene	Algtase

Teenistuskäik

2021–2023	PSG409, “Uue generatsiooni dünaamilised meetodid kütte- ja jahutussüsteemide dimensioneerimiseks vahelduva kasutusega hoonetes”
2021–2022	LEEEE21133, “Energeetikaalase konsultatsiooni pakkumine seoses masinõppe mudelitega”
2021–2021	LEEAE21059, “Elektripaigaldise töökindluse hindamine koos kohapealsete mõõdistamistega”
2020–2023	EE20107, “Energiatarbimise juhtimise paindlikkustoote pilootprojekt - 2. etapp”
2019–2021	Lep18101, “Kompensaatorite monitooring kasutuskohas: tehnoloogilise lahenduse kontseptsiooni väljatöötamine”
2017–2021	PUT1680, “Jõuelektroonikal baseeruv energia juhtimissüsteem liginullenergia ehitistele”
2020–2020	EE20012, “Energiatarbimise juhtimise paindlikkustoote pilootprojekt - 1. etapp”
2018–2018	Lep18038, “Virtuaalse elektrijaama arenduslabori väljatöötamine”
2016–2018	VERT16061, “Strateegiline partnerlus mehhatroonika valdkonnas Euroopa väikeste ja keskmise suurusega tootmisettevõtete innovatiivseks ja nutikaks kasvuks (MechMate)”
2018–2018	Lep18042, “Nutika spetsialiseerumise meetme arendusplaani koostamine kompensaatorite monitooringu pilootlahenduste väljatöötamiseks”
2017–2018	Lep17108, “Tehnoloogilise lahenduse eeluuring kompensaatorite monitooringuks kasutuskohas”
2017–2018	Lep17114, “Elektromehhaaniliste kontaktorite asendamine kontaktivabade pooljuhtseadmetega”